



This is to certify that the

thesis entitled


Computer Controlled Coulostatic
Instrumentation and Its Application to
the Study of Mercury Film on the Platinum Surface

presented by

Minchen Wang

has been accepted towards fulfillment
of the requirements for

Ph.D. degree in Analytical Chemistry


Major professor

Date Sept. 15, 1978

COMPUTER CONTROLLED COULOSTATIC INSTRUMENT AND ITS APPLICATION
TO THE STUDY OF MERCURY FILM ON PLATINUM SURFACE .

By

Minchen Wang

A DISSERTATION

Submitted to

Michigan State University

In partial fulfillment of the requirement
for the degree of

DOCTOR OF PHILOSOPHY

Department of Chemistry

1978

CONF

const

deliv

elect

curre

pulse

immed

by th

per d

seque

progr

quite

film

three

127000

ABSTRACT

COMPUTER CONTROLLED COULOSTATIC INSTRUMENT AND ITS APPLICATION TO THE STUDY OF MERCURY FILM ON PLATINUM SURFACE

By

Minchen Wang

A computer controlled coulостatic instrument was constructed. The basic function of this instrument is to deliver a predetermined amount of charge to the working electrode of an electrochemical cell by supplying constant current pulses. It can deliver currents up to ± 2.5 mA with pulses as short as $0.56 \mu\text{s}$. The potential response of the cell immediately after the coulостatic charging pulses is followed by the computer. The fastest sampling rate is about $13 \mu\text{s}$ per datum point. Under computer control, other polarization sequences can be performed simply by using the appropriate programs. This capability makes the coulостatic instrument quite versatile.

This instrument was used in the study of the mercury film formation on a platinum surface. On the platinum surface, three structures of mercury deposits were identified, namely;

8

o

m

re

ho

pl

int

on

comp

to t

be d

react

thick

trans

decre

surfa

mercury droplets, mercury patches and smooth mercury films. The structure of the mercury film depends on the deposition overpotential and the pretreatment of the platinum prior to the mercury deposition. On the freshly polished platinum surface, mercury droplets are formed at small deposition overpotentials while at higher deposition overpotential, mercury patches are formed. By repetitive oxidation and reduction of the platinum surface, an activated, more homogeneous platinum surface is produced which can be easily plated with smooth mercury film.

The plated mercury reacts with the platinum to form an intermetallic compound. The rate of this reaction is dependent on the thickness of the intermetallic compound. For a given compound thickness, the transformation of the metallic mercury to the compound form is proportional to $t^{\frac{1}{2}}$. This relation can be described in terms of the diffusion process of the reactants through the intermetallic compound layer. As the thickness of the compound increases, the rate of the transformation of the metallic mercury into the compound decreases.

A new approach to plate a mercury film on a platinum surface was also devised. In this approach, the chloride ion

is

pr

on

of

ef

pl

is utilized as a masking agent during the mercury plating process. The chloride ion forms an insoluble calomel film on the deposited mercury surface which prevents the formation of mercury droplets. This approach is found to be quite effective for creating a thin smooth mercury film on the platinum surface.

En

gr

mon

ser

prey

guid

appr

Help

are)

while

to my

thank

throu

ACKNOWLEDGEMENT

I would like to express my thanks to Professor Christie Enke for his guidance and patience during the course of my graduate study. His advice and friendship in many critical moments will always be remembered.

Thanks to Professor Weaver for taking the hardship and serving as my second reader at the last moment of thesis preparation. Thanks go also to the other members of my guidance committee. I also like to express my special appreciation to Dr. Atkinson for his help and friendship. Helps from my fellow members of the Enke research group are highly appreciated.

Thanks to my wife, Hwai-Lin, who typed the whole thesis while taking a full time job to support our family. Thanks to my parents-in-law for their selfless help. And above all, thanks to my parents who have always shown their support throughout my life.

Chapt

LIST

LIST

I.

II.

III.

TABLE OF CONTENTS

Chapter	Page
LIST OF TABLES.....	vii
LIST OF FIGURES.....	ix
I. A COMPUTER CONTROLLED GENERAL PURPOSE COULOSTATIC SYSTEM.....	1
A. Introduction to the Coulostatic Instrumentation.....	1
B. Instrument.....	7
C. Performance of the Instrumental System.....	23
D. Applications of the General Purpose Coulostatic Instrument.....	51
II. INTRODUCTION TO THE STUDY OF THE MERCURY FILM ON PLATINUM.....	64
A. The Search for a Mercury Film Electrode.....	64
B. Mercury Film Preparation.....	68
C. Interaction between Mercury and Platinum	73
D. Additional Problems with Platinum- Based Mercury Film Electrodes.....	74
E. Objective of Study.....	75
III. EVALUATION OF THE FACTORS AFFECTING THE STRUCTURE OF THE MERCURY ELECTROPLATED ON THE PLATINUM SURFACE.....	77

A.	Platinum Surface State Characterization.....	77
B.	Methods of Examining the Smoothness of the Mercury Film on the Platinum.....	83
C.	Experimental Set-up.....	84
D.	Experiments and Results.....	94
1.	Creating Platinum Surface with Varying Roughness Factors.....	94
2.	Influence of the Potential and the Roughness Factor on the Mercury Deposition.....	103
E.	Discussion.....	111
1.	Structure of the Mercury Deposit Versus the Plating Potential.....	111
2.	Effect of Surface Roughness Factor on the Structure of the Mercury Deposit.....	117
3.	Other Factors that Influence the Formation of the Mercury Deposit.....	120
F.	Conclusion.....	123
IV.	A NEW METHOD OF MAKING A SMOOTH MERCURY FILM ON A PLATINUM SURFACE.....	125
A.	Introduction.....	125
B.	Procedures of Making a MFE Using Chloride Ion as a Masking Agent.....	127
C.	Results and Discussion.....	127
1.	Product of Primary Plating.....	127
2.	Continual Mercury Plating.....	131
3.	Factors that Influence the MFE Obtained..	131

V.

E

C

D

VI. F

APPEN

APPEN

M

P

S

P

P

S

S

S

V. DETERMINATION OF THE PLATINUM-MERCURY REACTION RATE ON THE MFE.....	134
A. Introduction.....	134
1. Scope of the Pt-Hg Reaction Rate Study.....	134
2. Relevant Results Obtained by Other Workers...	135
B. Experimental.....	139
C. Experimental Results.....	140
1. Methods Used for the Pt-Hg Reaction Rate Study.....	140
2. Anodic Stripping of MFE in Mercurous Solution.....	143
3. Disappearance of Metallic Hg on the PMOCPE.....	145
D. Discussion.....	155
1. Reaction of Platinum and Mercury on PMOCPE.....	155
2. Accounting for the Pt-Hg Reaction Rate.....	157
VI. Future Study.....	164
APPENDIX 1 Computer Interface.....	165
APPENDIX 2 Program Listings.....	168
Macros and Registers Assignment.....	169
Program QUANTIF.FTN.....	172
Subroutine QUANTM.MAC.....	175
Program SLOPE.FTN.....	178
Program CAPF3.FTN.....	180
Subroutine CAPM3.MAC.....	184
Subroutine LINFIA.FTN.....	186
Subroutine AMP.FTN.....	187

Program VDEPOF.FTN.....	189
Subroutine VDEPOM.MAC.....	191
Program CHRONF.FTN.....	193
Subroutine CHRONM.MAC.....	195
Program DEPOSF.FTN.....	198
Subroutine DEPOSM.MAC.....	200
Program ETREAF.FTN.....	202
Subroutine ETREAM.MAC.....	204
Program PLATNZ.MAC.....	207
Program STRIPF.FTN.....	210
Subroutine STRIOM.MAC.....	212
REFERENCES.....	214

T

1-

1-

1-

1-4

1-5

1-6

1-7

1-8

1-9

1-10

LIST OF TABLES

Table	Page
1-1	Slopes of the Pulse Charge Content, Current Channel 1 with Negative Current.....34
1-2	Slopes of the Pulse Charge Content, Current Channel 1 with Positive Current.....34
1-3	Slopes of the Pulse Charge Content, Current Channel 2 with Negative Current.....38
1-4	Slopes of the Pulse Charge Content, Current Channel 2 with Positive Current.....38
1-5	Slopes of the Pulse Charge Content, Current Channel 3 with Negative Current.....42
1-6	Slopes of the Pulse Charge Content, Current Channel 3 with Positive Current.....43
1-7	Variation of the SCC with the Pulse Width for Current Channel 1.....47
1-8	Variation of the SCC with Pulse for Current Channels 2 and 3.....47
1-9	Charge Produced by a 1.56 μ s, 2.5 mA Current Pulse.....48
1-10	Determination of Cell Capacitance and Faradaic Resistance with High Amplitude Current Pulses.....55

3

3

5-

5-

Table		Page
1-11	Determination of Cell Capacitance and Faradaic Resistance with Low Amplitude Current Pulses.....	60
3-1	Platinization of Platinum with Alternating Current Steps.....	102
3-2	Potential Dependence of the Mercury Deposit on the Bright Platinum Electrode.....	106
3-3	Dependence of the RF of the Mercury Deposited at 200 mV.....	106
5-1	Disappearance of Metallic Mercury in the Current Reversal Experiment.....	147
5-2	Disappearance of Metallic Mercury in the Aging Experiment.....	152

[illegible]

LIST OF FIGURES

Figure	Page
1-1	Equivalent Circuit and Current Impulse Response of Electrochemical System.....4
1-2	Computer Controlled Coulostatic System.....8
1-3	Pulse Generator.....12
1-4	Pulse Generator Circuit.....14
1-5	Current Generator.....17
1-6	Digital to Analog Converter Card.....19
1-7	Data Acquisition System.....21
1-8	Shortest Current Pulses.....27
1-9	Cathodic Charging Curve with Current Channel 1.....31
1-10	Anodic Charging Curve with Current Channel 1.....33
1-11	Cathodic Charging Curve with Current Channel 2.....36
1-12	Anodic Charging Curve with Current Channel 2.....37
1-13	Cathodic Charging Curve with Current Channel 3.....40
1-14	Anodic Charging Curve with Current Channel 3.....41
1-15	Cathodic Charging Curve with Current Channel 4.....45
1-16	Potential Decay of a Dummy Cell with High Amplitude Current Pulses.....53

Figur

1-17

1-18

1-19

1-20

3-1

3-2

3-3

3-4

3-5

3-6

3-7

3-8

3-9

3-10

1-17	Curve Fitted Potential Decay of a Dummy Cell with High Amplitude Current Pulses.....	54
1-18	Potential Decay of a Dummy Cell with Small Amplitude Current Pulses.....	57
1-19	Improvement of Data through the Curve Fitting and Signal Averaging Process.....	59
1-20	Simulated Potentiostatic Polarization by the Coulostatic Instrument.....	62
3-1	Flow Cell.....	88
3-2	Potential Response to the Solution Oxygen.....	91
3-3	Flow Diagram of Hg Deposition Experiment.....	93
3-4	Cyclic Chronopotentiograms of Pt Electrodes with and without Aqua Regia Treatment.....	95
3-5	Cyclic Chronopotentiograms of Pt Electrodes in 0.1 M HCl and 0.1 M HClO ₄	99
3-6	Creating Platinized Pt Electrodes by Alternating Current Steps.....	101
3-7	Two Types of Mercury Deposit on Pt Surfaces.....	105
3-8	Plating Mercury on Pt Surface with Small Current, -24 μ A.....	109
3-9	Plating Mercury on Pt Surfaces with Large Current, -1000 μ A.....	110
3-10	Plating Mercury on Thick Hg Coated Pt Electrodes with Large Current, -1000 μ A.....	112

F

4

5-

5-

5-

5-1

5-5

5-6

5-7

5-8

5-9

Figure	Page
4-1	Mercury Plating at a Constant Potential in 1.2 N HCl and 0.1 M HgCl_2 Solution.....128
5-1	Potential-Charge Response of MFE under Anodic Current in 0.1 M HClO_4137
5-2	Current Programs used for Pt-Hg Reaction Rate Study.....142
5-3	Anodic Potential-Charge Characteristic of the MFE in 0.1 M HgClO_4 Solution.....144
5-4	Potential-Charge Response with Current Reversal Polarization.....146
5-5	Potential-Charge Variation during Reduction of Mercurous Ions from 0.1 M HgClO_4 Solution Using High Reduction Current.....149
5-6	Potential-Charge Variation during Repetitive Deposition-Stripping of Hg with Varying Aging Intervals.....151
5-7	Disappearance of Metallic Mercury with Aging.....154
5-8	Effect of Pt-Hg Compound Thickness on the Reaction Rate of Pt and Hg.....156
5-9	Hg Concentration Profile in the Pt-Hg Compound.....158

A.

stu
occ
of
tran
syst
appl
whic
Reinn
amoun
in a
poten
is di
stead
injec
elect
charg
the p
of the
elect

CHAPTER I

A COMPUTER CONTROLLED GENERAL PURPOSE COULOSTATIC SYSTEM

A. Introduction to Coulostatic Instrumentation

Several methods have been developed over the years to study the charge transfer and mass transport processes occurring at electrode surfaces. To avoid the interferences of the mass transport phenomenon, most methods of charge transfer study rely on the response of the electrochemical system immediately after an excitation signal has been applied. Among these methods is the coulостatic technique which was independently and simultaneously proposed by Reinmuth (42) and Delahay (28). In this method, a known amount of charge is delivered to the electrode double layer in a very short time. The application of charge changes the potential of the electrode to a new value. Thus the electrode is disturbed from the reaction conditions (equilibrium, steady state, no reaction) which existed prior to the charge injection. The potential change may induce a change in the electrochemical reaction conditions which consumes the charge stored on the electrode double layer. As a result, the potential relaxes back toward the prior value. The rate of the potential decay is a function of the rate of the electrochemical reaction and the value of the double-layer

o

i

t

co

De

st

el

(4

of

cha

tha

at

This

as t

time

over

unuse

depen

termi

equiv

circu

parall

capacitance. Thus the rate of the electrochemical reaction induced by the charge pulse can be deduced from the potential-time curve.

Two techniques have been used to accomplish the coulometric charging process. The earlier technique of Delahay and Reinmuth used a small, high quality capacitor to store the charge which was then discharged across the electrochemical cell. The second technique, by Wier and Enke (45), used a current impulse to deliver the desired amount of charge. This method has two advantages over the capacitor charging method: the potential during pulsing can be lower than with the capacitor method in which the peak potential at the first instant of charge dumping must be quite high. This high voltage drives the input of measuring devices such as the oscilloscope to their limit. Since a certain period of time is required for the device to recover from being overdriven, the information within this period of time is unusable (43). In addition, since the pulse duration is not dependent on cell resistance, it is better defined and it is terminated more sharply than with an exponential decay.

An electrochemical cell can be analyzed in terms of an equivalent circuit as shown in Figure 1-1. A. This equivalent circuit is composed of a double-layer capacitor C_d , in parallel with resistors R_f and Z_m , and in series with another

r
s
t.
po
is
oc
im
a
so.

as
res
At
unt.
gra
pot
of
in
the
n
rea
vs

resistor R_s . The double-layer capacitance is determined by several factors: the material and the surface condition of the electrode; the composition of the electrolyte and the potential of the electrode. The faradaic resistance, R_f , is a function of the rate of the electrochemical reaction occurring at the electrode surface. The mass transport impedance is Z_m and R_s is the solution resistance which is a function of the electrolyte concentration in the cell solution.

When a current impulse, I , as in Figure 1-1B, is applied as an excitation function to this equivalent circuit, the response function, E , is observed as shown in Figure 1-1C. At the beginning of the impulse, the potential rises immediately until it is equal to $i_t R_s$. Then the potential increases gradually as C_d charges until the current pulse is ended. The potential now drops by $i_t R_s$. After this point, the discharge of the double-layer capacitor dominates the potential variation in the circuit. In the absence of mass transport limitation, the potential follows a simple exponential decay law with $\eta = \eta_{t=0} \exp(-t/R_f C_d)$. The exchange current I_0 of the reaction can be calculated directly from the slope of the $\log \eta$ vs t curve from the relationship:

$$\text{Slope} = (nF/2.303RT) (I_0/C_d)$$

A

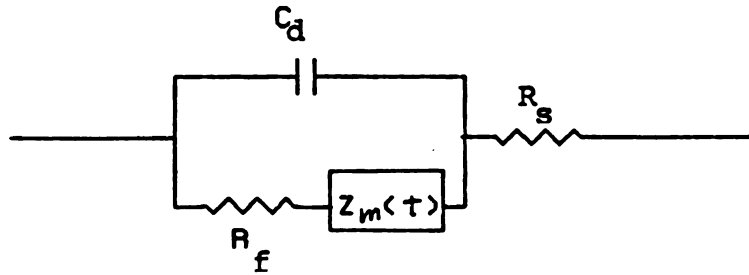
I

B.

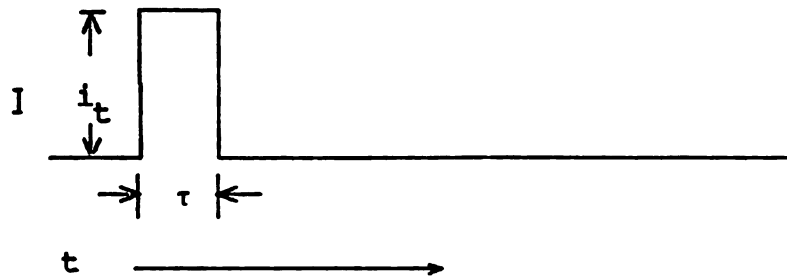
Ei

C.

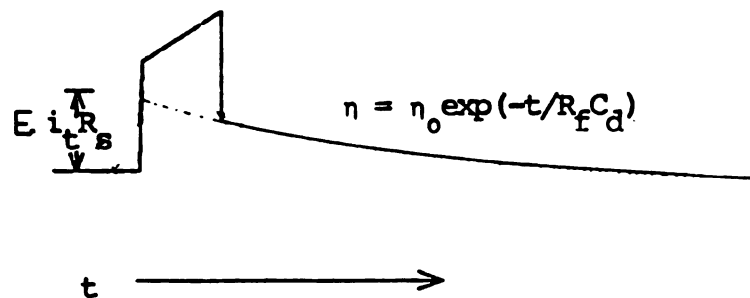
Fig



A. EQUIVALENCE CIRCUIT FOR ELECTROCHEMICAL CELL



B. EXCITATION FUNCTION: CURRENT IMPULSE



C. POTENTIAL RESPONSE

Figure 1-1. Equivalent Circuit and Current Impulse Response of Electrochemical System

ob

th

For

mus

occ

the

the

curv

cell

the

enha

coul

the

In the case of a reaction that is mass-transport limited throughout the pulse response, the potential decay follows the equation :

$$\eta = \pm \frac{2nFC^0D^{\frac{1}{2}}}{\pi^{\frac{1}{2}}C_d} t^{\frac{1}{2}}$$

In either case, the double-layer capacitance C_d can be obtained experimentally by the ratio of the total charge in the current impulse to the initial potential $\eta_{t=0}$. For an accurate determination of $\eta_{t=0}$, the pulse duration must be short enough so that a negligible amount of reaction occurs during the pulse time.

There are two significant advantages associated with the coulостatic technique : the double-layer capacitance at the electrode can be obtained from the same potential-time curve and the measured potential need not be corrected for cell resistance because there is no current through R_s when the potential is being measured.

The capability of a coulостatic system is greatly enhanced with an on-line computer. The computer controlled coulостatic system improves this polarization technique in the following aspects :

ex

with

is

by

the

pola

curr

of a

capab

plati

plati

adsor

cover

be ca

a cle

accor

1. Capability of performing other types of polarization techniques (30).
2. Versatility of experiment control.
3. Ease of data processing including signal averaging.

These advantages are illustrated in the following examples :

Controlled potential polarization has been achieved with the computer controlled coulостatic system. The potential is maintained within a few millivolts of the desired value by constantly adding short charging pulses as necessary to the electrical double layer (30). Controlled current polarization is realized by adjusting the pulse width, the current amplitude, and the pulse repetition rate.

The experiment can be programmed according to the need of a particular electrochemical system under study. This capability has been critical in the study of the mercury-platinum interaction reported here. The behavior of a platinum electrode is greatly affected by trace impurities adsorbed on the platinum surface, and by the degree of coverage of the oxide film on the surface. The electrode must be carefully pretreated just before the experiment to generate a clean and reproducible electrode surface. This is accomplished by programming the potential of the electrode.

The electrode is first held to a positive potential to oxidize all impurities and then is changed to a negative potential to remove the oxide film on the surface.

Improvement of the data collected is realized by the averaging of the data obtained from repetitive runs of an experiment. The signal-to-noise ratio increases at a rate proportional to the square root of the number of averages for random noise. The digitization error which arises from the resolution of analog-to-digital conversion is improved as well.

B. Instrument

The computer controlled coulometric system is shown in Figure 1-2. It consists of a minicomputer and its peripherals, a pulse generator, a current generator, a sample cell and an analog data conversion unit. All controls and data collection are performed by the minicomputer under program control.

When a current pulse is needed, the computer sets up the pulse width, pulse amplitude and the current channel number. Then it issues a pulse command upon the request of the operator or of the program. The data collection sequence is started at a predetermined rate. These data are either transferred to a mass storage device for future analysis or

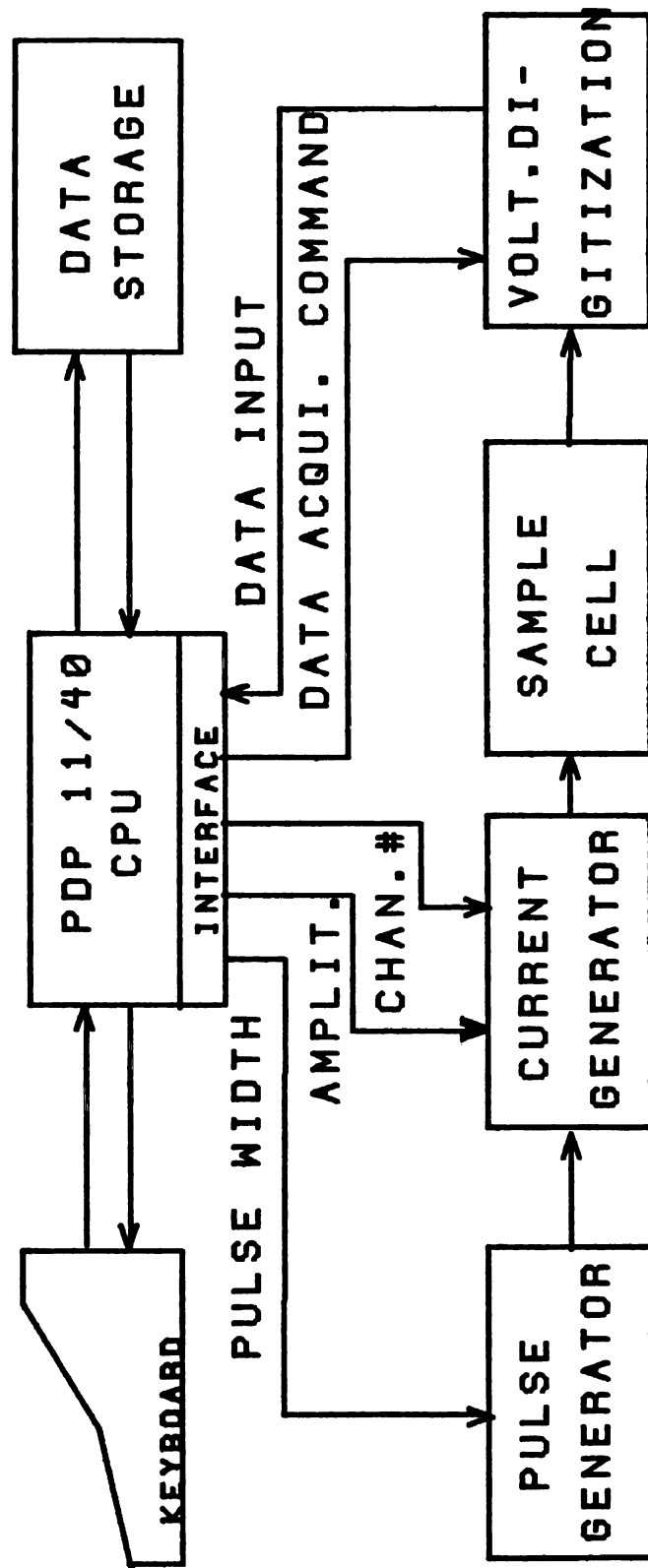


Figure 1-2. Computer Controlled Coulostatic System

they

cont.

expe.

curve

next

in th

for t

secti

1. Co

Digit

It is

The m

mass

(also

T4010

print

copy

was b

during

they undergo preliminary processing to obtain experiment control parameters. An example of the latter is the experimental sequence that uses the analysis of an E vs t curve to establish the charge content and the timing of the next pulse.

Each portion of the instrument is described separately in the following sections. Detailed description is provided for the purpose of reconstruction. Readers could skip to section C for the performance study of the system.

1. Computer and Interface

The computer used is a PDP 11/40 minicomputer from Digital Equipment Corp.. This computer has a 28K core memory. It is a 16-bit word machine with 8 general purpose registers. The machine cycle time is approximately one microsecond. The mass storage units available are a RK05 moving head disk (also from DEC) and a SYKES dual floppy disk.

The operator controls the instrument through a Tektronix T4010 terminal. An ASR33 teletype and a Printronix line printer/plotter are also available for producing the hard copy of data and the program listings. A real time clock was built on the computer bus. This is used for timing during experiments.

The computer interacts with the coulometric instrument through an interface. The interface is composed of a DR11-C interface card located on the computer unibus and wired as an emulator which generates control signals similar to the PDP-8 computer. An interface buffer unit functions as an isolator between the DR11-C and the instrument. The details of this interface are described in Appendix 1.

The operating system used is the DOS/BATCH V9-20. This is a disk based operating system. This operating system provides routines for the creation, editing and running of programs. Most programs were written in Fortran and some programs which perform the actual experimental control were written in a machine language call Macro- an assembly language which provides more effective real time control. Some of the programs are listed in Appendix 2.

In addition to the experimental control and data collection, the computer is also used to process the collected data. Data averaging, statistical analysis, data smoothing, and curve fitting processes are performed. Routines are also available for data display during and after experiments.

2. C

a. P

long

can r

To pr

are f

is is

and g

signa

the c

Gate.

the c

the r

risin

star

numb

zero

unde

to t

2. Coulostatic Instrument

a. Pulse Generator

The pulse generator generates TTL level pulses. The longest pulse is 4096 times a selected time-base unit which can range from one microsecond to one hour.

Figure 1-3 shows the block diagram of the pulse generator. To produce a current pulse, the time base and the pulse width are first loaded from the CPU. Then a signal called Reset T.B. is issued to actually reset the time base to this new value and generate another signal called Pulse Init. The Pulse Init signal opens the gate of the T.B. gate control which allows the clock pulse to pass another logic gate called Timebase Gate. This gate is used to synchronize the clock pulse with the opening of the gate so that the pulses at the output of the Timebase Gate would be only whole clock pulses. The first rising edge at this output turns on the flip-flop which starts the current pulse. The clocking pulses decrement the number latched in the Pulse Width Counter until it reaches zero. Then the next pulse causes the counter to generate an underflow pulse. This pulse signals the Timebase Gate Control to terminate the current pulse.

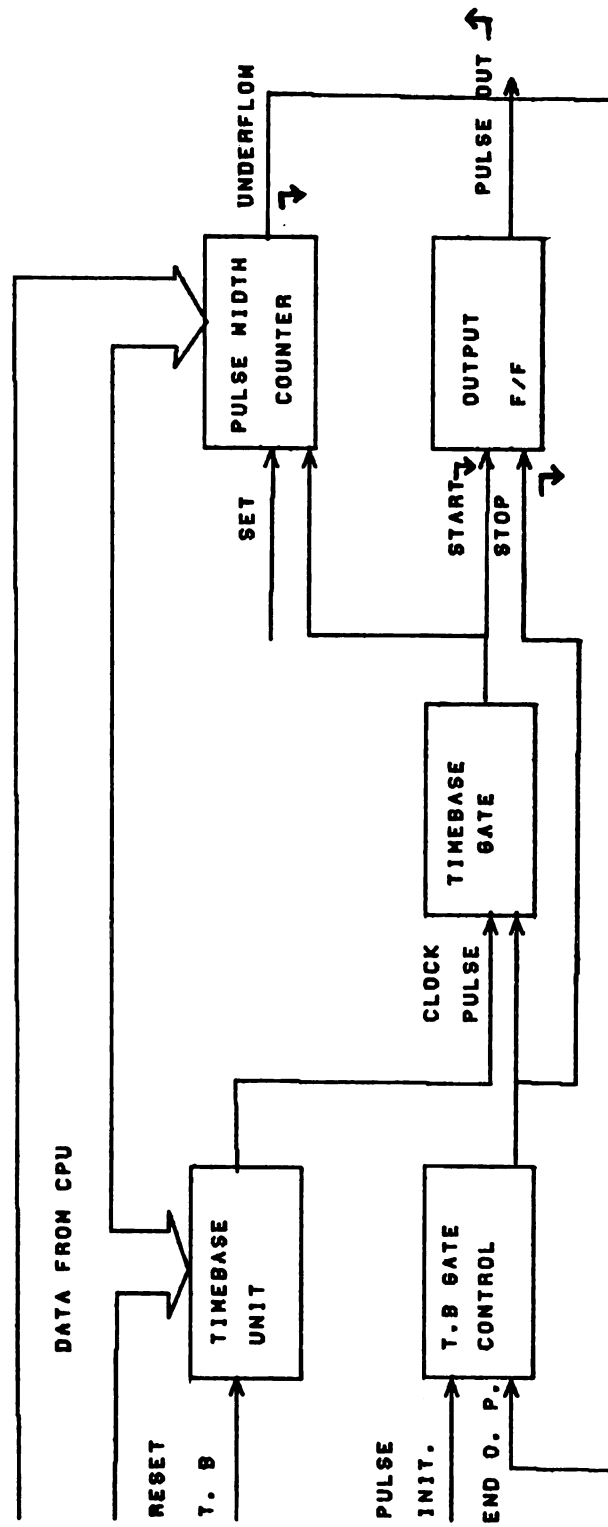


Figure 1-3. Pulse Generator

pulse

buffer

(IC's

to pr

Width

and 1

count

before

is us

(block

Count

The f

1M Hz

channel

is ge

signal

monos

MK500

another

This

is se

Figure 1-4 shows the detailed circuit diagram of the pulse generator. The device select codes from the interface buffer are decoded by two 7442 BCD decoder integrated circuits (IC's). These decoded signals are gated with IOP timing pulses to provide control signals. The signal L.L. loads the Pulse Width Counter from CPU into three 4-bit latches (blocks 6, 11 and 16).

The signal L. Counter is used to set three up/down counters, (blocks 7, 12 and 17) with the pulse width counter before the starting of the current pulse. The signal L. TB is used to load the time base into a four bit data latch, (block 18). This latch selects the time-base for a MOS Counter Time-Base IC, MK5009 manufactured by MOSTEK Co.. The fundamental timebase of the MK5009 is provided by a 1M Hz crystal oscillator.

The signal L. CHAN. loads the data latch (block 5) with the channel number to be used. The pulse command signal, PULSE CMD is generated similarly on another circuit card. When this signal is produced, a 10 μ sec pulse is initiated by a monostable. This pulse, RESET T.B. resets the timebase of the MK5009 to the value set by last L. TB signal. It also causes another monostable to produce a 1 μ sec pulse, PULSE INIT. This pulse sets one flip-flop (10-A). Once this flip-flop is set, the clocking pulses from the MK5009 are allowed to

L. CH

[illegible]

3	
2	
1	
0	
L	T

1615
PULS

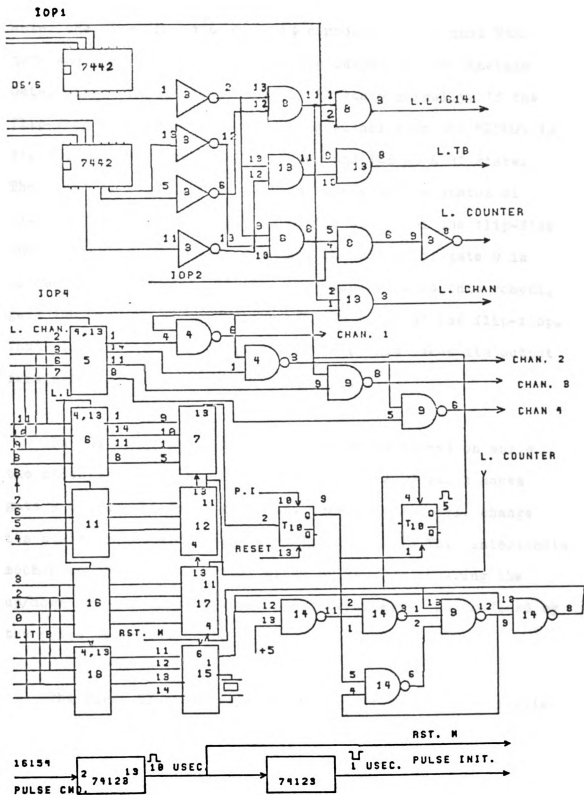


Figure 1-4. Pulse Generator Circuit

ent

gate

Gate

flip

HI,

The

gate

and/

LO d

gate

Thus

remai

the c

gate

its s

mecha

up/do

the p

14D t

These

up/do

13 of

enter the Timebase Gate which is composed of one quad NAND gate and one 3-input NAND gate. The output of the Timebase Gate, pin 8 of gate 14D, stays at HI state normally. If the flip-flop is set while the clocking signal from the MK5009 is HI, gate 14A will be at a LO state, and 14B at a HI state. The state of gate 9 is determined solely by the status of gate 14C which in turn depends on the status of the flip-flop and/or the status of gate 9. Since the output of gate 9 is LO due to the LO state of the flip-flop prior to this moment, gate 14C remains HI regardless of the status of the flip-flop. Thus all three inputs of gate 9 are HI. This makes its output remain LO and makes gate 14D remain HI.

On the other hand, if the flip-flop is turned on while the clocking signal is LO, gate 14B becomes LO which makes gate 9 HI and activates gate 14D. Thus gate 14D will change its state when the clocking signal becomes HI. This interlocking mechanism prevents a partial clock pulse from entering the up/down counter so that a precise time interval is produced by the pulse generator (31).

The first HI-to-LO edge of the clocking pulses from gate 14D turns on the output flip-flop 10B, and starts the pulse. These clocking pulses decrement the number loaded in the up/down counter until an underflow pulse is produced at pin 13 of counter 7. This pulse causes flip-flop 10A to change its

state and turns off the pulse at Q of flip-flop 10 B. The output pulse from the pulse generator is gated with the channel selecting latch, block 5. Only the channel chosen allows the pulse to appear.

b. Current Generator

The current generator consists of a 12-bit digital to analog converter, a buffer amplifier, a fast operational amplifier and a quad FET analog switch.

Figure 1-5 shows the wiring diagram of the current generator. The current amplitude is determined by a 12-bit data latch. The voltage from the DAC is buffered by a buffer amplifier. A CA3140 operational amplifier is used for this purpose. The output of the buffer amplifier is connected with four parallel precision resistors. The resistances are 2 M Ω , 200 K Ω , 20 K Ω and 2 K Ω within $\pm 1\%$. The other end of the resistors are independently connected to the sources of the analog switches. The drains of these switches are connected to the summing point of the high speed operational amplifier. These switches are controlled independently by the pulses from the pulse generator. Each switch is driven by an open collector driver tied to +15 V through a small resistor to reduce the leakage current. The switches come from a quad analog switch AH5011 made by

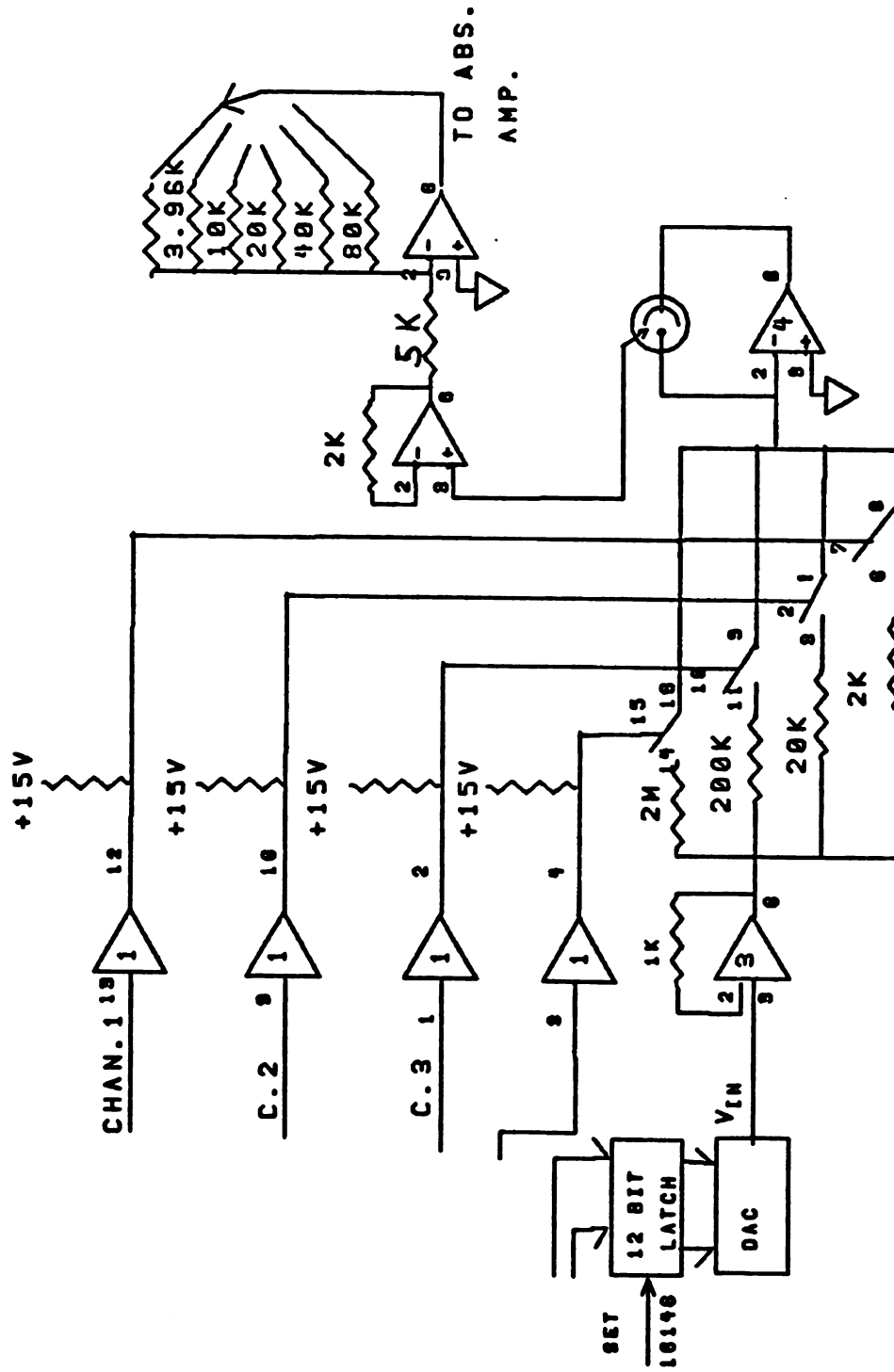


FIG. I-5 CURRENT GENERATOR

National Semiconductor Co.. These switches have a switching speed of 150 nsec and an "ON" resistance of 30Ω , which allows extremely short, reproducible current pulses to be produced.

The high speed operational amplifier is a AM405-2 manufactured by DATEL Co.. It has a slew rate of 150 V/ μ sec with a settling time of 400 nsec. A small capacitor, 20pf, is used to stabilize the operational amplifier.

The voltage control is shown in Figure 1-6. The device select codes from the interface buffer are decoded by two BCD decoders. The decoders were wired to decode device 14. The device select signal is gated by the timing pulse, IOP2. When both are issued from the CPU, a command pulse, NEW AMP. CMD. is produced which latches the pulse amplitude data from the interface buffer into three 4-bit data latches (5,8, and 12). These latched data control the voltage output of the DAC. The DAC is a 12-bit digital to analog converter, DAC 85C from Burr-Brown Co. The DAC was wired to produce voltages between +5.000 V and -5.000 V. Since four channels are available, the current generator provides four decades of current range with the same resolution. The maximum current is ± 2.5 mA.

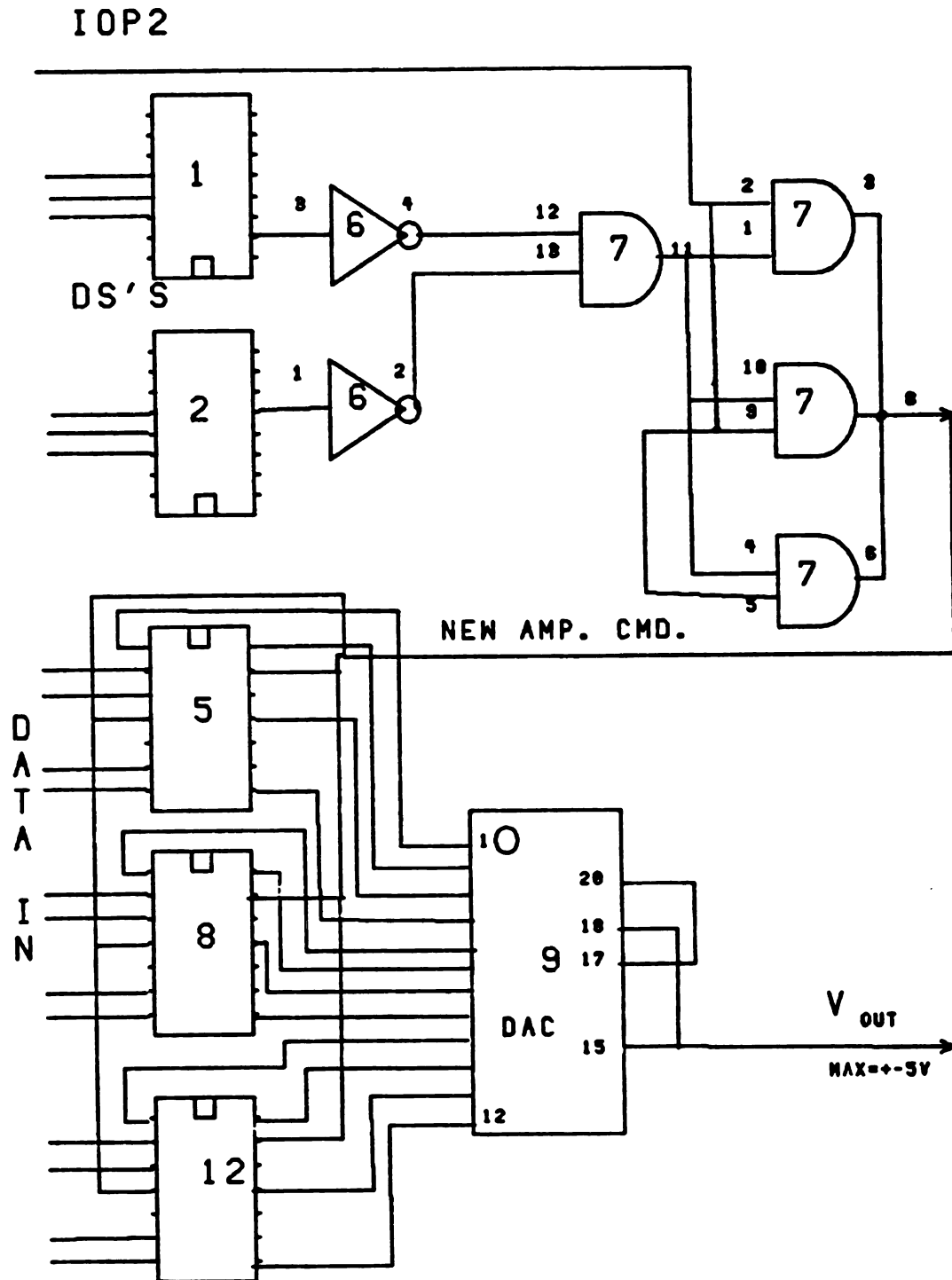


Figure 1-6. Digital to Analog Conv. Card

c.

se

vo

pr

dec

wit

and

elec

for

fast

by a

manua

an ab

voltage

conve

circu

perfo

(An

(CA3

case

c. Data Acquisition System

This section of the instrument amplifies the voltage sensed by the reference electrode, digitizes the resulting voltage and transfers the digitized data to the CPU under program control. The circuit is shown in Figure 1-7.

Three control signals are produced by the device select decoders and the timing pulses. Device code 56 is combined with IOP1, IOP2, IOP4 to generate commands CONV. CMD., READY and DATA IN CMD. respectively.

As shown in Figure 1-5, the voltage at the reference electrode is sensed by a follower amplifier. A CA3140 is used for its extremely high input impedance of $10^{12} \Omega$ and reasonably fast response (slew rate 8 V/ μ s). The voltage is amplified by a second CA3140. The amplification factor is selected manually with a rotary switch. The output voltage is fed to an absolute value amplifier which produces a positive output voltage for an input voltage of either polarity. After the conversion, the voltage V_{in} is fed to the sample and hold circuit in Figure 1-7. An HA2425 gated op amp was chosen to perform the sampling and holding of the voltage input, V_{in} . (An option is also available which uses a follower op amp (CA3140) instead of the absolute value amplifier.) In this case, two jumper wires on the ADC have to be adjusted

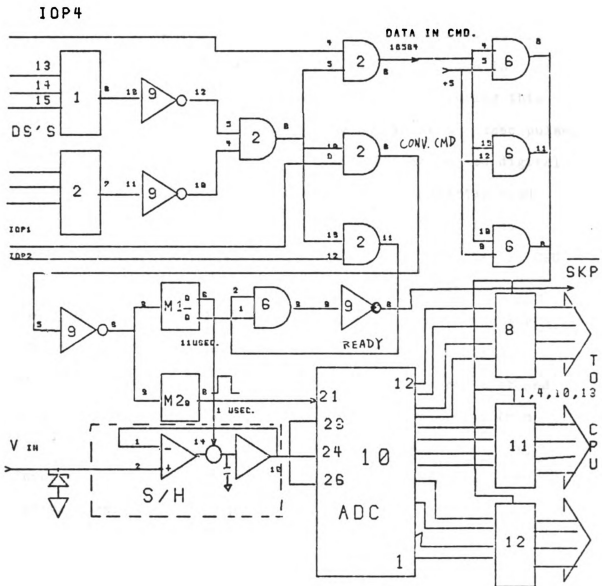


FIGURE 1-7. DATA ACQUISITION SYSTEM

accordingly to accommodate ± 5 V voltage range.)

When the data conversion command, CONV. CMD. is issued, two short controlling pulses are simultaneously generated by monostables, M1 and M2. M1 generates a 11 μ sec long pulse. This pulse is connected to the gate control of the sample and hold circuit. The output amplifier of this gated op amp is isolated from the input amplifier and the voltage is held at the same level by the holding capacitor during this pulse period. The other monostable M2 generates a 1 μ sec pulse. The falling edge of this pulse triggers the analog to digital conversion sequence of a A/D converter. The converter used is a ADC-12Z from DATEL, block 10. It takes 8 μ sec to do one conversion. The control signal READY is issued by the CPU during this period to check the status of M1. When the conversion is finished, \bar{Q} of M1 goes to HI. This makes the $\overline{\text{SKP}}$ line go LO and clears the flag bit of the control and status register of the DR11-C. The CPU acknowledges that and issues the DATA IN CMD. signal which latches the data from the ADC to three 4-bit data drivers (blocks 8, 11 and 12). These data are passed to the input register of the DR11-C and processed by the computer.

C. Performance of the Instrumental System

The most important performance factor for a coulometric instrument is the ability to deliver a precisely known amount of charge in a short time. Ideally, a current pulse of rectangular shape is generated by the pulse generator and the charge content of the current pulse is equal to the product of the pulse width and the current amplitude. However, several factors undermine the performance of the coulometric system, causing the system performance to deviate from the ideality. It is critical to determine these factors and evaluate their corresponding effects for the usage of such system.

1. Scope of the Instrument Performance

a. Pulse Generator

Although the timing pulses at the output of the timebase gate are the complete pulse cycles, the pulse width produced is not an exact integer multiple of μs . This is due to the delays caused by the output Flip-Flop and the logic gates. These delays increase the pulse width by $0.56 \mu\text{s}$. The shortest pulse produced is then $0.56 \mu\text{s}$.

b.

by

and

to

err

set

How

rel

amp

cha

app

in c

the

This

resi

impl

perc

inst

cha

The

the

the

sig

dis

b. Current Generator

The performance of the current generator is controlled by the digital to analog converter (DAC), the current switch and the operational amplifiers. Since the 12-bit DAC is wired to produce ± 5 V, the resolution is 2.4414 mV. The relative error caused by the resolution depends on the voltage setting. It increases as the voltage setting becomes smaller. However, since four current channels were implemented, the relative error can be reduced by switching from a higher amplitude current channel to a lower amplitude current channel. The current switch has an on-resistance of approximately $30\ \Omega$. The current limiting resistor is $2\ \text{K}\Omega$ in current channel 1. The on-resistance of the switch causes the current to drop by 1.5 % from the theoretical value. This error was offset using the matched current setting resistor. A current limiting resistor of $1961\ \Omega$ is actually implemented which reduces the error to within one half percent. The on-resistance of the current switch causes only insignificant error for other current channels. The other characteristic of the current switch is the switching speed. The typical value is 150 ns. The longer the current pulse, the less error is caused by the rise time limitation. When the current pulse is very short, this factor become more significant because the shape of the current pulse is distorted.

c.

am

Th

is

d.

a

The

dey

rec

and

sys

To

of

fol

any

the

tes

c. Operational Amplifiers

The slew rate and the settling time of the operational amplifier also affect the shape of the current pulse produced. These two effects are more significant when the current pulse is short.

d. Data Acquisition System

Since the analog to digital converter is wired to give a 10 V range, the digitization error is thus 2.4414 mV. The relative error contributed by the digitization error depends on the voltage to be measured. Its magnitude is reduced by the proper selection of the amplification factor and by the data averaging technique employed.

In summary, the current pulse produced by the coulостatic system is more ideal when the pulse width is not too short. To use a very short current pulse, the actual charge content of the pulse needs to be determined experimentally. In the following sections, the shapes of the extremely short, high amplitude current pulses are examined, and the results of the charge content determinations and the reproducibility tests are discussed.

2.

an

in

a.

dun

A t

ins

the

wit

fro

amp

the

Thi

is

pu

b.

a

a

2. Shapes of the Extremely Short Current Pulse

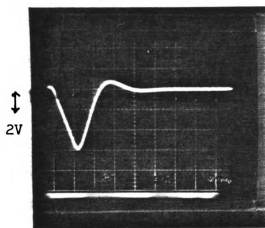
The extremely short current pulses were observed with an oscilloscope. The results of two such pulses are shown in Figure 1-8.

a. 0.56 μ s Pulse

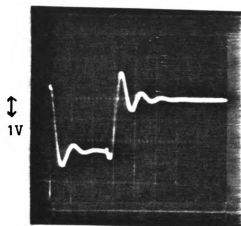
A 2.5 mA, 0.56 μ s current pulse was dumped into a dummy cell which consists of a 5 K Ω precision resistor. A triangular wave was observed as is shown in Figure 1-8 A instead of the expected square wave. The half-width of the pulse is 0.5 μ s. The peak height is only 6 V in contrast with the theoretical value of 10 V. This discrepancy comes from the relatively slow response of the buffer operational amplifier which is unable to drive the current pulse through the cell from 0 V to 10 V during the pulsing period. This pulse is not practical because the charge it carries is too small to be useful and the charge content of this pulse varies depending on the resistance of the cell solution.

b. 1.56 μ s Pulse

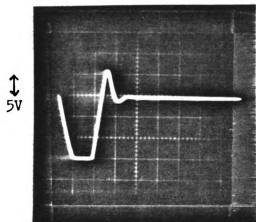
A 1.56 μ s long, 2.5 mA high current pulse was dumped into a dummy cell which consists of a 1 K Ω , 1 % resistor. The appearance of the wave is shown in Figure 1-8 B. The half-width



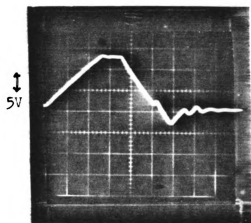
(A)



(B)



(C)



(D)

Figure 1-8. Shortest Pulses

of this wave is $1.56 \mu\text{s}$ and the amplitude is 2.5 V. Voltage ringing is present as a result of the sudden voltage change. The same current pulse was dumped into a resistor of $5 \text{ k}\Omega$. The result wave is shown in Figure 1-8 C. In this figure, the horizontal scale is $1 \mu\text{s}$ per division while the vertical scale is 4 V per division. A trapezoid is observed. The voltage ringing is still present but is reduced as compared with the previous wave. As the pulse width increases, the current pulse approaches that of an ideal square wave. Figure 1-8 D shows the voltage pattern observed at the input of sample and hold circuit after the voltage of Figure 1-8 B is amplified eight times. The horizontal scale is $0.5 \mu\text{s}/\text{div}$ as shown in Figure 1-8 B, while the vertical axis is $5 \text{ V}/\text{div}$. The distortion is quite obvious. This is because the operational amplifiers used for the amplification and voltage follower are the type CA3140 which have a slower response than the buffer operation amplifier. However, this distortion problem does not affect the data acquired because the fastest data rate is only $13 \mu\text{s}$ per datum point which allows sufficient time for these amplifiers to follow the voltage input.

3. Ch

a. De

In

gener

conte

calcu

ampli

of th

of th

pulse

relat

pulse

short

dummy

The v

The p

FTN a

progr

of th

QUANT

acqui

3. Charge Content of the Current Pulse

a. Dependence of the Pulse Charge Content on the Current Intensity

Since the current pulses produced by the current generator are not exactly rectangular in shape, the charge content of the current pulses are different from the values calculated using the equation $Q = \tau \times i$, where i is the amplitude of the current pulse and Q is the charge content of the current pulse of τ μ s long. Thus the charge content of the current pulses was determined experimentally. The pulse durations chosen for the following examples are relatively short, because the distortion of the current pulse becomes significant when the pulse width is very short.

A 0.01 μ F, 0.5 % precision capacitor is used in the dummy cell to store the charge carried by each current pulse. The voltage developed is measured under program control. The program used is called QUANT which consists of a FORTRAN. FTN and two subroutines QUANTM.MAC and AMP.FTN. The main program reads in the current channel to be tested, the name of the data file to be created and then calls the subroutine QUANTM to perform the discharging and the subsequent data acquisition. The amplification factors are manually selected.

7

8

T

c

t

cu

ca

1)

wi

Cuz

2.5

res

31.

thr

expe

equa

data

stan

devi

and

this

These factors are stored in the subroutine AMP.FTN and are retrieved by the main program to process the acquired data. The pulse command is issued by the operator. After each current pulse, an indicator light turns on which indicates that the processor is ready for the next pulse command.

Five pulses of different width were chosen for each current setting. Five current settings were examined each case. Each of the four current channels was examined.

1). Channel 1

Figure 1-9 shows the charge content vs. pulse width with current channel 1, using negative current pulses. Curves 5, 4, 3, 2 and 1 correspond to the amplitudes of 2.500 mA, 2.000 mA, 1.500 mA, 1.000 mA and 0.500 mA respectively. The pulse widths are 1.56 μ s, 7.56 μ s, 15.56 μ s, 31.56 μ s and 39.56 μ s. Each plotted point is an average of three data points from three separate runs of the identical experiments. The length of the data point in the figure is equal to twice the standard deviation associated with that data point. It seems that curve 2 carries the greatest standard deviation. With a 31.56 μ s pulse, the standard deviation is 3.3 %. With a 39.56 μ s pulse, it is 1.2 %, and within 1 % with others. Other experiments showed that this is not always the case.

1.0

CHARGE MICROCOUL.
V10 -5

0.00

Figure

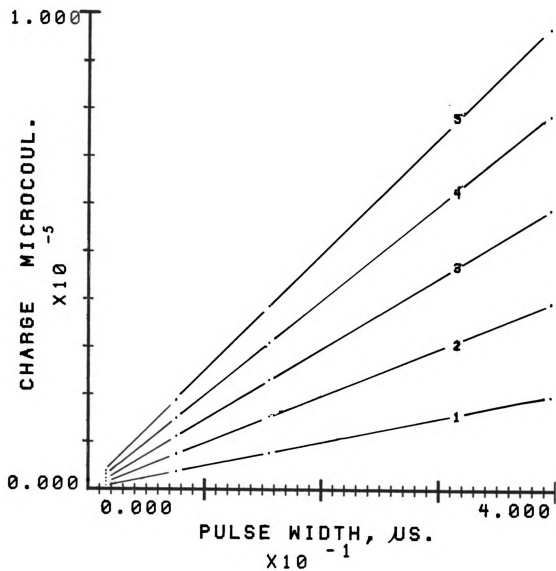


Figure 1-9. Cathodic Charging Curve with Current Channel 1

current

0.500

in the

point

is 3 %

include

specif

the s

per m

SCC s

Figure 1-10 shows similiar experiments with positive current pulses. The current amplitudes correspond to 0.500 mA, 1.000 mA, 1.500 mA, 2.000 mA and 2.500 mA in the order of curves 1, 2, 3, 4 and 5. The second data point on curve 3 shows the biggest standard deviation which is 3 %. Again good linearity is observed with every curve.

The slopes of these curves were calculated and are included in Table 1-1 and Table 1-2. A term called the specific charge content (SCC) is defined as the ratio of the slope to the current amplitude. The SCC is in nanocoul. per mA per μ s current pulse. For an ideal situation, SCC should be unity.

1.0

CHARGE MICROCOUL.
Y10⁻⁵

0.000

Figure

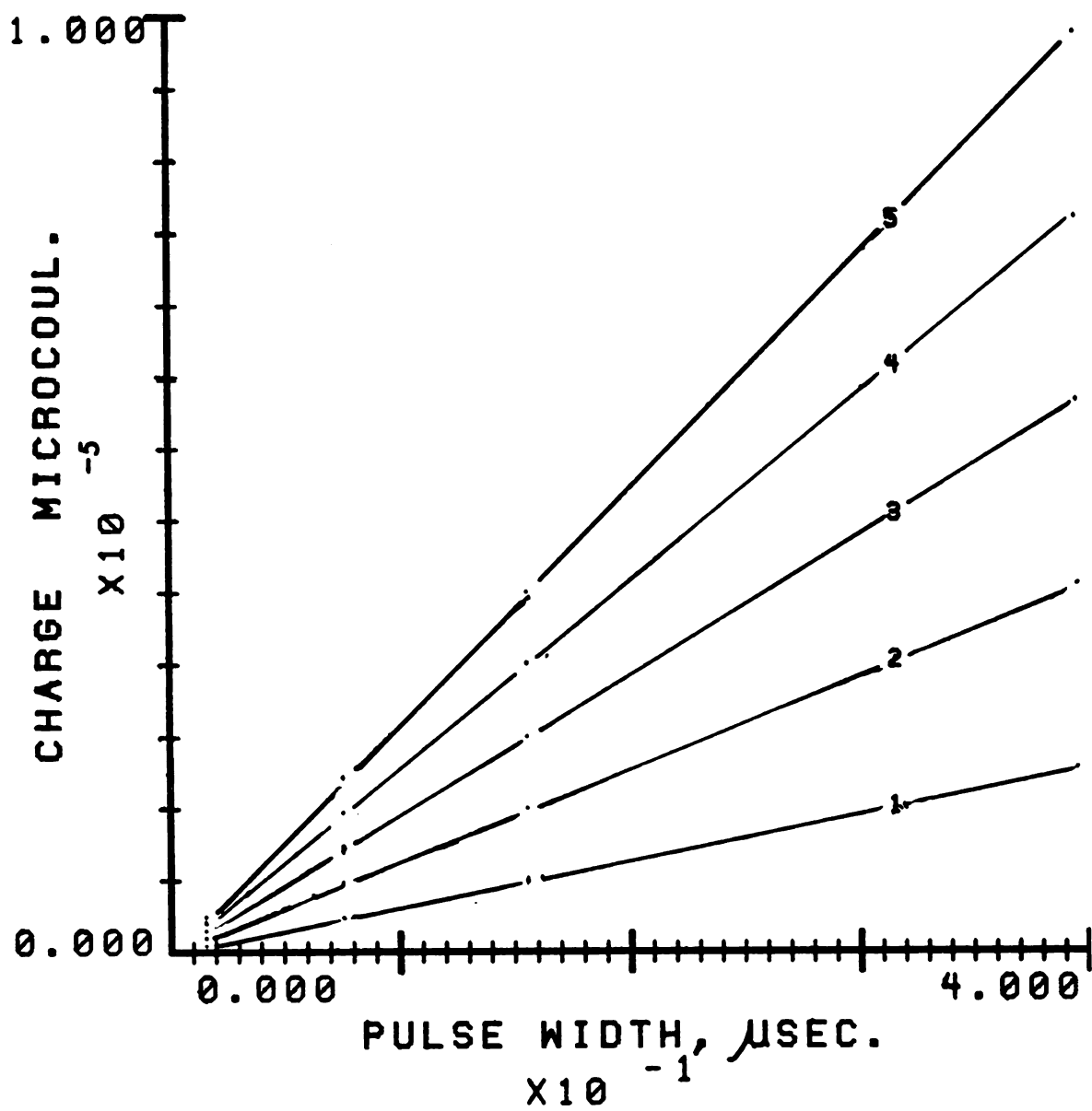


Figure 1-10. Anodic Charging Curve with Current Channel 1

Table 1-1. Slopes of the Pulse Charge Content
Channel 1. Negative Current

Current Amplitude mA	-2.500	-2.000	-1.500	-1.000	-0.500
Slope nanocoul/ μ s	2.4598	1.9748	1.4822	0.9863	0.4844
SCC nanocoul/ μ s-mA	0.9836	0.9870	0.9882	0.9862	0.9768

Average SCC = 0.9844 ± 0.0046

Table 1-2. Slopes of the Pulse Charge Content
Channel 1. Positive Current

Current Amplitude mA	0.500	1.000	1.500	2.000	2.500
Slope nanocoul/ μ s	0.4965	0.9896	1.4827	1.9772	2.4762
SCC nanocoul/ μ s-mA	0.9930	0.9886	0.9884	0.9896	0.9930

Average SCC = 0.9900 ± 0.00186

2). (

39.56

pulse

-1.00

-2.50

Table

pulse

1.000

2.500

Table

2). Channel 2

The pulse widths chosen for these experiments are 9.56 μ s, 39.56 μ s, 79.56 μ s, 149.56 μ s and 299.56 μ s.

Figure 1-11 shows the charge contents with negative current pulses. The current amplitudes are -5.00×10^{-2} mA, -1.000×10^{-1} mA, -1.500×10^{-1} mA, -2.000×10^{-1} mA and -2.500×10^{-1} mA. The slopes of these curves are shown in Table 1-3.

Figure 1-12 shows the charge contents with positive current pulses. The current amplitudes are 5.00×10^{-2} mA, 1.000×10^{-1} mA, 1.500×10^{-1} mA, 2.000×10^{-1} mA and 2.500×10^{-1} mA. The slopes of these curves are shown in Table 1-4.

8

:
 :
 :
 (
 (
 (
 (
 (
 (
 :
 :

1
2
3
4
5
6
7

0

Fig

CHANNEL 2

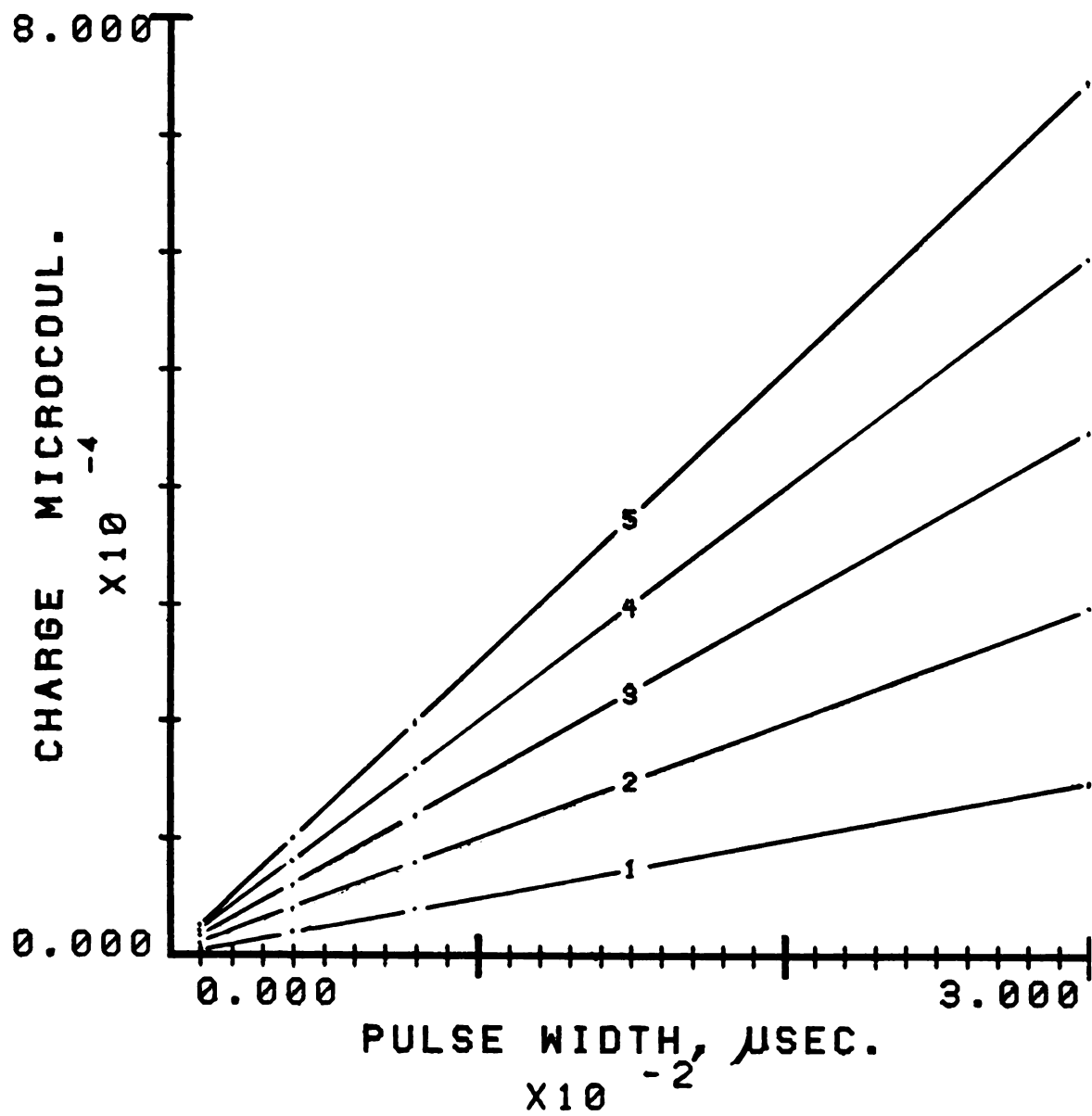


Figure 1-11. Cathodic Charging Curve with Current Channel 2

CHANNEL 2

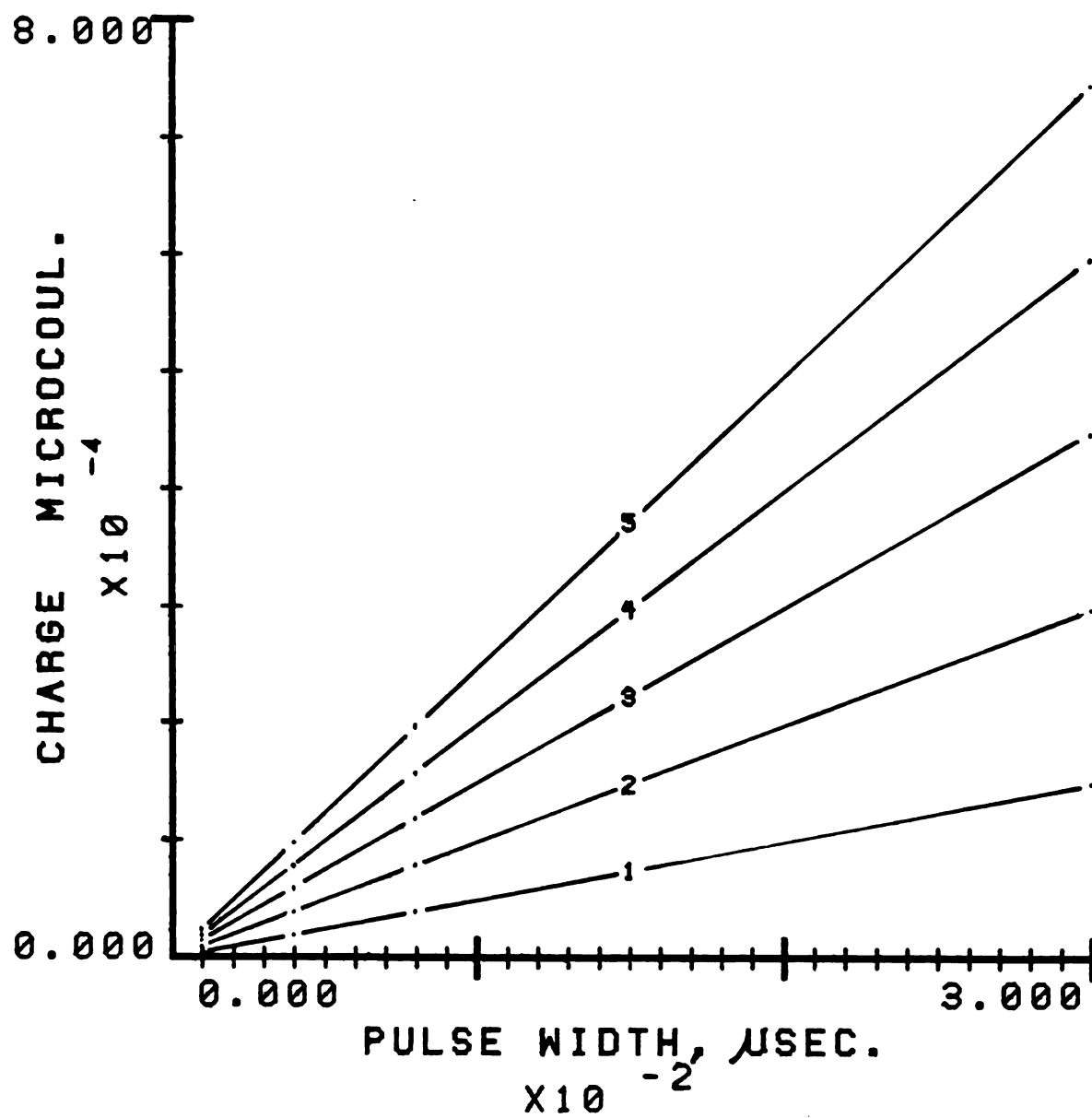


Figure 1-12. Anodic Charging Curve with Current Channel 2

Table 1-3. Slopes of the Pulse Charge Content

Channel 2. Negative Current

Current Amplitude uA	-250.0	-200.0	-150.0	-100.0	-50.0
Slope nanocoul/us	0.2474	0.1979	0.1484	0.09894	0.04947
SCC nanocoul/us-mA	0.9896	0.9896	0.9896	0.9894	0.9894

Average SCC = 0.9894 ± 0.0

Table 1-4. Slopes of the Pulse Charge Content

Channel 2. Positive Current

Current Amplitude uA	50.0	100.0	150.0	200.0	250.0
Slope nanocoul/us	0.04950	0.09903	0.1486	0.1980	0.2474
SCC nanocoul/us-mA	0.9900	0.9904	0.9906	0.9900	0.9900

Average SCC = 0.9910 ± 0.00002

3). (

and p

are \pm

± 2.0

9.56,

The s

in Ta

chann

3). Channel 3

Figure 1-13 and Figure 1-14 correspond to the negative and positive current pulses respectively. The current amplitudes are $\pm 5.000 \times 10^{-3}$ mA, $\pm 1.000 \times 10^{-2}$ mA, $\pm 1.500 \times 10^{-2}$ mA, $\pm 2.000 \times 10^{-2}$ mA and $\pm 2.500 \times 10^{-2}$ mA. The pulse widths are 9.56 μ s, 99.56 μ s, 499.56 μ s, 999.56 μ s and 1999.56 μ s. The slopes of the charge content vs. pulse width are listed in Table 1-5 and Table 1-6.

The findings are similar to those of channel 1 and channel 2.

5.00

CHARGE MICROCOUL.
X 10⁻⁴

0.00

Figure

CHANNEL 3

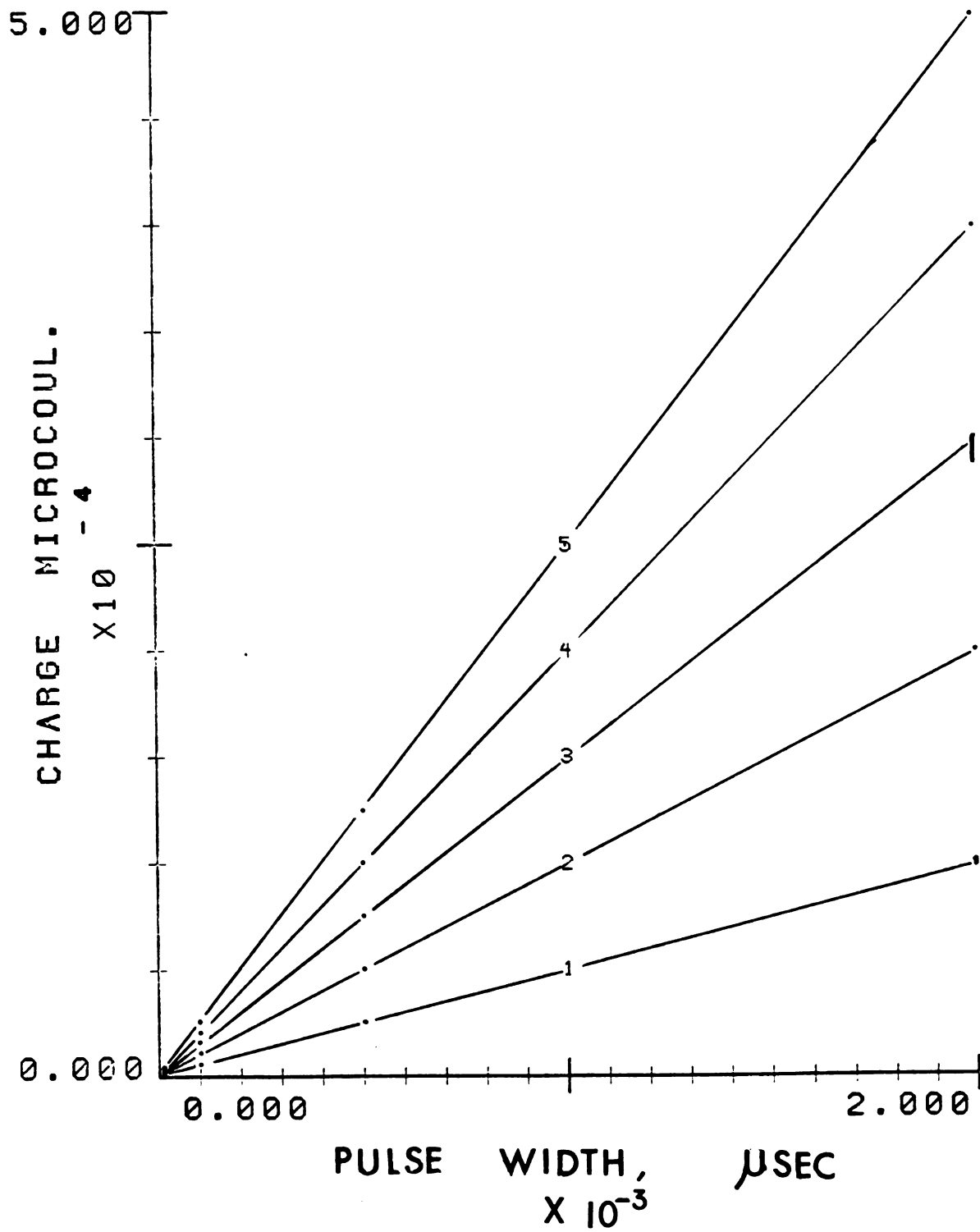


Figure 1-13. Cathodic Charging Curve with Current Channel 3

5.0

CHARGE MICROCOUL.

0.0

Figure

CHAN. 3

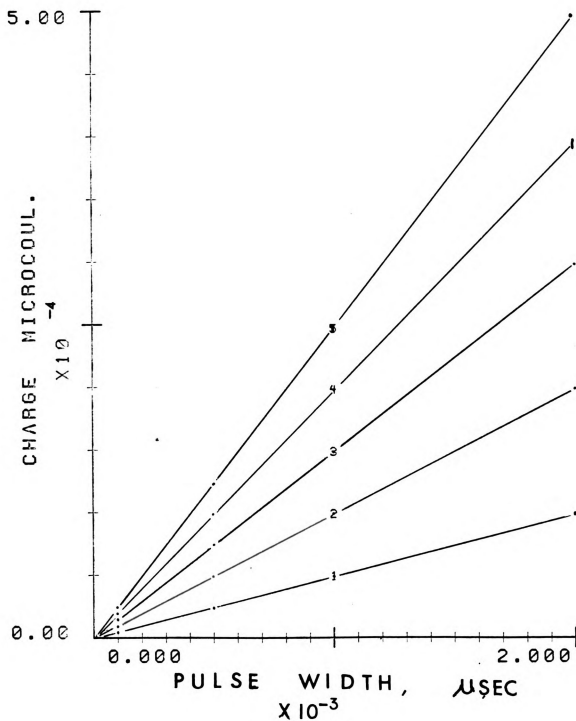


Figure 1-14. Anodic Charging Curve with Current Channel 3

Table 1-5. Slopes of the Pulse Charge Content

Channel 3. Negative Current

Current Amplitude μA	-25.0	-20.0	-15.0	-10.0	-5.0
Slope nanocoul/ μs	0.02472	0.01982	0.01484	0.00987	0.00493
SCC nanocoul/ $\mu\text{s-mA}$	0.9888	0.9910	0.9894	0.9870	0.9860

Average SCC = 0.9884 ± 0.00198

Table 1-6. Slopes of the Pulse Charge Content
Channel 3. Positive Current

Current Amplitude μA	5.0	10.0	15.0	20.0	25.0
Slope nanocoul/ μs	0.00498	0.00965	0.01470	0.01976	0.02474
SCC nanocoul/ $\mu\text{s-mA}$	0.9960	0.9650	0.9800	0.9880	0.9896

Average SCC = 0.9838 ± 0.0118

4).

999

-0.

A 1

sig

thr

At

bal

the

are

4). Channel 4

The pulses chosen are 49.56 μs , 99.56 μs , 499.56 μs , 999.56 μs and 3999.56 μs long. The current amplitudes are -0.500 μA , -1.000 μA , -1.500 μA , -2.000 μA and -2.500 μA . A log-log plot is used to display the data as in Figure 1-15.

The first two data points of each curve deviate significantly from the straight line drawn through the other three points. This is caused by the offset of the amplifier. At such level of charge quantity, the amplifier needs to be balanced very carefully. In addition, any stray charge from the environment affects the result significantly. The charges are in the range between 10^{-11} coul. and 10^{-9} coul..

0.

LOG CHANGE, MICROCOUL.

-6.0

Figure

POTENTIAL DECAY

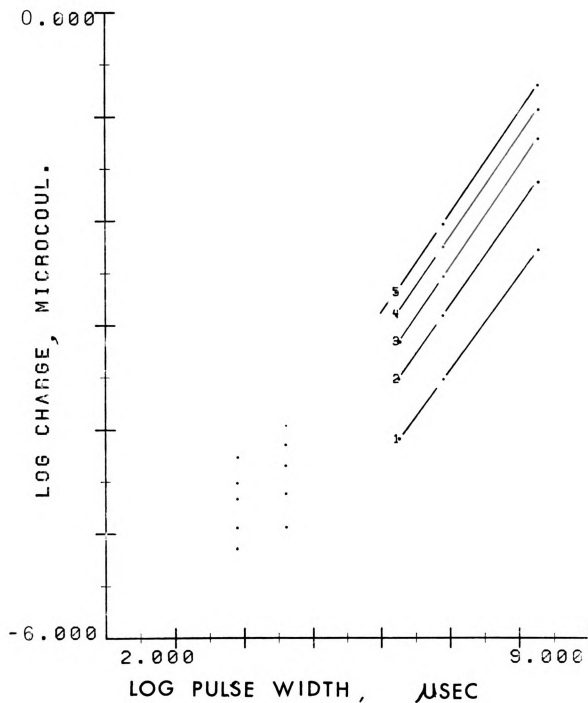


Figure 1-15. Cathodic Charging Curve with Current Channel 4

b. Dependence of the SCC on the pulse width

The data obtained in the previous sections are used to calculate the specific charge content for each pulse width.

The results are listed in Table 1-7 and Table 1-8.

Table 1-7 includes the results obtained using current channel 1.

Table 1-8 includes results obtained using current channel 2. and channel 3.

Table 1-7. Variation of the SCC with the Pulse Width for
Current Channel 1

P.W., μs I= mA	1.56	7.56	15.56	31.56	39.56	from ** slope
2.5	1.012	0.996	0.992	0.992	0.980	0.993
2.0	1.011	0.992	0.995	0.991	0.993	0.989
1.5	1.015	0.990	0.990	0.992	0.991	0.988
1.0	1.041	0.991	0.995	0.974	0.984	0.986
0.5	1.080	1.000	0.999	0.993	0.990	0.993
-2.5	0.988	0.989	0.993	0.993	0.993	0.983
-2.0	1.001	0.989	0.995	0.994	0.993	0.987
-1.5	1.001	0.976	0.990	0.993	0.993	0.988
-1.0	0.978	0.989	0.990	0.992	0.994	0.986
-0.5	0.954	0.989	0.983	0.994	0.996	0.977

100

162

Table 1-8. Variation of the SCC with the Pulse Width for

a) Current Channel 2

$\begin{matrix} P.W, \mu s \\ I, mA \end{matrix}$	9.56	39.56	79.56	149.56	299.56	from** slope
0.250	1.465	1.012	1.000	1.000	1.000	0.991
-0.250	1.000*	0.988	0.992	0.996	0.992	0.989

* This value is exceptionally high.

b) Current Channel 3

$\begin{matrix} P.W, \mu s \\ I, \mu A \end{matrix}$	9.56	99.56	499.56	999.56	1999.56	from** slope
25.0	0.1414	0.106	0.996	0.996	0.992	0.984
-25.0	0.0773	0.966	0.984	0.986	0.992	0.988

** obtained from section a

th

le

c. Reproducibility

The reproducibility of the system is generally quite good. A typical case is shown which utilized a 1.56 μ s wide, 2.5 mA current pulse. The set-up is the same as the charge content determination experiments. The results are listed in Table 1-9.

Table 1-9. Charge Produced by a 1.56 μ s, 2.5 mA
Current Pulse in nanocoul.

3.891	3.899	3.899	3.925	3.861
3.876	3.896	3.915	3.851	3.825

average = 3.884 \pm 0.03118 nanocoul.

The reproducibility of the pulse generator is better than 1 % for consecutive tests. Yet the long term drift is less favorable, approximately \pm 2 %.

3.

the

is :

of t

less

curre

aver

aver

to r

shor

resul

with

the

1 %,

cause

disco

A/D

reduc

stat

3. Discussion

No regular pattern of SCC variation was observed when the current amplitude was changed. This indicates that SCC is independent of the current amplitude and that the variation of the SCC is caused by other parameters.

Except for the very short current pulse, the SCC is 1 % less than unity, the average value is 99.2. With the shorter current pulse, the SCC value appears higher than the averaged value for the anodic pulse and lower than the averaged value for the cathodic pulse. Thus it is imperative to run calibrations along with the experiment when these short current pulses are used in order to obtain a more precise results. The SCC is used for the longer current pulse without significant error. Although the reproducibility of the current pulse in the consecutive run is better than 1 %, the instrument does show a long term drift. This drift causes the result to vary by approximately ± 2 %. It was discovered that most of the errors came from a defective A/D converter. With a new A/D converter, the error is reduced to below 1 %.

The error has two types, the systematic error and the statistical deviation. The systematic errors originated from

the

the

the

from

error

the

A de

be la

tech

tech

case

capa

± 2 .

can

with

as f

the

For

the

the calibration error and the non-ideal characteristics of the system. This type of error can be compensated for by the careful calibration work. The statistical error comes from the noise pick-up from the environment, the digitization error as well as other noise sources such as shot noise in the system. This type of error can be quite large.

A deviation of several percent is possible. Such error can be largely corrected by employing various data manipulation techniques, such as data averaging and data smoothing techniques. These techniques are quite effective, in many cases, in reducing the statistical errors.

In summary, the coulometric system constructed is capable of delivering current pulses as short as $1.56 \mu\text{s}$ at $\pm 2.5 \text{ mA}$. The charge content of current pulses delivered can be calculated for the current pulses over $10 \mu\text{s}$ long to within 1 % error. The potential variations can be followed as fast as $13 \mu\text{s}$ per data point. This data rate approaches the conversion time, $8 \mu\text{s}$, of the A/D converter used. For any faster application, both the pulse generator and the data acquisition system would have to be modified.

D. Application of the General Purpose Coulostatic Instrument

1. Determination of the Double Layer Capacitance and the Faradaic Resistance

The capacitance and the resistance of a dummy cell were determined with the coulostatic technique. The dummy cell as shown in Figure 1-1 A, consists of a 0.01 μF capacitor in parallel with a precision resistor which is either 100 $\text{K}\Omega$ or 200 $\text{K}\Omega$ and a resistor R_g which is 250 $\text{K}\Omega$.

A program called CAP3 was written to perform the experiments. This program is composed of a FORTRAN main program CAPF3.FTN, a MACRO subroutine CAPM3.MAC and FORTRAN subroutine LINFIA.FTN. The main program reads in the pulse width, pulse height data, data points to be fitted to an exponential equation and the name of the data file for storing the collected data, then it calls the subroutine CAPM3.MAC to deliver the current pulse and collect data. The first data is collected 10 μs after the pulse is initiated. One hundred data readings are collected at intervals of 39.38 μs . The logarithm of the collected data is calculated and fitted to a linear equation :

$$\log \eta_1 = \log \eta_0 - \frac{t_1}{R C}$$

w

v.

d.

ex

sm

a.

se

to

Cur

cur

1.0

a 1

3ac

dec.

to

Fig

acc

the

where η_1 is the potential at time t_1 , η_0 is the extrapolated value of η_1 at $t=0$. The capacitance C is calculated by dividing the charge of the pulse by η_0 .

Current channel 1 was used exclusively in the following experiments. Large amplitude current pulses as well as small amplitude current pulses are included for comparison.

a. Large Amplitude Current Pulses

Figure 1-16 shows the potential vs. time curve of several large amplitude current pulses. Curve 1 corresponds to the decay from a 3.56 μs long, -2.000 mA current pulse. Curve 2 corresponds to that of a 1.56 μs long, 2.000 mA current pulse. Curve 3 corresponds to that of a 1.56 μs long, 1.000 mA current pulse and curve 4 corresponds to that of a 1.56 μs long, 0.500 mA current pulse respectively. Each point represents a single data reading. The potential decay appears exceptionally smooth. These data were fitted to a linearized exponential equation and replotted in Figure 1-17. The capacitance and resistance are calculated accordingly. Table 1-10 lists the results obtained from these experiments plus some additional experiments.

8.0

MVOLT

0.0

POTENTIAL DECAY

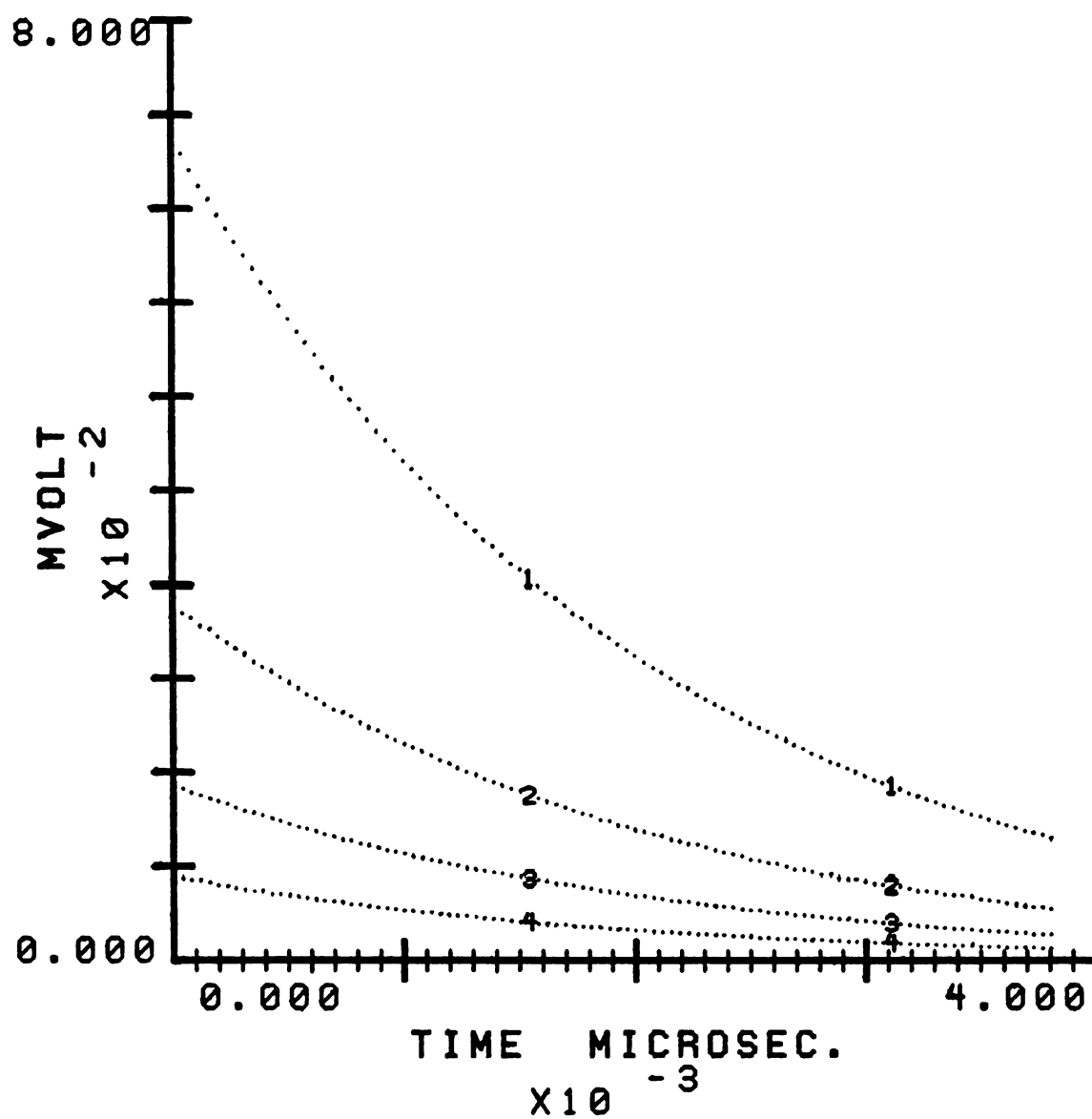


Figure 1-16. Potential Decay of a Dummy Cell with High Amplitude Current Pulses.

$C=0.01 \mu F$, $R=100 K\Omega$

8

MYC: T

0.

Fig 16

POTENTIAL DECAY

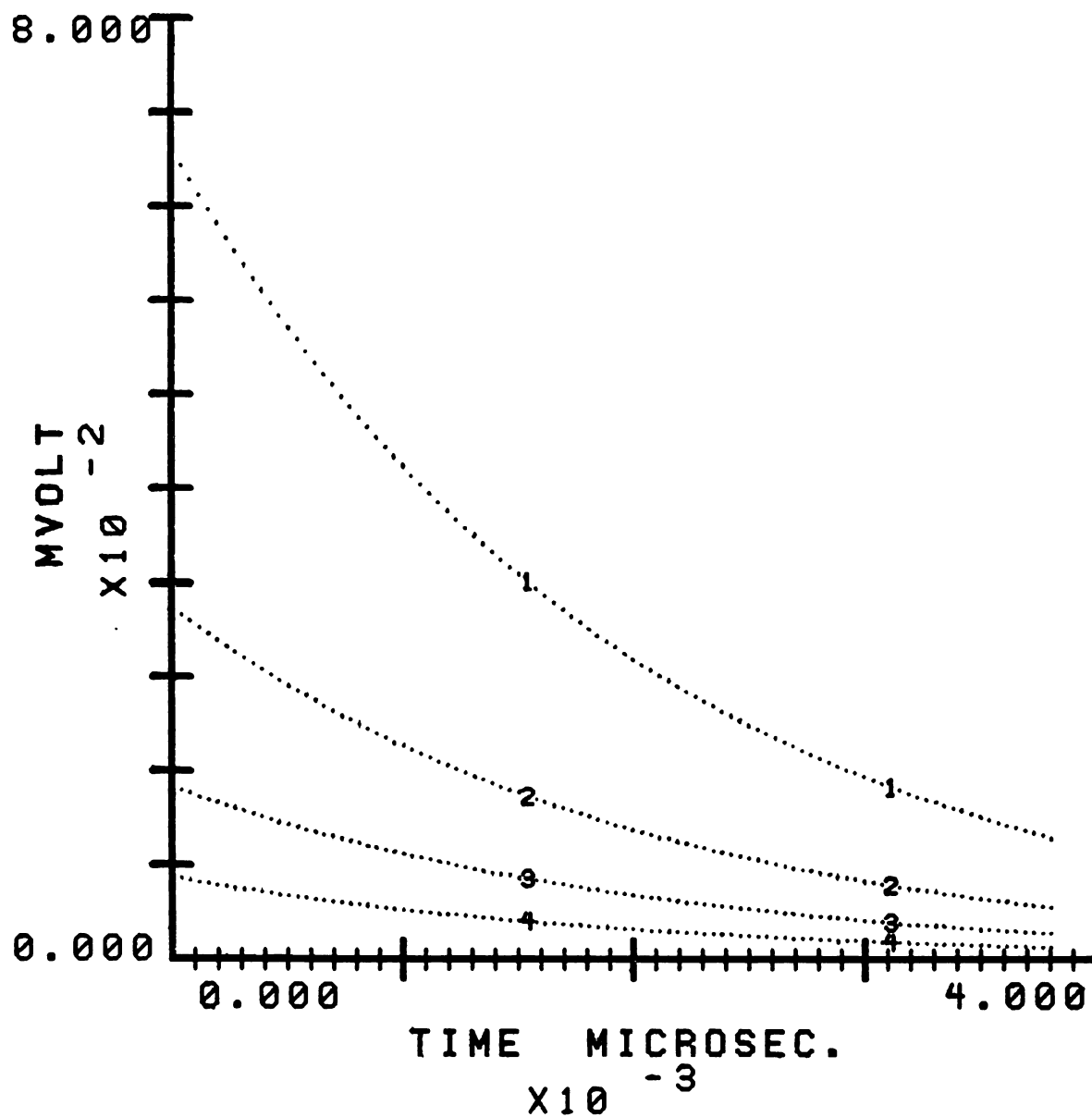


Figure 1-17. Curved Fitted Potential Decay of a Dummy cell
with High Amplitude Current Pulse.

$C = 0.01 \mu F$, $R = 100 K\Omega$

Table 1-10. Determination of Cell Capacitance and Faradaic Resistance with High Current Amplitude Pulse

Pulse Width μ s	1.56				3.56
Current Amplitude mA	2.000	1.000	0.500	-1.000	-2.000 -1.000
C _{exp} , μ F	0.01012	0.00999	0.00999	0.00985	0.01009 0.00990
R _{exp} , K Ω	97.6	103.45	103.45	101.35	99.53 101.55

C = 0.01 μ F , 0.5 %

R = 100 K Ω , 0.01 %

Note : No SCC correction was performed in these experiment

va

th

ca

wi

da

da

b.

pu.

a

a

ob

pu

cur

for

dis

for

In

The

no

av

The normal value of RC is $1.0 \mu\text{F-K}\Omega$. The experimental values with a $3.56 \mu\text{s}$ current pulse shows a better agreement than values obtained with a $1.56 \mu\text{s}$ current pulse. In both cases, the RC product agrees with the predicted value to within 3 %. With these high current amplitudes, the fitted data shown in Figure 1-17 completely overlaps the original data shown in Figure 1-16.

b. With Small Current Amplitude Pulses

The potential decay vs. time with small current amplitude pulses are shown in Figure 1-18. Curve 1 was obtained with a $1.56 \mu\text{s}$, $200 \mu\text{A}$ current pulse. Curve 2 was obtained with a $1.56 \mu\text{s}$, $100 \mu\text{A}$ current pulse, curve 3 and curve 4 were obtained with a $3.56 \mu\text{s}$, $-50 \mu\text{A}$ and a $1.56 \mu\text{s}$, $+50 \mu\text{A}$ current pulses respectively. These curves appear noisier than the curves obtained with higher amplitude current pulses. Except for curve 4, all the noise could be attributed to the digitization error. Since the amplification factor is 16 for all these data, the digitization error is $\pm 0.15 \text{ mV}$. In curve 4, the small data values are buried under the noise. The maximum voltage in curve 4 is 2.0 mV .

Two techniques were adopted to improve the signal to noise ratio of the collected data. One of them is signal averaging. Curve 5 in Figure 1-18 shows the result using

2.6

MVOLT

0.

Fl

POTENTIAL DECAY

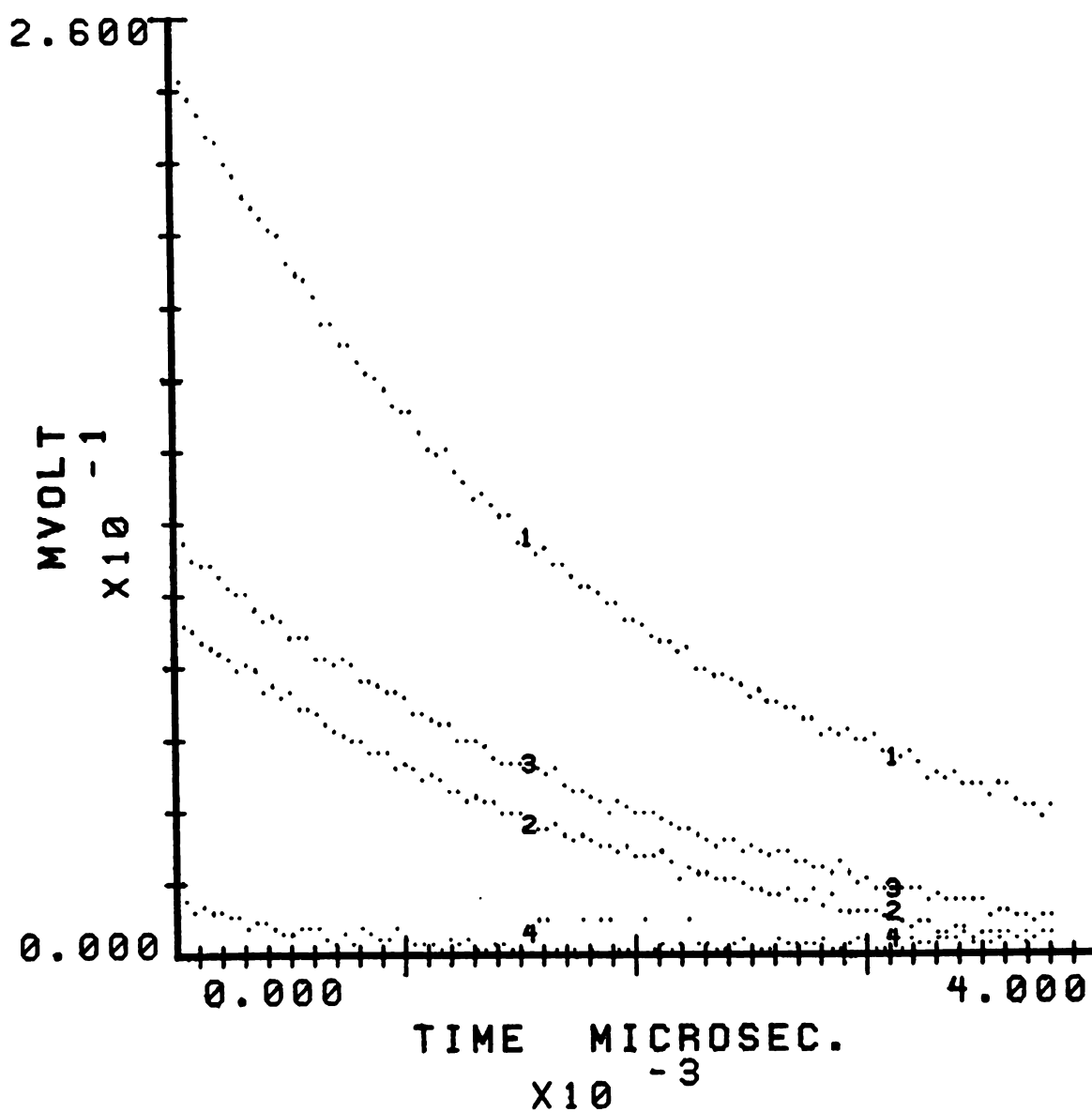


Figure 1-18. The Potential Decay of the Dummy Cell Using
Some Small Current Pulses

v
a
a
t

a
t
e
us

wi
re
me
ch
do

data averaging. A Fortran routine called AVG was written to do this job. Corresponding data from eight separate experiments were averaged together. The current pulse used was $2.56 \mu\text{s}$ long and $+50 \mu\text{A}$ high. The improvement is significant. The digitization error is greatly reduced. The second technique is to fit the equation to the linearized exponential equation using the first 20 points. The results are shown in Figure 1-19 with curves 1-4. The capacitance and the resistance of the dummy cell were calculated from these fitted data. Table 1-11 lists the results.

As the charge of the pulse become smaller, the capacitance and the resistance obtained experimentally deviate more from the correct values. This deviation comes from the inaccurate estimate of the real charge content in the current pulse used. Although in each successive run the charge content is within 1 %, it does drift over time. The accuracy of the resistance measurement relies on the accuracy of the capacitance measurement which in turn depends on the accuracy of the charge determination. The accuracy of the time constant, RC , does not depend on the charge determination.

POTENTIAL DECAY

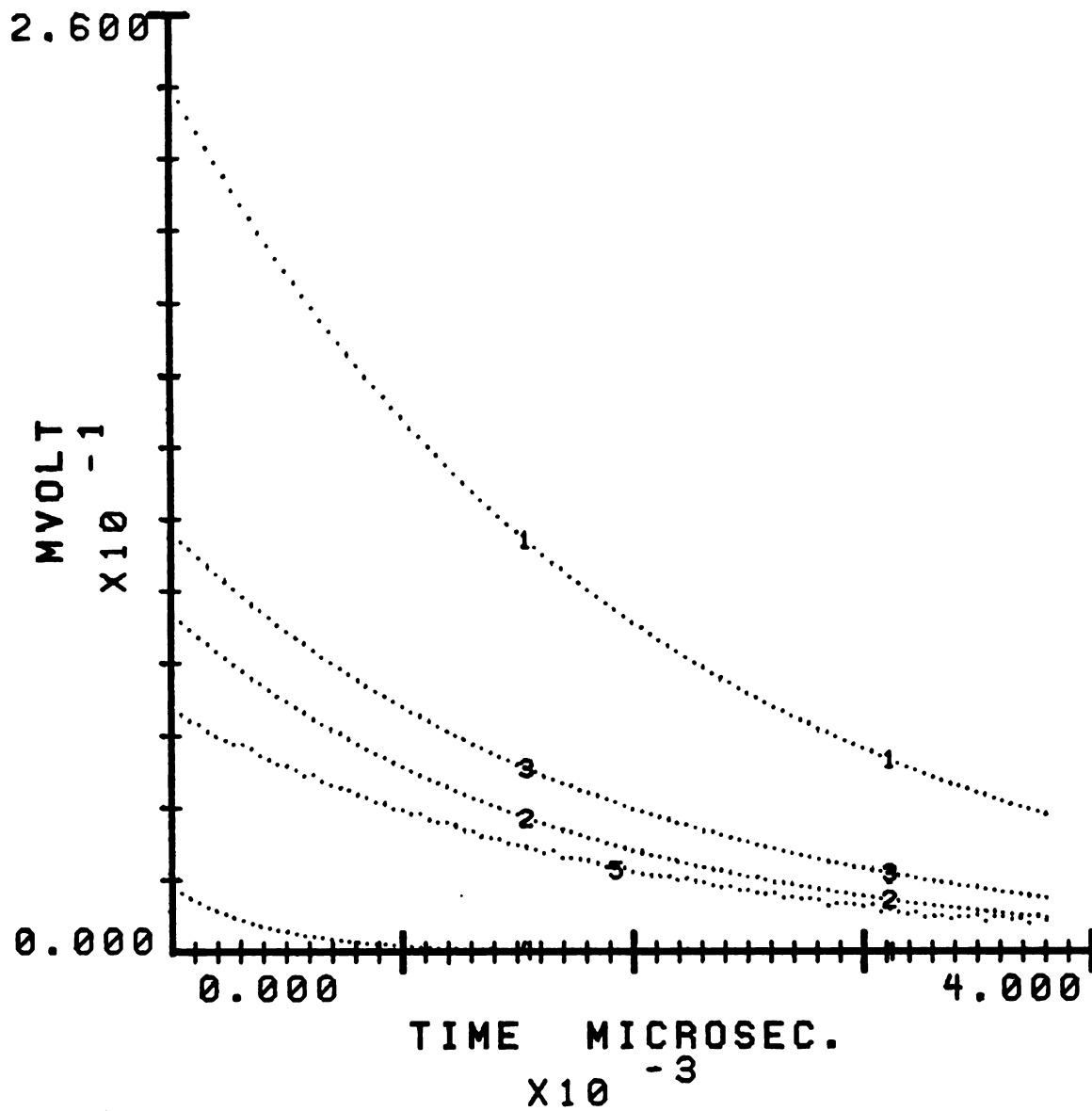


Figure 1-19. Improvement of the Data through the Curve
Fitting and Signal Averaging Technique

Table 1-11. Determinatio of Cell Capacitance and Faradaic
Resistance with Small Current Amplitude Pulses

		Pulse Width, μ s					
		1.56			3.56		
Current Amplitude μ A		+300.0	-300.0	100.0	-100.0	50.0	-50.0
RC		9.9868	9.655	8.482	10.07	10.67	9.279
C _{exp} , μ F		0.0104	0.00954	0.010280	0.00936	0.00793	0.00149
R _{exp} , K Ω		94.89	101.2	82.51	107.6	134.55	62.28

C = 0.01 μ F, 0.5 %
R = 100 K Ω , 0.01 %
(normal values)

Note : No SCC correction was performed on these data.

2. Po

perfo

This

the

requ

the

injec

retu

inst

the

call

from

pote

simpl

ampl

The

1-20

at t

the

the

caus

2. Potentiostatic Polarization with the Coulostatic Instrument

The potentiostatic polarization technique can be performed by the computer controlled coulostatic instrument. This is possible because the computer continuously monitors the potential of the electrochemical cell and makes the required adjustment in a very short time. A small shift of the potential value causes the computer to issue command to inject additional charge which forces the potential to return to the predetermined value.

The precision of the potential maintenance by this instrument relies on the electrochemical system as well as the algorithm of the program used for the purpose. A program called VDEPO was written for the deposition of the mercury from the mercurous perchlorate solution at a constant potential. The algorithm for the process control is quite simple. It uses a continuous cathodic current with varying amplitude. The potential to be maintained is 200 mV vs. R.H.E.. The variation of the potential vs. time is shown in Figure 1-20 a. A current pulse of very high intensity is applied at the beginning until the potential drops to 200 mV and then the current amplitude is reduced which eventually brings the potential back to about 400 mV. The anodic potential causes the computer to increase the current amplitude again.

7.0007

7.0007

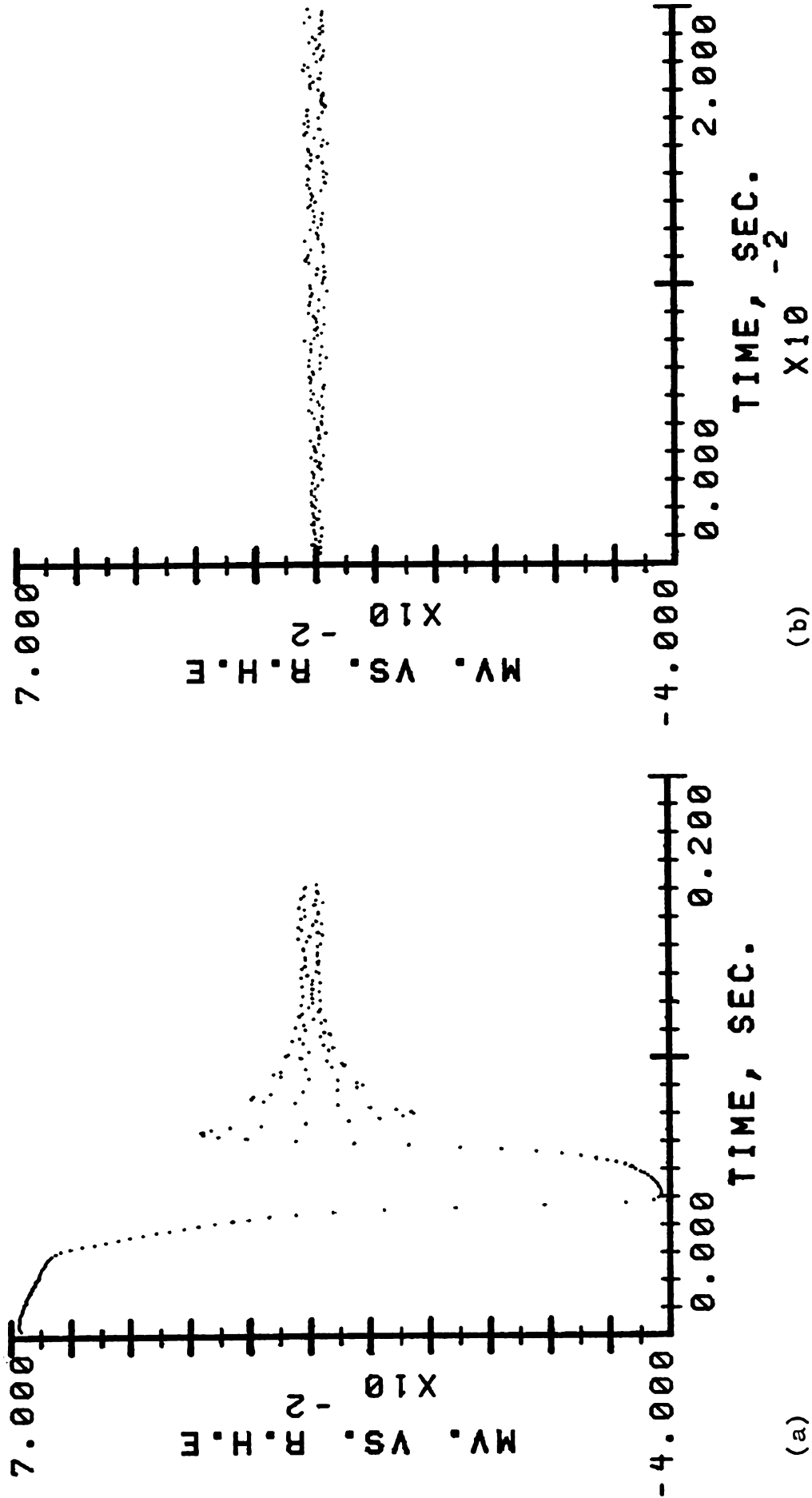


Figure 1-20. Simulated Potentiostatic Polarization by the Coulostatic Generator

The resulting potential shows a damped oscillation which converges to a constant value within approximately 0.1 sec. Figure 1-20 b, shows the same potential-time curve at an expanded scale during the 200 sec deposition period. The computer is able to maintain a fairly constant potential after it converges. The oscillation of the potential observed using this technique can be substantially reduced with a more sophisticated program. However, the program development is time consuming. Better results can easily be obtained with a regular inexpensive potentiostat if the special features of capacitance measurement, no IR error, quantized charge addition, and change in polarization technique in mid-experiment are not needed.

c
c
c
p
o
In
sp
te
te
ca
cal
Dur
red
the
sev
per
the
ste
con

CHAPTER II

INTRODUCTION TO THE STUDY OF THE MERCURY FILM ON PLATINUM

A. The Search for Mercury Film Electrodes

Despite the well-known problems associated with the environmental hazard, mercury has played and will still continue to play an important role in electroanalytical chemistry. One of the reasons is that mercury electrodes provide high sensitivity and reproducibility unmatched by other types of electrodes used for trace metal analysis. In many cases, the sensitivity is even higher than with spectroscopic techniques. This is demonstrated by the technique called anodic stripping voltammetry (48). In this technique, the mercury electrode is first kept at a selected cathodic potential for a predetermined time. This is commonly called the preconcentration step in the stripping analysis. During this step, the trace metal ion in the solution is reduced on or into the mercury. After preconcentration, the electrode is allowed to sit idle for some time, typically several minutes, without any current passing. After this period of time, the electrode is made anodic to dissolve the metals that had accumulated during the preconcentration step. By analyzing the resulting stripping response, the concentration of the metal in the original solution can be

s

F

i

M

t

me

se

pr

me

fo

Fi

determined. Successful determinations down to several picogram per ml concentration have been achieved (48).

The sensitivity achieved by this method depends on several factors : the experimental conditions during the preconcentration, the electroanalytical method adopted for the stripping step (49), and the electrode used.

One of the most commonly used electrodes for the stripping analysis is the hanging mercury drop electrode. However, detailed analysis of the stripping technique indicates that increasing the area to volume ratio of the mercury results in a significant improvement of this technique. This causes an increasing attractiveness of the mercury film electrode for application in stripping analysis.

The advantages of using mercury film electrode can be seen clearly by the following comparisons : During the preconcentration step the concentration of the interested metal in the mercury is given by equations (1) and (2) for HMDE (Hanging Mercury Drop Electrode) and MFE (Mercury Film Electrode) respectively (50).

where

inc

in

wit

the

ass

und

pre

thi

ele

$$(1) \quad C = \frac{3 I_L \tau}{4 \pi r_o^3 nF} \text{ mole/cm}^3$$

$$(2) \quad C = \frac{I_L \tau}{A l nF} \text{ mole/cm}^3$$

where I_L : limiting current in Amperes

τ : time of preconcentration in Seconds

r_o : radius of the mercury drop, typical value 0.5 mm

l : thickness of the mercury film, normally 1-100 μ m

n : oxidation state of the metal ion

F : Faraday constant

Under the same preconcentration process, this means an increase in concentration by two to three orders of magnitude in the thin film of one micron thickness as compared to HMDE with the same surface area.

There is also an advantage of the MFE in the duration of the rest period. Equations (1) and (2) are derived under the assumption that the metal distribution inside the mercury is uniform. This condition is met some time after the preconcentration is stopped. For an HMDE of usual dimensions, this uniformity is achieved approximately 200 sec after the electrolysis. With an MFE of 10^{-3} cm thickness, uniformity is

reach
perfo
for t.
mercu
might
metal
the r

the r
and co
is it.
quite
the t

other
with
chara
This
allow
and a
surfa
tradi
advan
stabi

reached to within 0.5 % in 3-4 sec. During stripping, the performance of these two electrodes is compatible except for the extremely thin mercury film. When an extremely thin mercury film is used, the dissolution of one metal element might be completely finished before the ionization of another metal with a close oxidation potential. This effect improves the resolution of this technique.

Since the film is built on some rigid, inert support, the resulting electrode provides good mechanical stability and could be used under severe conditions. One such example is its use under high speed rotation. This property is quite important during the preconcentration step to decrease the time needed to reduce a desired amount of metal.

The mercury film electrode could also be used in many other electrochemical applications replacing other electrodes with improved performance. Such electrodes exhibit characteristics similar to that of the mercury drop electrode. This includes the high hydrogen reduction overpotential which allows the observation of a wide range of cathodic processes and a good surface reproducibility of the reformable liquid surface. The MFE could be used in many applications traditionally performed by the dropping mercury with the advantage of easy electrode handling and good mechanical stability.

t
i
a

of
gl.
gra
(59

ele
The

an
that
Thes

but
rate
carb
show
resu

B. Mercury Film Preparation

To be a candidate for the supporting material for the mercury film, a material should possess several qualities : good electrical conductivity, wettability with mercury while maintaining chemical inertness toward mercury, and chemical inertness toward metals dissolved in the mercury. No material that has been used meets all these criteria. These materials include various constructions of graphite, silver, platinum and nickel.

The graphite based mercury film has drawn the attention of many researchers lately. The materials tested include glassy carbon (58), graphite-epoxy (55), wax impregnated graphite (WIG) (56, 57), and radiation cured polymer-graphite (59). The mercury film could be made extremely thin on these electrodes because the mercury forms no compound with carbon. The sensitivity is quite high with these electrodes. However, an examination of the films made on these electrodes showed that the mercury forms droplets instead of a smooth film (58). These electrodes are quite stable in basic or neutral solution but deteriorate quickly in acidic media. The deterioration rate depends on the construction of the electrode. The glassy carbon which is the most expensive among these electrodes shows the best stability (60). The reproducibility of the results is not good. This is not surprising knowing that the

dro

fil

dis

com

as

ana

sta

tha

and

1-3

6-8

that

with

resu

film

Oste

is c

The

amal

thic

film

seve

is e

droplets change sizes with the potential employed for film making (58).

Gold (51, 52) is readily wet by mercury. However, gold dissolves in mercury and forms a series of intermetallic compounds. The resulting film is thus not pure mercury and as such is useless for reducing other metals for stripping analysis. Using silver as a substrate, Zakharov and Trushina stated that the results obtained with mercury films thinner than 2 μm are irreproducible (53). According to Igolinskii and Stromberg (54), Silver electrodes with mercury films of 1-3 μm thickness gave reproducible results only during 6-8 sec after plating, while Gardiner and Rogers (6) reported that a few days of reproducible performance were obtained with 2-4 μm thickness film. These seemingly contradictory results reflect the fact that the property of the mercury film depends on the film preparation procedure. Stojek, Osterpczuk and Kublik (64) found that this irreproducibility is caused by the amalgamation of silver at the contact. The amalgamation rate of silver is greatly reduced as the amalgam thickness is increased. By controlling the thickness of this amalgam layer, they found that mercury films as thin as 0.1 μm gives reproducible results within several hours of preparation (62, 63, 64). This improvement is encouraging for the silver based mercury film electrode.

most

succ

merc

were

Under

wire

merc

the

with

surf

resu

Vand

in m

by i

merc

diff

type

with

sens

W

easy

on p

Platinum, due to its chemical inertness, has been the most widely used solid electrode material. It has been successfully used as the supporting material for stationary mercury electrodes (12, 13, 39, 40). Various approaches were utilized to make the mercury platinum contact. Underkofler and Shain (39) etched the tip of a platinum wire sealed in a piece of soft glass and then deposited mercury drop on it. Ramaley, Brubaker and Enke (13) plunged the electrochemically reduced platinum into a mercury pool without interrupting the current to wet the platinum surface with mercury and then deposit more mercury on the resulting platinum surface from mercuric nitrate solution. Vandeer Leest (40) merely immersed the platinized platinum in mercury pool. Moros (12) made the mercury platinum contact by immersing the platinum in sodium amalgam.

Provided that the contact is perfectly covered with mercury, the polarization curves obtained with such electrodes differ very little from those obtained with the HMDE. This type of electrode has been used for as long as two months with no detectable changes in its residual current or sensitivity (6).

While making a platinum supported hanging mercury drop is easy and reliable, the construction of a smooth mercury film on platinum is difficult. When a small amount of mercury is

dep

fou

Thi

mer

big

is

a l

pro

on

mad

mer

sati

ess

pre

at -

cons

cont

the

obta

occu

curre

same

Cox

from

solu

deposited on the platinum, mercury droplets are frequently found instead of the desired smooth mercury film (7, 10). This phenomenon causes no problem if a large amount of mercury is deposited because small droplets grow into bigger drops and eventually a coalesced mercury coating is formed. As long as the mercury coverage is complete, a large drop can form that should have electrochemical properties similar to the HMDE.

The success of making the smooth mercury film depends on some empirical step in the process. Marple and Rogers (7) made the mercury film by plating mercury from saturated mercuric nitrate followed by cathodizing the electrode in saturated potassium chloride solution. The last step is essential and must be repeated frequently. Neeb (10) prepared mercury plated platinum electrodes by electrolysis at -1.5 V vs. S.C.E. in 0.1 % $\text{Hg}(\text{NO}_3)_2$. The electrode obtained consists fine mercury droplets. By using the solution containing 0.005 % $\text{Hg}(\text{NO}_3)_2$, 0.5 M NH_4OH and 0.05 M EDTA at the same cathodic potential, a smooth mercury coating was obtained. At this potential vigorous hydrogen reduction occurs. Decreasing the cathodic potential to obtain a 100 % current efficiency for the mercury reduction reaction in the same solution produced mercury droplets. Hartley, Hiebert and Cox (14) employed a current of 10 mA/cm^2 to deposit mercury from a solution containing 0.05 M $\text{Hg}(\text{NO}_3)_2$ and 0.1 M HClO_4 solution to form mercury droplets. The electrode

w

w

me

of

de

re

Ma

wi

wou

One

met

rol

dep

cle

cle

elec

this

obta

of t

depe

and

was then subjected to a high cathodic current in 0.1 M HClO_4 with hydrogen gas generated by the electrode reaction. Smooth mercury films were observed.

Except for the Marple and Rogers' method, the success of these methods to produce smooth mercury film seems to depend on the large cathodic potential employed which greatly reduces the surface tension of the mercury droplets. In Marple and Rogers' method, two 1.5 volt batteries were used with saturated $\text{Hg}(\text{NO}_3)_2$ solution as electrolyte. The potential would have been quite cathodic at the working electrode. One other important but less apparent factor in the successful method is the conditioning of the platinum electrode. The role played by the KCl which was used before and after the deposition of mercury in Marple and Rogers' method is not clear. Hartley, Hiebert and Cox's method employed an electrode cleaned by dissolving the mercury deposited on the platinum electrode with hot nitric acid. The platinum surface obtained this way is quite different from the fresh platinum surface obtained by mechanical polishing. The surface after removal of the mercury appears spongy showing brown to black color depending on the degree of the reaction between the platinum and the mercury at the contact (17, 29).

mercu

that

mercu

in th

film

C. In

system

with

(14,

compo

polar

(13,

poten

vs. E

the

inter

respe

One problem associated with the creation of smooth mercury films by the induced merging of mercury droplets is that little control can be exercised at the interface between mercury and platinum. Ion or solvent molecules may be entrapped in the interface and thus affect the behavior of the mercury film electrode especially when thin films are employed.

C. Interaction Between Mercury and Platinum

The most undesirable property of the mercury-platinum system for making thin mercury films is that platinum reacts with mercury. This process proceeds at a significant rate (14, 17), and transforms deposited mercury into an intermetallic compound which cannot be used for stripping analysis purpose.

When the mercury coated platinum is subject to anodic polarization, three distinct processes can be identified (13, 15, 29). With constant current, Brubaker found three potential plateaus at 0.65 volt, 1.25 volt and 1.80 volt vs. R.H.E. which correspond to the ionization of the mercury, the ionization of the mercury from the mercury-platinum intermetallic compound and the oxidation of the solvent respectively.

the

exis

Surv

comp

PtHg

body

The

one

inte

it h

drop

slow

This

seve

D. A

F

thei

of c

cad-

maxi

Studies on the mercury-platinum system indicate that the intermetallic compound between platinum and mercury exists in many forms. An X-ray study by Plaskin and Survorovskaya (19) found three phases of the intermetallic compound with structures corresponding to PtHg , PtHg_2 , and PtHg_4 . The crystal structure of PtHg_4 was identified as body-centered cubic with ten atoms in one unit cell (31). The structure of PtHg_2 is tetragonal with three atoms in one unit cell. Only one stoichiometry has been found at the interface between the platinum and mercury metal (15, 33, 41); it has the structure of PtHg_4 .

Judging from the long life of the platinum-based mercury drop electrode, the mercury-platinum reaction rate must slow down as the intermetallic compound layer thickens. This view has been confirmed directly or indirectly by several studies (13, 14).

D. Additional Problems with Platinum-Based Mercury Thin Film Electrode

Gardiner and Rogers (6) used the thin mercury film for their anodic stripping analysis to determine the concentration of cadmium and discovered that the recovery of the reduced cadmium determined by the stripping current peak reached a maximum value until the film thickness reached $1\text{ }\mu\text{m}$. No

C

S

M

S

W

B

T

B

M

E.

SU

pr

of

pr

st

wh

of

wit

explanation was given for this phenomenon.

Kemula, Kublik and Galus (9) discovered that when the stripping analysis of Cd and Zn was performed with a hanging mercury drop and a thin mercury film electrodes, Cd was stripped off at the same potential from both electrodes while the Zn peak was missing with the film electrode. The behaviors of antimony and tin were found analogous to zinc. These authors suggested that intermetallic compounds formed between platinum (or the Pt-Hg compound) and these metal might be responsible for such behavior.

E. Objective of the Study

To summarize, mercury film formation on the platinum surface is dependent on the surface state of the platinum prior to the mercury deposition. Understanding of the nature of this relation paves the way for devising effective procedures for film formation. This is essential for the study of the formation for the platinum-mercury system in which a growing layer of intermetallic compound exists.

The objective of this study is to correlate the nature of the film formed and the surface state of the platinum with the aim of devising an effective process for constructing

reproducible and smooth mercury films, and to determine the rate of the intermetallic compound formation so that a sound prediction may be made on the conditions under which the mercury plated platinum electrode can be effectively used.

A.

used

enp

in

Erub

merc

A m

the

acco

sur

The

the

of

sur

fir

CHAPTER III

EVALUATION OF THE FACTORS AFFECTING THE STRUCTURE OF THE MERCURY ELECTROPLATED ON THE PLATINUM SURFACE

A. Platinum Surface State Characterization

As discussed in the preceding chapters, the processes used for making mercury coated platinum have been largely empirical. The success of obtaining a good mercury coating in each attempt depended on chance as was observed by Brubaker. If any kinetic data is to be drawn on the mercury-platinum interaction, this situation must be avoided. A method of making a smooth reproducible mercury film on the platinum surface has to be found. To be able to accomplish this, a good understanding of the platinum surface under the experimental conditions is necessary. The dependence of the structure of the mercury deposit on the surface states of the platinum and the other conditions of the experiment has to be determined. The effect of the surface state of the platinum electrodes will be considered first.

1.

gr

pl.

pl.

su

fo

the

As

res

und

has

thi

the

and

be

pla

and

is

sur

nat

it

pla

1. The Characterization of the Surface State of Platinum

The electrochemical behavior of a platinum electrode is greatly influenced by the treatment performed on the platinum. For instance, the catalytic activity of the platinum is found to be greatly increased after it has been subjected to anodic-cathodic cycling. This phenomenon was found decades ago (3) and was attributed to the removal of the impurities irreversibly adsorbed on the surface.

As a consequence of the great interest shown by numerous researchers on platinum in the past several decades, our understanding of the electrochemical behavior of this metal has been improved (8). The electrochemical properties of this metal are dependent on its surface structure (36), the preparation (1), the electrolyte solution used (2), and the process being carried out (8).

A description of the state of the platinum surface can be divided into the chemical and physical aspects. The platinum surface exposed to the air always has an oxide film and this is one of the reasons that this type of platinum is not in the active state. Mercury can't wet this type of surface even after a long time of contact (49). Although the nature of the surface oxide is still controversial (8), it is generally agreed that the adsorption of oxygen on the platinum surface in the anodic process is irreversible,

th
be
th
ma
co
th
ea
on

wit
nat
on
is
pla
amo
str
fac
pol
ele
is
pla
on
to
rec
sur

that the irreversibility increases as the potential applied becomes more anodic, and that oxygen is capable of entering the platinum crystal lattice (18). When the potential is made cathodic enough, the platinum electrode surface is covered with an adsorbed layer of hydrogen. In contrast to the oxide film, the adsorbed hydrogen film can be removed easily. The adsorption and the ionization of the hydrogen on and from the platinum surface is a reversible process.

The physical state of the platinum surface is associated with its physical structure on the surface. Although the nature of the dependence of the electrochemical properties on the physical state is not fully understood, the importance is well recognized. For instance, the activity of the platinum surface for hydrogen adsorption was found to vary among different crystal planes. The control of the physical structure of the platinum is difficult. Platinum forms a face-centered cubic crystal. Both single crystal and polycrystalline platinum electrodes have been used in electrochemical studies. The polycrystalline platinum which is most commonly used is composed of numerous grains of platinum crystallites. Several grain boundaries are exposed on the surface. As the initial step, the platinum electrode to be used in the electrochemical study is commonly polished mechanically or electrochemically in order to create a fresh surface. This process creates a microscopically rough

s

t

E

v.

ti

of

qu

su

be

2.

nee

of

rep

may

on

and

bee

of

ele

inc

of

ele

ber

surface. The surface actually exposed is always larger than the geometric area. The ratio of the actual area to the geometric area is called the roughness factor. This value varies from almost unity for a very smooth surface to several thousand for platinized platinum (24). The most common method of measuring the actual surface area is to measure the quantity of charge required to completely cover the platinum surface with hydrogen atoms. One hydrogen atom is assumed to be adsorbed by one surface platinum atom (4, 21).

2. Effects of Pretreatment on the Surface State of Platinum

After the initial mechanical polishing, it is always necessary to pretreat the platinum surface by a combination of chemical and electrochemical methods in order to obtain reproducible results from the platinum electrodes. The major concern is to remove any trace of impurities adsorbed on the platinum surface. Various processes have been proposed and according to their promoters, reproducible results have been obtained (1, 2, 17). These processes in general consist of a cleaning step followed by a treatment step which includes electrochemical oxidation and reduction. In spite of our incomplete knowledge of the platinum oxidation process, most of these methods prescribe a strong oxidation. The platinum electrodes from different treatment methods show different behavior. If the platinum is cycled between the anodic and

cat

inc

sur

Man

Dur

sur

and

app

cat

red

sur

wou

pla

of

wit

was

ele

3.

is

thr

cathodic potentials, the resulting electrodes show an increase in catalytic activity (3). In addition, the platinum surface is altered by the anodic-cathodic cycling process. Many observers obtained a smoother platinum surface (23, 24). During the anodic cycle, the platinum at the electrode surface is oxidized. A certain amount of platinum is ionized and dissolved in the solution which depends on the potential applied and the electrolytes used. During the following cathodic cycle, part of the dissolved platinum ions are reduced. Thus many observers reported that the platinum surface was platinized by the potential cycling process (5, 25).

The reduction of the oxide film on the platinum surface would also be obtained without the occurrence of surface platinization (1, 5). F. Anson (5) reported that the reduction of the oxidized platinum with hot 12 M HCl produced platinum without forming platinization. This type of platinum surface was named "stripped platinum" to differentiate it from the electrochemically reduced surface, "red platinum".

3. Classification of Platinum Surface According to the Surface Roughness Factor

The electrochemical behavior of the platinum electrode is greatly affected by the platinum surface state. At least three factors concerning the surface roughness influence the

str

ac

dis

pro

It

to

sur

a.

b.

c.

app

in

eff

of

by

structure of the mercury deposit formation, namely the activity of the surface platinum, the local electrical field distribution on the platinum surface during the deposition process and the crystal structures of the platinum surface. It is logical to classify the platinum surface according to roughness factor in the study of the effects of the surface state on the mercury film formation.

Three types of surface can be differentiated :

- a. Bright platinum. This type of surface is characterized by a small roughness factor, typically between 1 and 2.
- b. Lightly platinized platinum. The platinum in this category has roughness factors ranging from 3 to well over 10.
- c. Heavily platinized platinum. The platinum surface in this class has a high value of the roughness factor, typically between 100 and several thousands.

From the discussion that follows in this chapter, it is apparent that the roughness factor is an important factor in characterizing the state of the platinum surface. Its effects on the mercury deposition are examined. The effects of the surface tension on the mercury deposition as suggested by Hartley, Hiebert and Cox (14) and real role of potassium

ch.

B.

two

pot

phy

dep

mer

sur

rou

as

mer

a v

0.1

pot

mer

abc

of

sta

chloride during the mercury plating are also discussed.

B. Methods of Examining the Smoothness of the Mercury Film on the Platinum

The smoothness of the mercury deposit is examined by two methods : microscopic examination and analysis of the potential-time behavior of the resulting electrode. The physical shape of a thin coating of electrochemically deposited mercury is examined under a microscope. If the mercury coverage of the surface is complete, the resulting surface looks like a mirror. Otherwise, the surface appears rough. With a 10X object lens, mercury drops with a size as small as two microns can be resolved.

The platinum surface which is completely covered with mercury shows a very large hydrogen overpotential even with a very thin mercury film. With a platinum electrode in 0.1 M HClO_4 electrolyte, hydrogen evolves vigorously at potentials more anodic than -0.1 V vs. R.H.E. With smooth mercury film electrodes, no hydrogen evolution is detected above -0.6 V vs. R.H.E. The cathodic hydrogen overpotential of a mercury plated platinum electrode varies with the states of the mercury coverage.

C.

1.

a.

sol

use

aci

the

whi

des

net

con

dis

mer

hav

was

Hg(

was

use

C. Experimental Set-Up

1. Chemicals

a. Mercury Solution

Mercury forms ions with two common oxidation states in solution. Both mercuric and mercurous solution have been used as the plating solution for mercury. Since in perchloric acid solution, no significant difference is expected in the choice of the oxidation state of the mercury ion from which to plate. In the study of the film making process described in this chapter, mercurous ion was used exclusively.

Mercurous perchlorate was prepared following Pughe's method (22). Reagent grade mercuric oxide was dissolved in conc. perchloric acid. The solution was shaken with triply distilled mercury which converted all mercuric ion into mercurous ion. The solution was filtered and diluted to have 0.1 M in Hg_2^{++} and 0.1 M in perchloric acid. The solution was stored in brown bottles. No disproportionation of the Hg(I) ion was detected after several months of storage.

The exact concentration of the mercurous perchlorate was determined by a gravimetric method. Sodium chloride was used to precipitate the mercurous ion. The precipitate was

f

T

b

24

th

is

gr

ne

su

is

ac

for

fiv

ele

wit

sur

rea

of

desc

filtered and dried at 110°C for an hour before weighing.

The concentration was found to be 0.107 M.

b. Platinum

The platinum electrode is made by sealing a piece of 24 guage platinum wire in soft glass tubing so that only the cross-section of the wire is exposed. The platinum is reported to be 99.9 % pure.

The tip of this platinum wire is polished with 600 grit silicon carbide polishing paper each time before a new mercury deposition in order to have a fresh platinum surface unless noted otherwise. After polishing, the electrode is cleaned by dipping it in boiling concentrated perchloric acid briefly. The electrode is then etched in hot aqua regia for one minute or in room temperature aqua regia for over five minutes to amooth the surface. A bright platinum electrode is obtained by reducing the resulting electrode with hot 12 M HCl or with reducing current. The platinum surface obtained after this step is free from oxide and is ready for the electroplating of mercury. The geometric area of this electrode is $2.5 \times 10^{-3} \text{ cm}^2$.

The preparation of the platinized platinum will be described in the experiment section. A series of oxidation-

c

pl

of

En

th

wi

wor

d.

rea

e.

l F

f.

oxid

reduction cycles achieved by means of alternating current steps are employed.

c. Gases

The working solutions are deaerated by bubbling purified H_2 gas or N_2 gas through the solution. Purification of the H_2 gas is done with a catalytic column produced by Englehard Industries. The residual oxygen content is less than 1 ppm. The N_2 gas from the gas cylinder is deoxygenated with a hot copper catalytic column. Before going into the working solution, gases are saturated with water.

d. Perchloric Acid

The 0.1 M perchloric acid is made by diluting 70 % reagent grade perchloric acid.

e. Sulfuric Acid

The platinization of the platinum is carried out in 1 F H_2SO_4 . Reagent grade H_2SO_4 is used for dilution.

f. HCl

Reagent grade 12 M HCl was used to reduce the surface oxide.

2.

of
dro
thi

3.

a.

sur
for
exp
mer
Tef
wor
for
per
ele

and

and

2. Microscope

A microscope from Bausch and Lomb is used for inspection of the mercury deposits. A 10X object lens is used. Mercury droplets with diameter of 2 microns can be resolved under this condition.

3. Flow Cell

a. Construction

It was suggested by some workers that the platinum surface could not be considered clean after exposure to air for as brief a time as two seconds (8). To prevent the exposure of the treated platinum to the air before the mercury deposition, a flow cell made of pyrex glass and Teflon stopcocks has been used. With this flow cell, the working solution is switched from the perchloric acid used for electro-cleaning of the electrode to the mercurous perchlorate used for plating mercury without exposing the electrode to the atmosphere.

The flow cell is composed of two solution reservoirs and a reaction chamber as shown in Figure 3-1. The reservoirs and the chamber are connected by a two way Teflon stopcock.

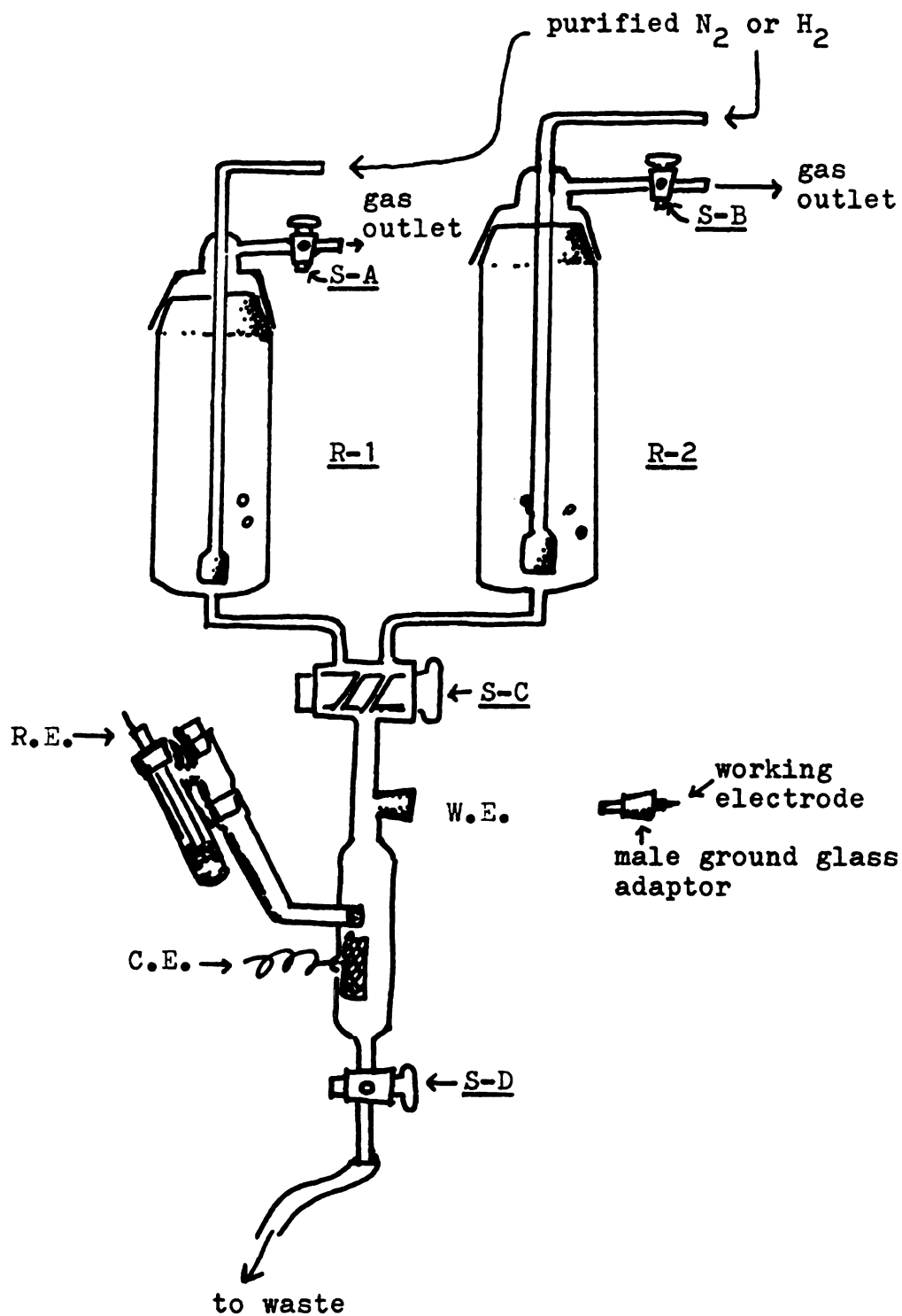


Figure 3-1. Flow Cell

One

At

gla

wit

be

coun

char

from

of

to

b. P

the

volu

from

elec

dead

rese

the

air-

chan

by

One solution is allowed to enter the chamber at a time. At the top of the reaction chamber, an adapter made of ground glass is constructed so that the working electrode (sealed with silicon rubber in a male ground glass adapter) could be inserted. A platinum wire mesh, which serves as the counter electrode, is sealed at the lower part of the chamber. The reference electrode compartment is isolated from the chamber by a medium pore glass frit. The diameter of the chamber at the working electrode has been minimized to reduce the solution dead volume.

b. Performance

The most important parameters of the flow cell are the dead volume and the dead time. These are the solution volume and the time needed for the solution to be transported from the bottom of the solution reservoir to the working electrode. The dead volume is 0.65 cm^3 for this cell. The dead time varies slightly with the solution volume in the reservoir. It is determined primarily by the orifice at the exit stopcock. The typical value is 0.25 second.

It is critical that the reaction chamber must be air-tight, allowing no air oxygen to diffuse into the chamber during the experiment. The performance is examined by measuring the potential variation with time as is shown

in

The

bubb

oper

is a

the

B by

decr

of

sudd

at

cal

read

stop

unc

to

S-D

cha

inc

con

Fin

all

S-D

in the experiment described below and in Figure 3-2.

The solution was exposed to the air prior to point-A. The potential was quite anodic. Then hydrogen gas was bubbled through the reservoir R-1 solution with stopcock S-C open to this reservoir. The gradual decrease in potential is a noticeable indication that H_2 molecules diffused into the reaction chamber. The solution flow was started at time B by opening the exit stopcock S-D. This produced a sharp decrease of potential which indicated that the concentration of H_2 molecules at the working electrode surface was suddenly elevated. The potential stabilized quickly as shown at time D. The value of the potential agrees with the value calculated by the Nernst equation for the H_2 reduction reaction. The chamber was isolated by closing both entrance stopcock S-A and exit stopcock S-D. The potential remained unchanged over tens of minutes. The stopcock S-A was opened to reservoir R-2 which was bubbled with N_2 and the stopcock S-D was opened allowing the N_2 bubbled solution to enter the chamber and replacing the H_2 saturated solution. The gradual increase of potential was observed indicating that the H_2 concentration at the working electrode surface was diminishing. Finally, the reservoir was exposed to the air and the solution allowed to pass into the chamber at time F by opening stopcock S-D. The potential returned to the anodic potential.

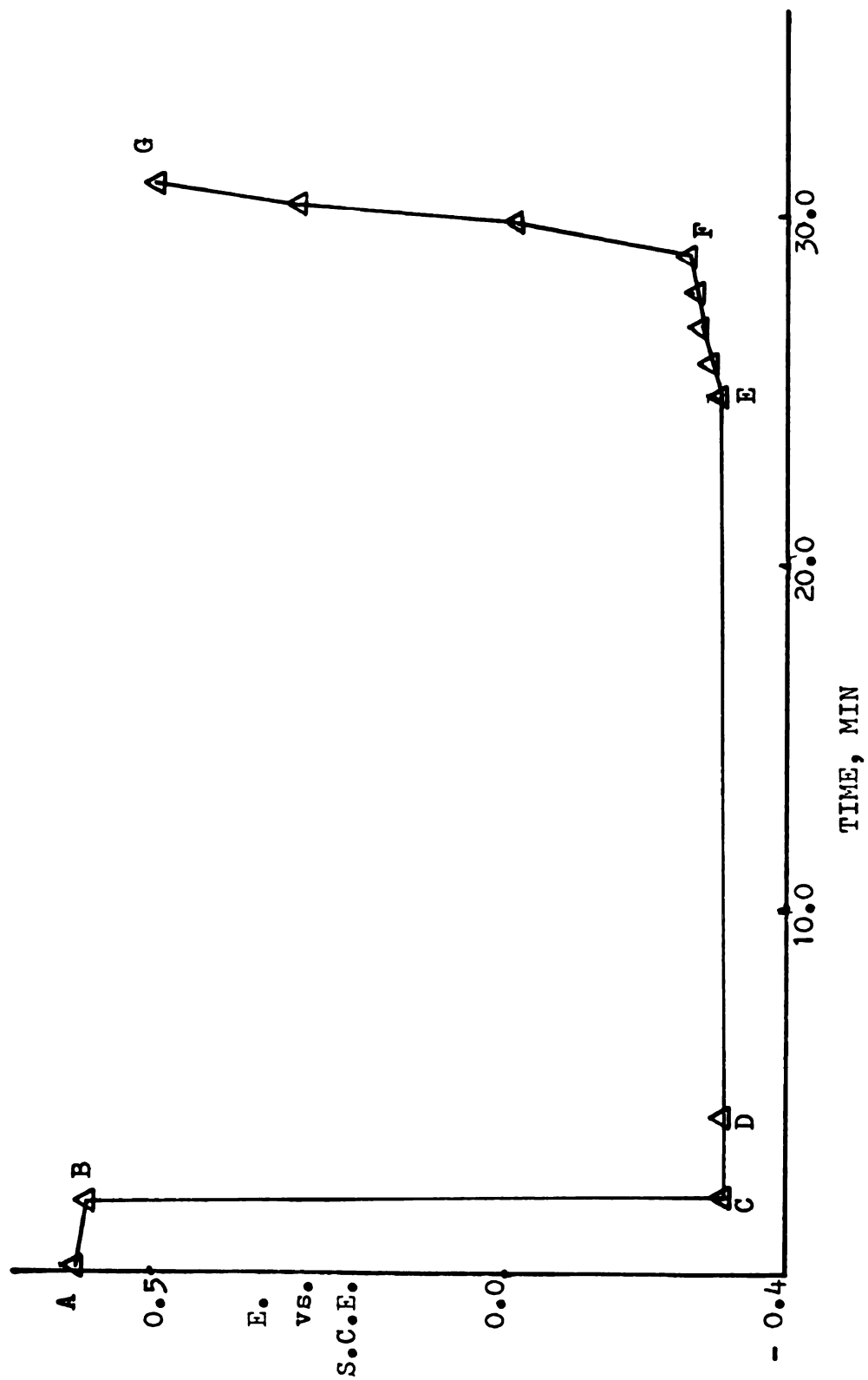


Figure 3-2. Potential Response of the Flow Cell to the Solution Oxygen

o

u

a

e

t

a

pr

by

cu

po

on

the

ele

the

a r

amo

This experiment clearly shows that the flow cell satisfactorily keeps an air-tight environment. All the potential values reported in the whole thesis refer to the reversible hydrogen potential (R.H.E.) unless specified otherwise.

4. Typical Experimental Sequence

The computer controlled coulостatic system offers the user great flexibility in varying experimental sequences according to the requirements of the experiment. A typical experimental sequence is shown in Figure 3-3 which includes the electrochemical pretreatment of the platinum electrode and the electrodeposition of mercury.

The experimental sequence is initiated with the pretreatment of the electrode. The process is controlled by a program called ETREA. Repeated cycles of anodic-cathodic current pulses are applied to the cell with the resulting potential-time curves shown on the computer terminal for on-line inspection. The working electrode is discarded if the results show that any impurity has remained on the electrode. If the result shows a clean platinum surface, the mercurous solution is introduced. Within a short time, a reduction current pulse is issued which deposits the amount of mercury selected by the operator. The computer

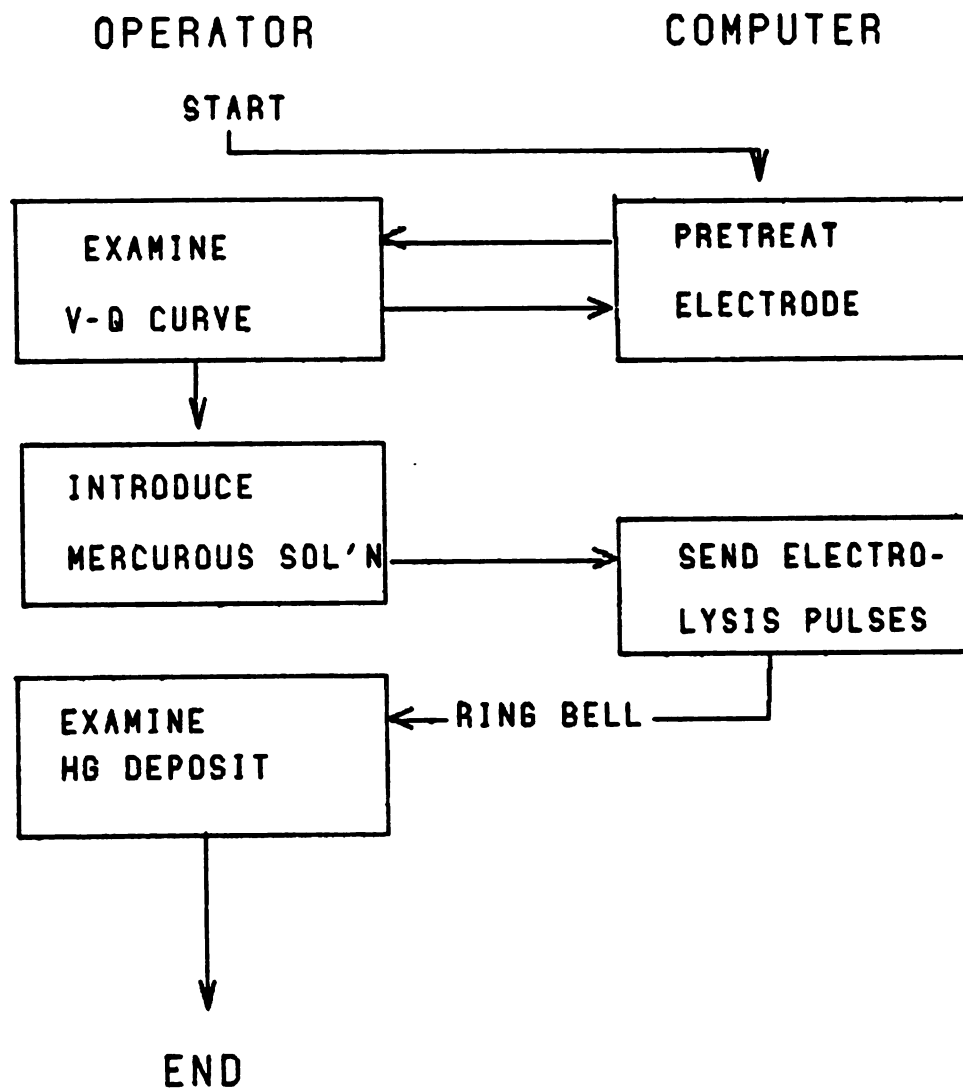


FIGURE 3-3. HG DEPOSITION EXPERIMENT

rings a bell as soon as the reducing pulse is ended. The electrode is removed and examined with a microscope to inspect the structure of the mercury deposit.

D. Experiments and Results

1. Creation of Platinum Surfaces with Varying Roughness Factors

a. Anodic-Cathodic Cycling of Platinum and Roughness Factor Measurement

A clean platinum electrode exhibits a characteristic potential-charge relationship under constant current anodic-cathodic cycling (reverse current chronopotentiometry). Typical potential-charge responses are shown in Figure 3-4. A solution of 0.1 M HClO_4 was used as the electrolyte for both curves. Curve 2 resulted from a freshly polished, hot concentrated perchloric acid treated platinum electrode. Curve 1 was obtained with the same electrode after it was boiled in hot aqua regia for one minute following the concentrated perchloric acid treatment.

These curves are characterized by several distinctive regions. On the anodic current side, the curve starts with the hydrogen desorption region. In this region, the

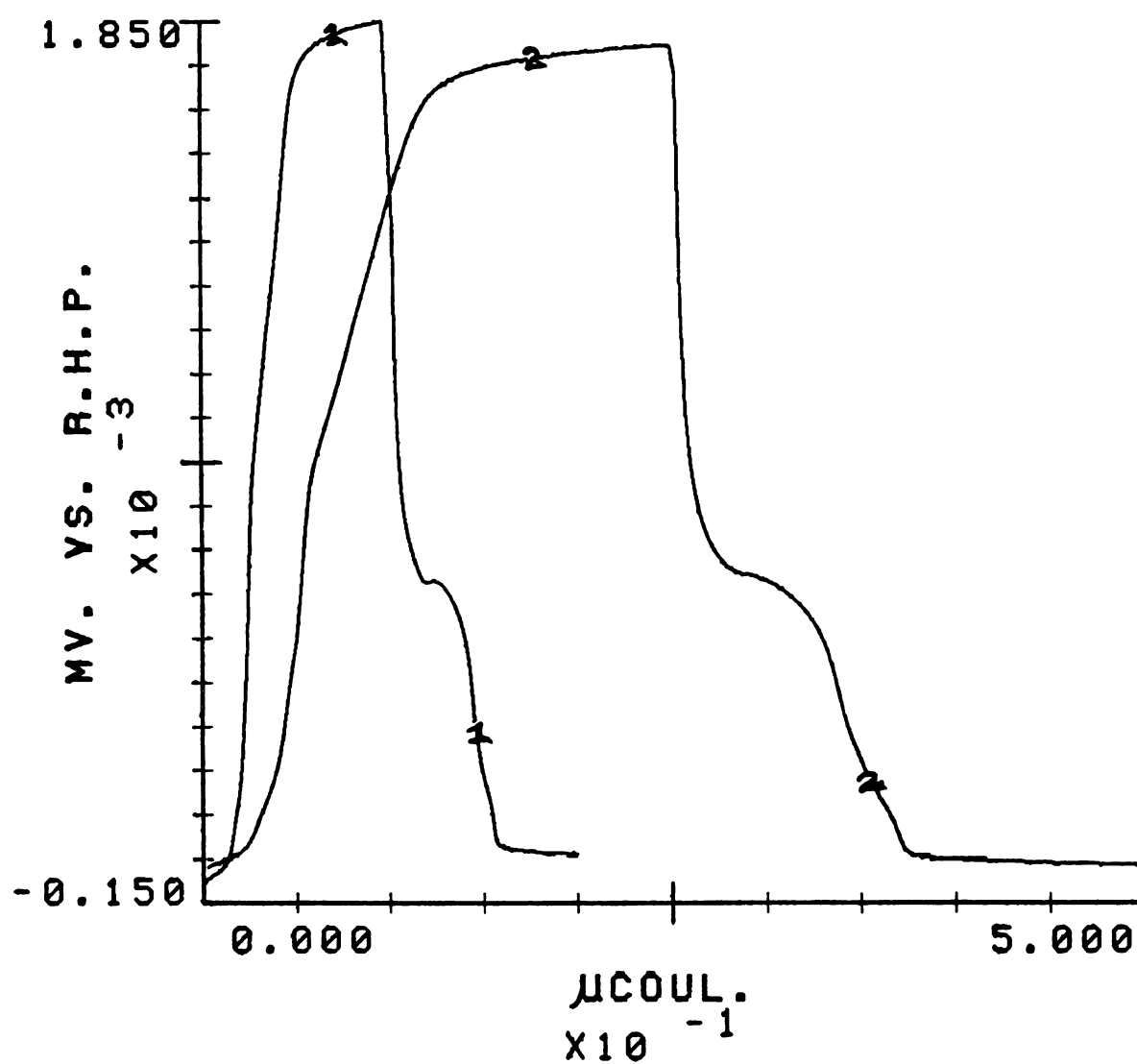


Figure 3-4. Cyclic Chronopotentiogram of Pt Electrode in 0.1 M HClO₄

potential rises slowly until all hydrogen that was adsorbed on the platinum surface is depleted (at a potential of 0.2 V). The potential rises sharply thereafter until a new electrochemical reaction begins. The fast rising potential region is associated with the electrical double layer charging. The new reaction, the oxidation of the platinum surface, begins at about 0.8 V. At 1.8 V, the oxidation reaction becomes the formation of oxygen gas. Shortly after this point, the current polarity is reversed which results in a very sharp plunge of the potential down to 0.6 V. The oxide just formed begins to be reduced. The potential continues to drop, passing the brief double layer charging region, into the hydrogen adsorption region and eventually to the beginning of the hydrogen evolution reaction. The potential remains fairly constant after that point.

These curves are used for two purposes :

(1). To ensure the surface cleanliness. These curves serve as the fingerprints for the clean platinum surface. Surface contamination causes a deviation from these curves and calls for further cleaning of the surface. Furthermore, this cycling process drives the potential above 1.8 V which is enough to oxidize some contaminants. In 0.1 M HClO_4 , the anodic-cathodic cycling causes no apparent surface

roughening up to several thousand cycles. The surface area remains unchanged.

(2). To determine the roughness factor. The roughness factor (RF) is determined by multiplying the time required during the hydrogen ionization or adsorption by the current used to get the charge equivalent of real surface area and dividing this value by the charge equivalent to the geometric area. One cm^2 polycrystalline platinum surface adsorbs about 210 microcoul. charge equivalent of hydrogen.

b. Bright Platinum

The platinum surface obtained by mechanical polishing shows a rather large roughness factor. Curve 2 in Figure 3-4 was obtained with this type of electrode. A 2.5 $\mu\text{coul.}$ charge was used for ionization of the adsorbed hydrogen. This corresponds to a roughness factor of 4.8. After aqua regia treatment, the surface area was reduced because the fine platinum grains on the surface were dissolved in the solution. Curve 1 in the same figure was obtained with an aqua regia treated electrode. It shows a roughness factor of 1.6. The platinum surface obtained in this way is used as the "bright platinum" in the studies that follow.

c. Lightly Platinized Platinum

Platinum is reported to be platinized following the anodic-cathodic cycling process (5, 25). This phenomenon was utilized to make the lightly platinized platinum in this study. The method used is a modification of the method used by F. Anson (5). Instead of using 60 Hz ac as in Anson's study, alternating current steps were used in this study. Each step lasts 15 msec, and has an amplitude of either +1.0 mA or -1.0 mA. The whole process is under the control of the program called PLATNZ.MAC. A multiple of 20,480 current steps is chosen by the operator.

Since the platinum dissolution in halogen acid is one to two orders of magnitude higher than in other acid (25), HCl solution seems to be the choice for the platinization. However, in HCl, the evolution of chlorine gas occurs at very low potential, and electrically insulating bubbles are formed on the platinum surface. Thus HCl is not a good choice for the purpose of platinization. In Figure 3-5, curve 2 shows a characteristic potential-charge curve in HCl. Curve 1 was measured in 0.1 M HClO_4 solution.

Solutions of 2.0 M and 0.1 M HClO_4 were tested as platinization electrolytes. No apparent surface roughness

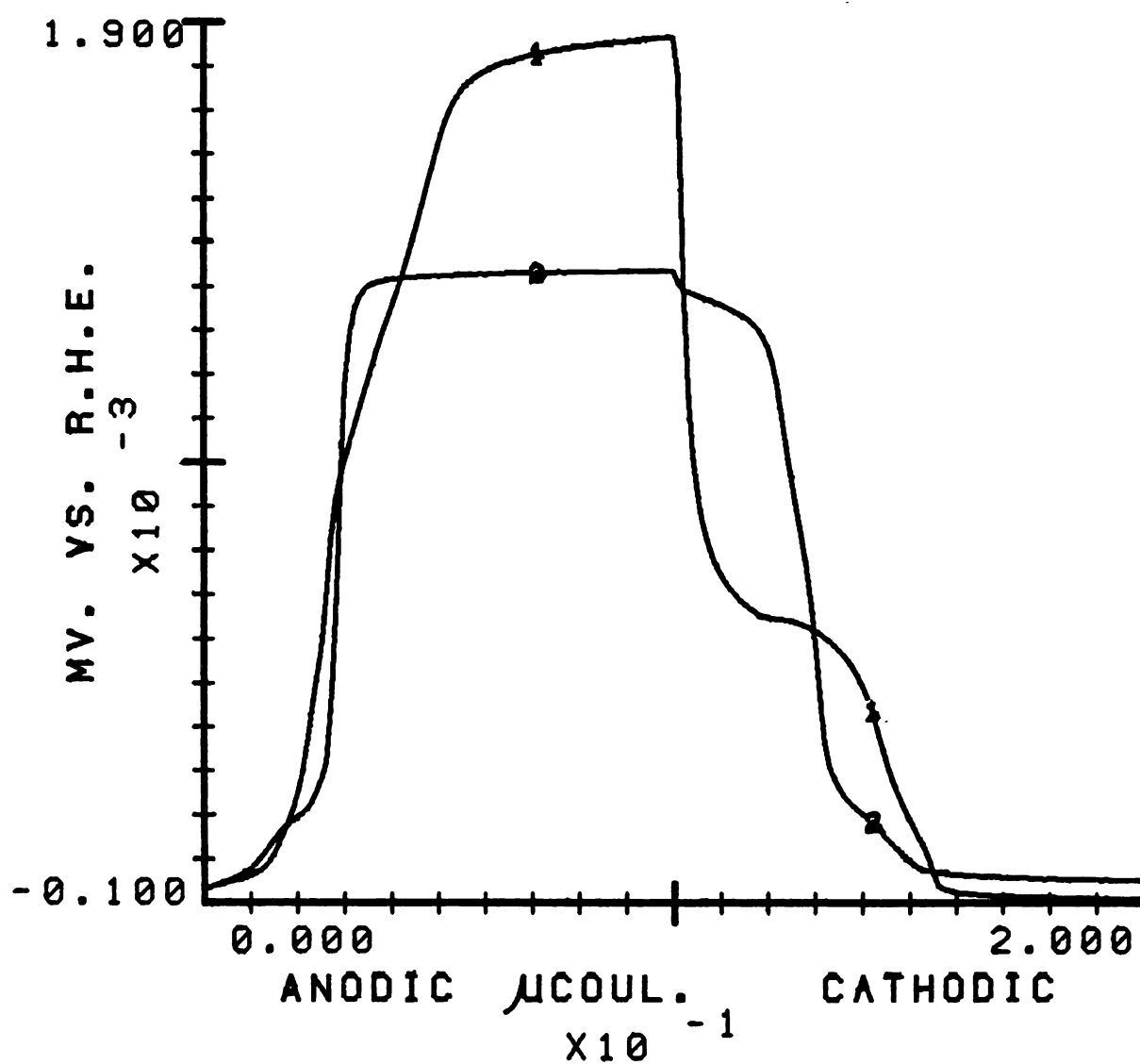


Figure 3-5. Cyclic Chronopotentiogram of Pt Electrode in
(1) 0.1 M Perchloric Acid
(2) 1.0 M HCl

increase was detected after 20,480 current steps and these electrolytes were therefore abandoned.

The 1.0 M H_2SO_4 solution used by F. Anson (5) gave satisfactory results. Variations of the potential-charge curves measured in 0.1 M HClO_4 with an increasing number of current steps are seen in Figure 3-6. The y-coordinates of the curves are moved successively downward by 0.1 V for clarity. The expansions of the hydrogen ionization region and hydrogen adsorption region are on the graph. Table 3-1 lists the roughness factors corresponding to these curves.

Apparently the roughness factor does not vary linearly with the number of the current steps. This might be caused by the interference of the gas bubbles generated during the process. The roughness factor also varies from one electrode to another with the same number of current cycles. An oscilloscope is quite helpful in estimating the roughness factor attained during the process. This is done by connecting the scope probe to the output of the absolute value amplifier (Fig. 1-5) and observing the time required for hydrogen adsorption in each current cycle.

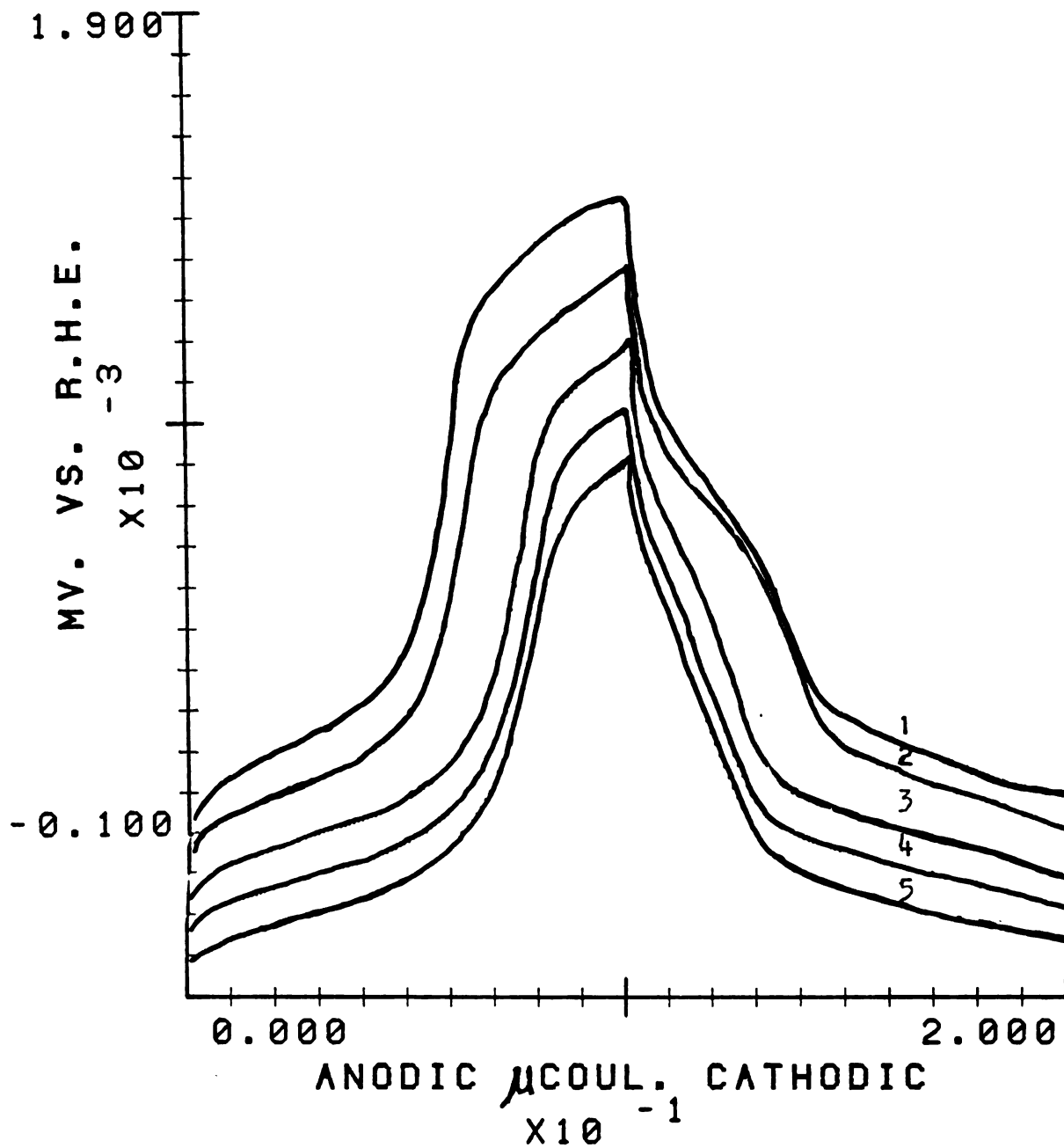


Figure 3-6. Platinized Electrode.

Y-coordinates is drawn with respect to curve 1, other curves are shifted downward successively by 0.1 volt.

Table 3-1. Platinization of Platinum with

Alternating current Steps

Curve (multiple of 20,480 (alternating current steps)		Roughness Factor
Before platinization		4.8
1		8.6
2		9.5
3		11.4
4		>12.0
5		>12.2

2. Influence of the Potential and the Roughness Factor on the Mercury Deposition

The effects of the potential and the roughness factor on the structure of the mercury deposit are determined by examining the structure of mercury deposit formed on bright platinum as well as on platinized platinum electrodes under the following conditions : a. potentiostatic, b. galvanostatic. With the potentiostatic method, the potential is suddenly stepped to a predetermined value and is then held at the same potential until the process is over. With galvanostatic method, a current step is applied. The potential varies with time during the process and is used for the analysis of the plating process.

a. Potentiostatic Experiments

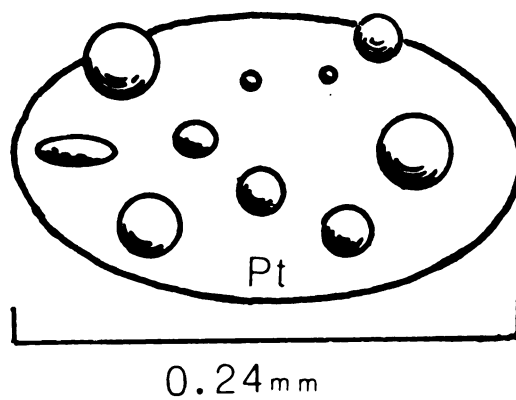
(1). Bright platinum electrode

Two schemes were used to examine the potential effects of the mercury deposit : (a) the deposition was carried out at several selected potentials and the resulting deposit was examined under microscope, (b) the mercury deposit obtained at a moderate overpotential, ie. 400 mV vs. R.H.E., was held at several more cathodic potential values for several

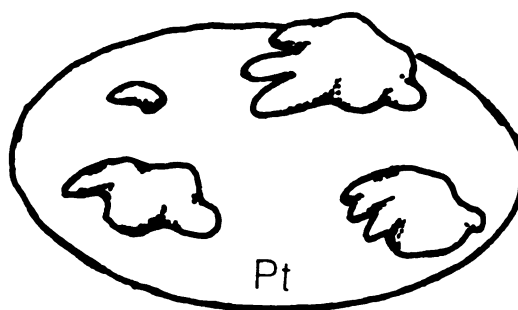
minutes in 0.1 M HClO_4 solution. The electrode surface was examined with a microscope prior to the application of a new potential to detect any difference in the appearance of the mercury deposit.

(a). The mercury plating was conducted at some selected potentials. The results obtained are listed in Table 3-2. Two distinct appearances were detected, the mercury droplets and the mercury patches. The mercury droplet appears spherical or oval in shape. Each droplet has a small contact area with the platinum. The shape of the mercury patches is quite irregular. Each patch has a large platinum-mercury contact area. A drawing of these two configurations is in Figure 3-7. Most frequently, both configurations of mercury deposit appear to distribute randomly over the platinum surface with varied sizes.

(b). A mercury coated electrode with mercury patches produced at 400 mV was held at more cathodic potentials in 0.1 M HClO_4 until the potential was as low as -0.8 V. Hydrogen gas was evolving vigorously at such a cathodic potential. Several mercury patches merged together to form bigger mercury patches, but some area of the platinum surface appeared to remain free from mercury coverage under microscopic inspection.



(a) Mercury Droplets



(b) Mercury Patches

Figure 3-7. Two Types of Mercury Deposit on Platinum Surface

Table 3-2

Potential dependence of the mercury deposit
on the bright platinum electrode

Potential mV vs. R.H.E.	Appearance of Hg deposit
700	mercury droplets and patches
650	mercury patches
400	mercury patches
200	mercury patches
-50	mercury patches with H ₂ bubble

Note : Rest potential = 730 mV

The rest potential in 0.1 M HgClO₄ & 0.1 M HClO₄
is 0.730 V.

Table 3-3

Dependence of the roughness factor of
the mercury deposited at 200 mV

RF	Appearance of plated mercury
3.4	mercury patches and scattered smooth mercury films
3.8	frequently smooth film
5.7	smooth film
9.5	smooth film

Note : Smooth mercury film is obtained with electrode having
RF \geq 3.8.

(2). Lightly platinized platinum electrode

Platinum electrodes with various roughness factors were electroplated with mercury at 200 mV. The results are listed in Table 3-3.

b. Galvanostatic Experiments

In galvanostatic cases, a current step is applied to produce mercury plating. The measured potential always shifts in the cathodic direction with time. The rate of the potential change depends on the current density applied. If the current density is quite small, the potential remains quite close to the rest potential. If a large current density is used, the concentration of the mercurous ion near the electrode surface drops to zero in a short time and this causes the potential at the platinum working electrode to become sufficiently cathodic for H_2 evolution. The platinized electrode used in the following experiments are chosen to have high RF which, according to results shown on Table 3-3, produces smooth mercury films at a suitable potential.

(1). Small current density

The potential-charge response to a current of $-24 \mu A$



for both the bright and lightly platinized platinum electrodes are shown in Figure 3-8. Curve 1 was obtained with a bright platinum which had a roughness factor of 1.0. Curve 2 was from a platinized platinum with RF of 9.5. The potential moves slowly cathodic. The charge passed during the electrolysis is enough to deposit over 600 monolayers of mercury. In both cases, mercury droplets were found. Much finer, evenly distributed mercury droplets were formed on the surface of the platinized electrode which might cause its potential response to be slightly anodic compared to the other electrode since the area exposed by the finer mercury droplets with same amount of mercury must be larger.

(2). High current density

A current of -1.0 mA was used to plate mercury. An unplatinized platinum with a RF of 2.7 gave curve 1 in Figure 3-9, while a lightly platinized platinum with RF of 9.5 gave curve 2. The overall platings took 10 sec.. The exhausting of the mercurous ion at the electrode surface caused the potential to plunge from 0.73 V to less than -0.3 V within one tenth of a second. The potential measured with the platinized electrode started at a more anodic value than that of the other electrode but soon became more cathodic. Hydrogen bubbles were formed in both cases. However, smoothly plated mercury was found on the platinized platinum electrode surface while mercury patches

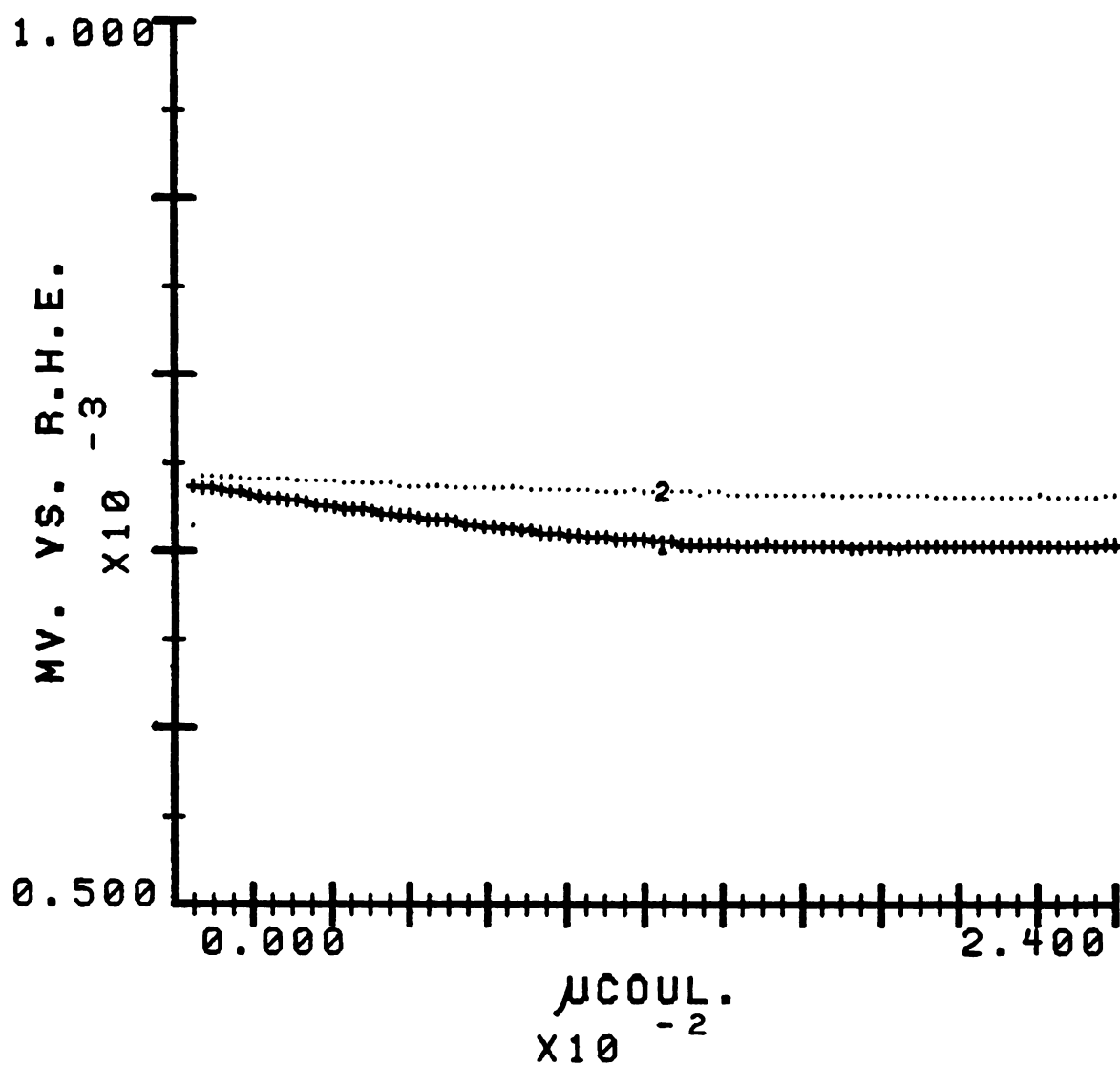


Figure 3-8. Plating of Mercury with $-24 \mu\text{A}$ Current on
1. Bright Platinum
2. Lightly Platinized Platinum

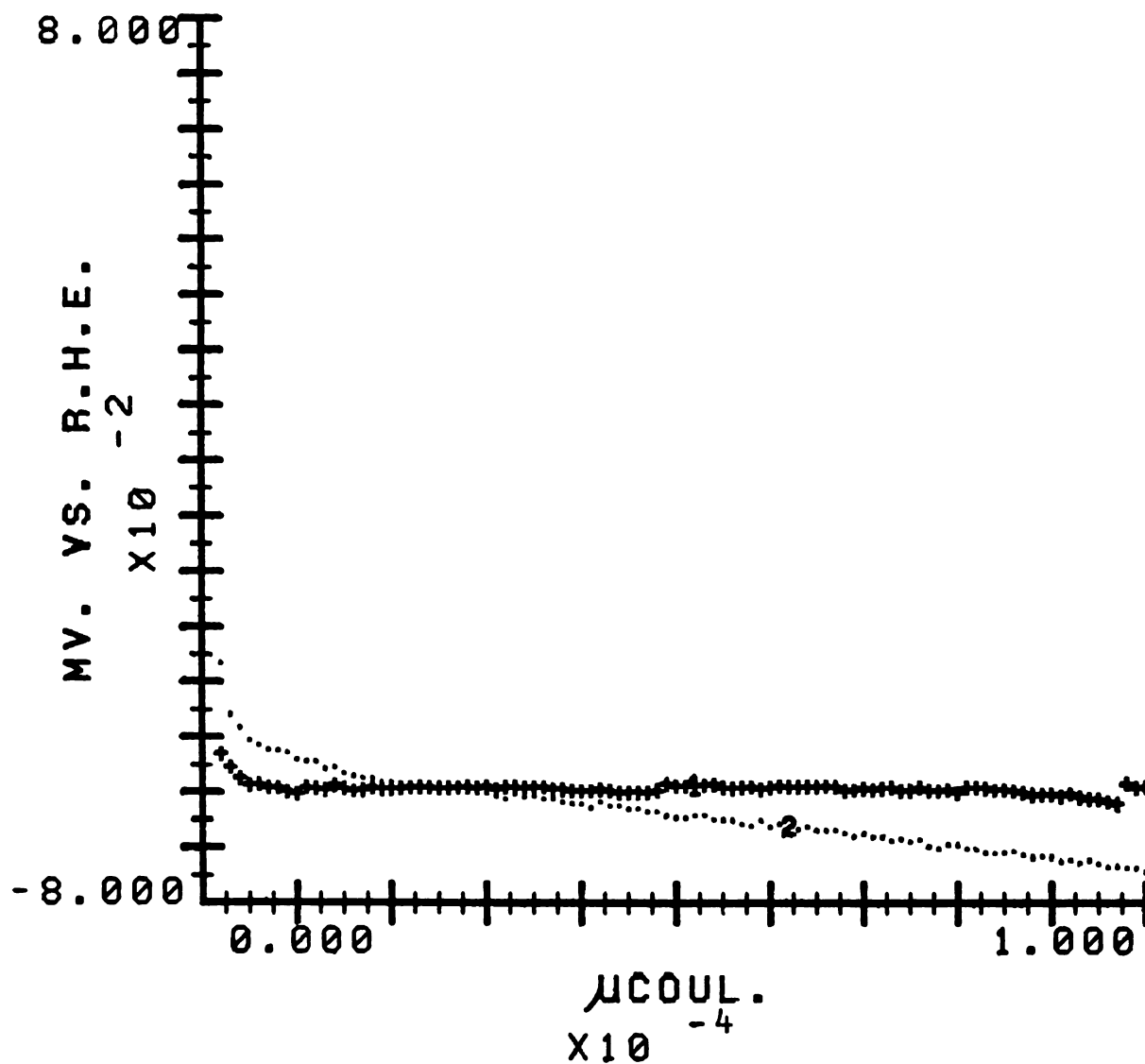


Figure 3-9. Plating of Mercury with -1000.0 μA Current on
1. Bright Platinum
2. Lightly Platinized Platinum

were formed on the unplatinized electrode. To compare the potential response, platinum covered with thick film of mercury, 57.9 mcoul, was tested under identical experimental conditions. Figure 3-10 shows the resulting potential-charge response. The X-coordinate of this figure has smaller scale so that the depletion of the surface mercurous ions is shown. The hydrogen overpotential of this electrode is at least 0.5 V more cathodic than the two freshly plated electrodes in Figure 3-9.

E. Discussion

1. Structure of the Mercury Deposit versus the Plating Potential

The mercury electrodeposited on the platinum surface is found to have three types of structure : mercury droplets, mercury patches and smooth film. At small potential polarization, both potentiostatic and galvanostatic experiments produced mercury droplets. This is true with bright platinum as well as with the lightly platinized platinum. At large overpotentials, mercury patches and/or mercury films were produced. The transition from one type of behavior to the other occurs at about 700 mV. Both mercury patches and droplets were found on the same surface at this potential. Formation of the droplets at low overpotential indicates

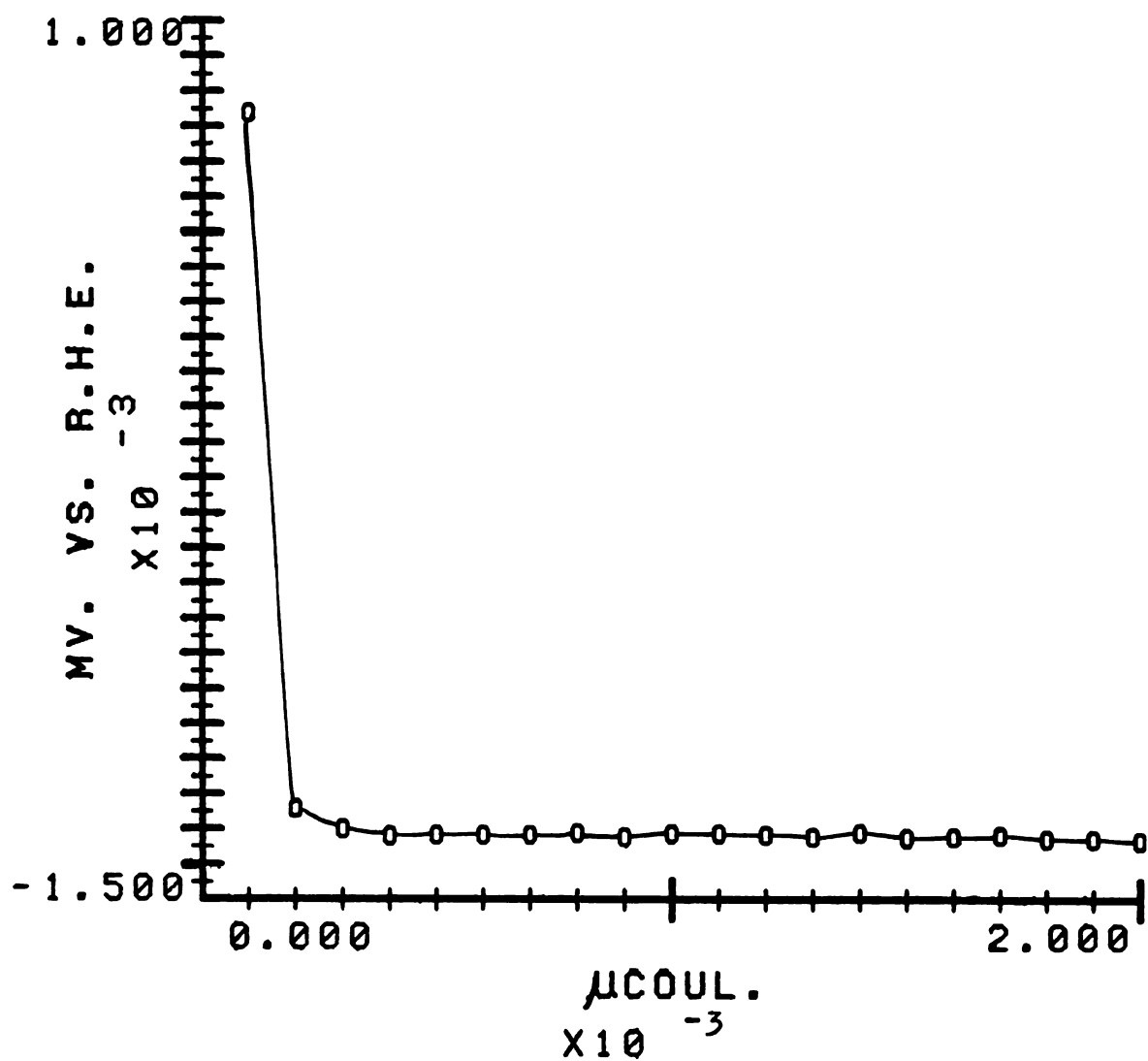


Figure 3-10. Plating of Mercury with -1000.0 μA Current
on a Thick Mercury-coated Platinum Electrode

that the deposition of the mercury on the platinum crystal lattice is not favorable at such potentials. This situation cannot be caused by the oxide film on the platinum surface because it had been deliberately reduced. The great majority of the platinum surface sites were free from oxide before mercury was plated. Furthermore, the reduction of oxide film on the platinum surface is an irreversible process, and a rather large overpotential is needed. The anodic-cathodic cycling in Figure 3-4 indicates that the reduction of the oxide film on platinum starts below 0.55 V. Thus if it had been caused by the residual surface oxide, the same structure of mercury deposit would have been produced for mercury deposited at the potential above 0.55 V. However, this was not the result observed at 0.65 V. The possibility of the interference from the hydrogen adsorption is remotely slim since its adsorption requires a potential as low as 0.3 V. In order to bring the mercury into direct contact with the platinum surface as in the patch structure, several kinetic steps are involved. These are the transportation of the mercurous ion to the platinum surface, the adsorption of the mercurous ion by the platinum surface in order to be reduced, the dehydration of the ion, and the incorporation of the mercury atom onto the surface crystal lattice of the platinum. All these steps, including the last two, require a certain amount of activation energy. The activation

energy required for the last step is much less when a mercury atom is deposited on a mercury surface. The droplet configuration of the mercury deposit indicates that the deposition of the reduced mercury on the existing mercury surface is preferred to deposition on the platinum surface. As the overpotential is increased, the energy transferred per mole of mercury during the reduction is increased according to $\Delta G = -nF\Delta E$, where ΔE is the overpotential, F is the Faraday constant, and n is the number of electrons associated with the reaction. The high potential of the transition of the structure from the mercury droplets to the mercury patches seems to indicate that a significant energy barrier exists for the deposition of the mercury on the average platinum surface sites.

The magnitude of this energy barrier depends on the structure of the platinum surface and is expected to vary among sites with different crystal environments (26). The bright platinum surface structure is complicated by many factors. Since the electrode is made with polycrystalline platinum, numerous platinum crystallite boundaries are present. Various crystal planes are exposed and numerous crystal defects are present on the surface. The defects include the edge vacancies, holes, steps and kinks on the

platinum surface. These surface features create various crystal environments on the surface and thus present various crystal sites, each carrying a different energy requirement for the mercury deposition.

The bright platinum surface created by mechanical polishing and aqua regia etching most frequently possesses a surface which is random in the constitution and distribution of these surface features. As a consequence, the distribution of the mercury deposit on the platinum surface under potentiostatic conditions will be random. This was confirmed by the experiments using bright platinum electrodes which produced either droplets or patches. Furthermore, at the potential of 700 mV, on part of the surface mercury patches were formed while on an other part of the surface mercury droplets were found. This is a strong indication of the non-uniformity of the platinum surface structure. However, in addition to the non-uniformity of the energy requirement associated with the crystal structure, a second type of non-uniformity might be operative. This is the non-uniformity of the local electrical field caused by the rough surface condition. Which of these two factors, the energy barrier or the electric field strength, is mainly responsible for the simultaneous formation of these two mercury deposit is not certain.

No noticeable difference was observed using the various overpotentials which result in the formation of mercury patches. This indicates that some sites of the platinum surface are always preferred for the mercury deposition in spite of the increase in the overpotential. A related study was done by Hassen, Unterecker and Bruckenstein who used the HgClO_4 solutions with concentration between 10^{-4} M to 10^{-6} M for the deposition of mercury. The potential during the deposition was held at 0.0 V vs. S.C.E. They found that on the mercury plated platinum surface, the capability to adsorb hydrogen is reduced. One deposited mercury atom displaces two hydrogen atoms when the mercury coverage of the platinum surface is low. When the coverage exceeds ~ 35 %, fewer hydrogen atoms are displaced for the same amount of mercury deposited. This suggests that there is a competition for the reduced mercury atom between the platinum atom and the mercury nuclei already deposited. As the overpotential is increased, more sites on the platinum surface become available for the mercury deposition to occur so that a wider area of mercury-platinum contact becomes possible. Since deposition of mercury on these nuclei is energetically more favorable than on the platinum atom, faster mercury deposition is expected on these sites. Therefore, the overall mechanism leads to the formation of mercury patches.

Assuming that the platinum surface exhibits no specific adsorption for the mercurous ion, the mercurous ion at the surface of the platinum in 0.1 M $\text{Hg}_2(\text{ClO}_4)_2$ solution constitutes less than one in 500 of the molecules and ions in contact with the platinum surface. Thus the usage of high overpotential seems to have no advantage. Hydrogen evolution occurs at much higher overpotential and creates a new situation. The evolving H_2 gas disturbs the solution with gas bubbles. These bubbles tend to exist preferentially at the platinum sites that are poorly covered with mercury. Since the H_2 bubbles block these sites from the solution ions, no real gain could be expected.

2. Effect of Surface Roughness Factor on the Structure of the Mercury Deposit

The results shown on Table 3-3 clearly demonstrate that at suitable potentials, a smooth mercury film is produced on the platinized platinum surface with higher RF value. Thus the platinization must assist the mechanism which leads to a smooth mercury film formation. What is happening during the platinization process which is comprised of repetitive oxidation and reduction cycles ?

During the platinization process in H_2SO_4 , a topological change is induced. Surface roughening was clearly observed in these experiments since the platinum surface changes appearance during the process. It loses the shiny metallic appearance, turns gray, and eventually becomes dark. The surface roughness factor increases as the process continues.

Roughening has been explained in terms of redistribution of surface metal atoms brought about by forming and breaking platinum-oxygen bonds (2, 23). Biegler (23) showed that the roughening only took place when more than one oxygen atom was associated with each surface platinum atom on the anodic step. Unterecker and Bruckenstein (27) demonstrated with the potential cycling method that the roughening process involved dissolution and redeposition of surface platinum. Thus a new platinum surface is generated by anodic-cathodic treatment.

Since the mercury droplets formed on the platinized platinum electrode showed a uniform distribution and a fine uniform diameter under the galvanostatic condition with a small current, a platinum surface with a more uniform surface condition must be created by the platinized treatment. Since an increase of RF value implies an increased amount of surface defects, the finer diameter droplets configuration with this surface condition would mean that these defect

sites are energetically more favorable for the reduced mercury atom. This is consistent with the theoretical calculation which predicts that the activation energy for the incorporation of the an atom during the electroplating process is less on the defect sites of crystal surface (44).

What is the threshold RF value for the smooth mercury film formation ? Table 3-3 shows that at a RF of 3.8, a smooth mercury film was obtained. It seems that the threshold RF for smooth film formation should be below this value. However, the concept of the threshold should be taken with caution since the RF value obtained at low platinization is easily affected by the surface condition prior to the platinization. The RF value alone cannot be used to specify the surface condition unless a treatment had been applied which could exactly reproduce the surface condition. This fact is demonstrated in the example shown in Figure 3-5. Two bright platinum electrodes were used. One of them, curve 1 had a RF value of 5.7. Despite of the high RF, the creation of a smooth mercury film on such a surface has been found to be very improbable.

It is interesting to compare the potential responses of a lightly platinized platinum electrode with a bright platinum electrode using a high plating current as shown in Figure 3-9.

The response potential of the lightly platinized platinum electrode (curve 2), which ended with a smooth mercury film, started at 0.1 V more anodic than the other electrodes, but became more cathodic as more mercury was plated. This means that the hydrogen overpotential on this electrode was increasing. This clearly indicates the mercury coverage of the platinized platinum electrode was improving. The potential response using the bright platinum is also interesting. During the plating process, the potential with hydrogen evolving stayed fairly constant. This value, -0.6 V, is quite cathodic compared to that of the platinum electrode which is about -0.03 V in 0.1 M HClO_4 solution. Except for the beginning, the potential did not vary with the charge consumed. This evidence strongly suggests that the reduction of mercury ions occurred on the existing mercury surface instead of the platinum surface which resulted in mercury patches.

3. Other Factors that Influence the Formation of the Mercury Deposit

1. Hydrogen Adsorption

Hassan, Untereker and Bruckenstein (17) studied the platinum surface covered with a submonolayer of mercury

and found that the hydrogen adsorbed decreased in direct proportion to the amount of mercury deposited up to 35 % mercury coverage of the electrode surface, then a smaller amount of hydrogen is displaced by an equal amount of mercury deposit. This indicates that mercury atoms must occupy the platinum sites at the expense of the hydrogen. However, the occurrence of hydrogen evolution did not seem to interfere with the smooth mercury film formation, except that H_2 bubbles that stick to the surface block current passage at those locations.

b. Surface Tension

Hartley, Hiebert and Cox (14) showed that the mercury droplets on the platinum surface merged to form a smooth film at a high cathodic potential. My results indicate that the platinum electrode covered with mercury patches produced at 400 mV showed an independence of the potential down to -0.8 V (section D-2, 1.b.). Although a 6 V battery was used by those cited workers, the overpotential could not have been more cathodic than -0.8 V unless a good coverage of mercury had already existed which is not the case for mercury droplets. The difference might come from the structure difference between these two types of deposits. The droplets, due to their lack of interaction with the platinum surface,

appear to be more susceptible to the influence of the surface tension variation as well as the physical agitation created by hydrogen evolution. The mercury patches, due to their strong interaction with the platinum surface as indicated by the contact area between the mercury and the platinum, are less susceptible to these influences. In addition, the interface between the mercury patches and the platinum becomes amalgamized quickly and loses the mobility of the liquid mercury. This bonding adds more inertness to the mercury patches.

c. Chloride ion

It was pointed out by Gardiner and Rogers (6) that treatment of the electrode with potassium chloride before and after the plating of mercury on the platinum surface is both essential and critical to have good mercury plating. This does not correspond to our experience as is shown by the results obtained above. The plating of a smooth mercury film on platinized platinum needs no KCl treatment. However, chloride ion was found to play an interesting role in the mercury coating process. It was discovered that the platinum surface reduced hot concentrated HCl could easily adsorb traces of chloride ion on the surface unless great precautions were taken. Since chloride ion reacts with mercurous ion easily, when such a surface was plated with

mercury, precipitates of mercurous chloride could easily be produced on the platinum surface. Since calomel precipitate shows a high affinity for the mercury surface (65), it is easily adsorbed on the mercury surface. The calomel film interferes with the growth of the mercury drop due to its poor electrical conductivity. This forces the further deposition of mercury to proceed at other locations on the platinum surface. As a result, the creation of a more evenly distributed mercury coating becomes easier. This process is explored further in the next chapter.

F. Conclusion

The structure of mercury deposited on the chemically or electrically reduced platinum depends on the plating-potential and the surface structure of the platinum.

When a small polarization potential is used for mercury plating, mercury droplets are formed. At higher polarization potential, mercury patches or mercury film are produced.

To create a smooth mercury film on bright platinum directly by an electroplating process is difficult because the platinum surface is quite inhomogeneous. The situation is changed when the surface is platinized by current cycling

which results in an increase in the surface area and probably a more homogeneous surface. The plating of a smooth mercury film is thus made easier.

CHAPTER IV

A NEW METHOD OF MAKING A SMOOTH MERCURY FILM ON A PLATINUM SURFACE

A. Introduction

One major factor seems to be responsible for the difficulty of making a smooth mercury film on a platinum surface. The platinum surface is normally quite inhomogeneous. The surface atoms display various affinities toward mercury atoms. This causes a preferential deposition of mercury atoms on certain sites when mercury is reduced electrochemically. Once some mercury nuclei are formed, these nuclei immediately become the center for newly reduced mercury because they compete much more favorably for mercury than the bare platinum atom. To solve this problem, several processes have been devised which include the usage of high negative reduction potentials (7), the immersion of platinum in a mercury pool (13) and the complexation of mercuric ions with EDTA species. The fundamental principle of these attempts is that by varying the experimental condition, the tendency of preferential deposition of mercury might be made less to allow a more homogeneous coverage of the Pt surface with Hg.

It was found during this study that there is a direct way of solving the mercury preferential deposition problem. In this method, a masking agent is utilized during the initial mercury plating to prohibit the deposition of mercury on the mercury nuclei. By masking, it forces the mercury plating to proceed on the bare platinum. Once the whole platinum surface is covered with this primary mercury layer, the masking agent can be removed and the mercury plating is resumed until a desired thickness is obtained. This process would be quite advantageous over the methods now being used because complete coverage of mercury on the platinum is guaranteed and the effect of the platinum surface status does not seem to have any direct influence on the success of the method.

The masking agent chosen must be able to react with mercury atom on the platinum surface preventing further deposition of mercury and yet leave the platinum surface uncovered for mercury deposition. Chloride ion which forms a very insoluble compound in the presence of mercurous ion, is chosen as the masking agent in this study.

B. Procedures of Making An MFE Using Chloride Ion As A Masking Agent

The platinum electrode to be coated with mercury is cleaned in hot perchloric acid and treated with aqua regia for several minutes. Two plating baths are used. One contains 1.2 N HCl and 0.1 N HgCl_2 . The other contains 0.1 N HgClO_4 and 0.1 N HClO_4 . The plating is first carried out in a HgCl_2 bath. A potential of approximately 1 V is used for this primary plating process for several seconds. Figure 4-1 shows a typical current response. Then the second solution is introduced after a brief dipping in hot conc HCl and rinsing with distilled water. The mercury plating is then resumed. A typical reduction current used is 5 mA/cm^2 . The reduction is continued until a desired thickness of mercury plate is obtained.

C. Results and Discussion

1. Product of the Primary Plating

The electrode surface appears gray after the primary plating. Under microscopic examination, the platinum surface is covered with a calomel precipitate which has a rugged spongy appearance.

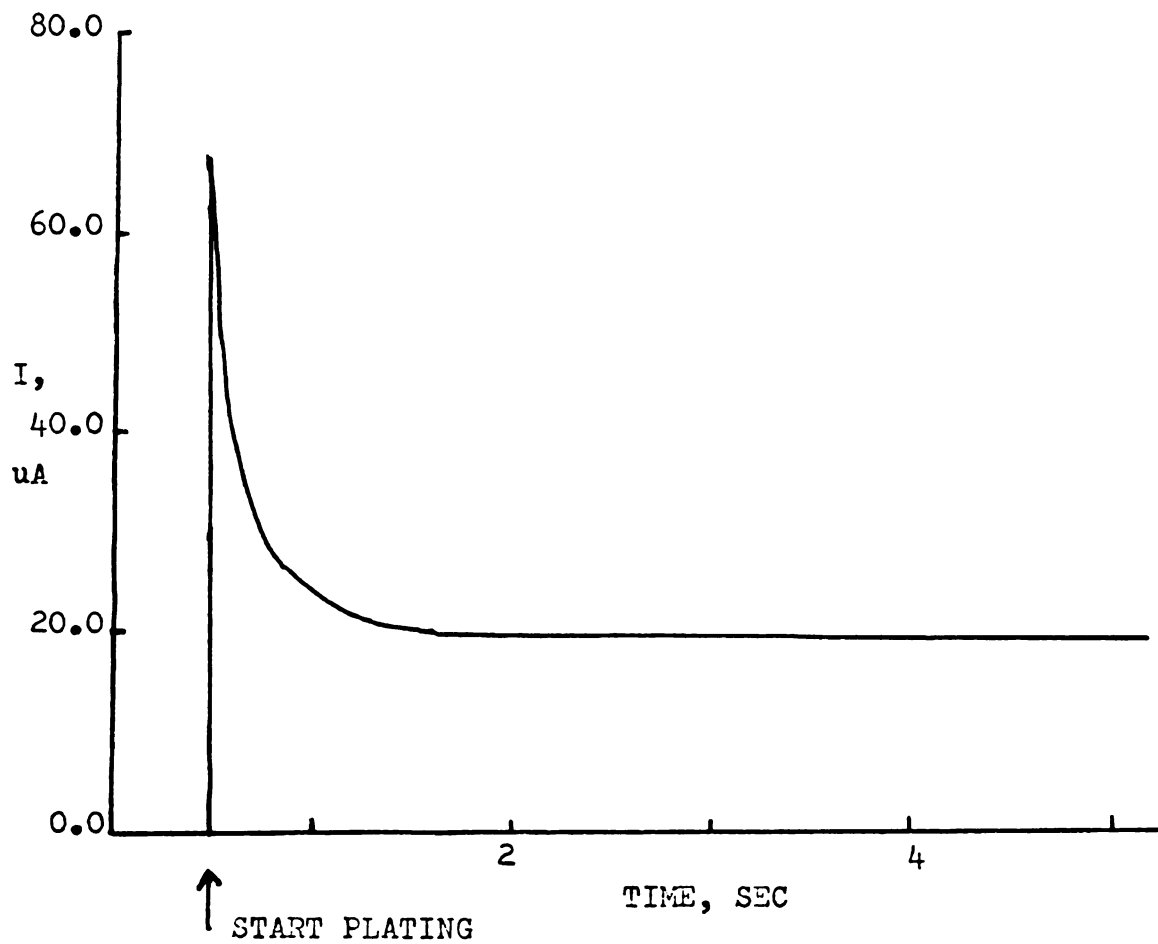
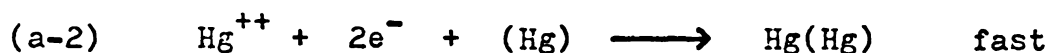
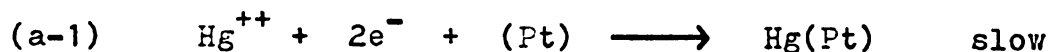


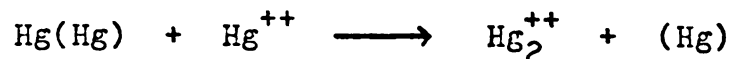
Figure 4-1. Mercury Plating at a Constant Potential,
Electrolyte Contains 1.2 N HCl and 0.1N HgCl₂

Several reactions are involved during the film making process. At the primary mercury plating stage, these are :

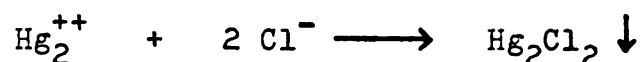
a. Electrochemical Reduction of Hg(II) Ion



b. Chemical Reduction of Hg(II) Ion



c. Precipitation of Hg_2^{++} by Chloride Ion



When the reduction current is applied, mercuric ions are plated on the platinum surface as indicated by reaction (a-1). The initial mercury is deposited on the most active sites of the platinum surface. Once these nuclei of mercury deposition are formed, a competition starts between deposition on the unplated Pt surface and deposition on these nuclei as indicated by reaction (a-2). The former sites are more favorable. In the meantime , a second reduction takes

place on these favored sites; that is, the chemical reduction of mercuric ion by mercury shown as reaction b. This reaction is known to be quite fast (37). The product of this reaction is mercurous ion which forms precipitate with the chloride ion in the solution immediately by reaction c.

Because the calomel formed is quite insoluble in the aqueous solution, it immediately precipitates and is adsorbed on the mercury surface.

The success of this plating process relies on the peculiar combination of reactions b and c. From reaction c, it is seen that the chloride forms a precipitate only with mercurous ion. But as reaction b indicates, the only place where these ions are generated is the place where mercury already exists. Thus, the precipitate is only formed on the place where mercury has been deposited. Once the precipitate forms, it creates an insoluble film over the mercury deposit and retards the electroreduction on these places. This forces the reduction to continue on places where mercury has not yet been formed. In this way, the plating of the mercury goes on evenly over the whole surface of the platinum electrode.

2. Continual Mercury Plating

By this time, the platinum electrode surface is covered with a thin film of calomel. This film is removed by the reduction reaction in hot conc **HCl**. The mercury plating proceeds smoothly after this step. After an appreciable amount of mercury is plated, the electrode surface appears mirror-like under the microscope.

It is interesting to note the difference in mercury obtained with and without the primary plating step. With the same reducing current density without the primary plating step, the platinum electrode surface is covered with mercury droplets.

3. Factors that Influence the MFE Obtained

a. Geometry of the Electrode

Electrodes with other geometry have been prepared including a spherical Pt electrode and a wire electrode. The spherical electrode is made by heating the tip of a Pt wire electrode. At the melting point, the Pt melts and forms a small Pt ball at the wire tip of about 1 mm in diameter. The wire electrode is made by sealing one end of

a piece of platinum wire in the soft glass leaving an approximately 1 cm length of wire exposed. The diameter of the electrode is approximately 1 mm. The plating procedure described earlier is performed. A smooth mercury film was obtained in both cases.

b. Influence of Aqua Regia

The pretreatment of aqua regia on the platinum surface seems essential for the success for making smooth mercury film after the electrode is polished with fine grit silicon carbide sandpaper (650 grit). Several attempts to plate mercury on the planar platinum electrode following all the procedures described above except the aqua regia treatment resulted in mercury droplets on the platinum surface. Since the Pt surface after the sandpaper polishing is quite non-uniform physically as evidenced by the random scratches and marks seen under microscopic examination. This causes the platinum to have a non-uniform surface activity and thus causes the failure to obtain a smooth mercury coating.

One other reason could be due to the surface changes associated with the aqua regia treatment. The aqua regia attacks the surface Pt atoms. Various compounds between chlorine and platinum have been found including PtCl , PtCl_2 , PtCl_3 and PtCl_4 . It is quite possible that after the aqua regia treatment, chlorine atoms are chemisorbed on the Pt surface. The chloride covered surface might be more hospitable for the plating of mercury than a platinum surface covered with either hydrogen or oxygen. This might be the reason that the Pt surface without treatment of aqua regia is difficult to plate with a smooth mercury film.

CHAPTER V

DETERMINATION OF THE Pt-Hg REACTION RATE ON THE MERCURY COATED PLATINUM ELECTRODE

A. Introduction

1. Scope of the Pt-Hg Reaction Rate Study

The application of the mercury film electrode (MFE) in electrochemical studies has not gained its full potential for some apparent reasons. Making a smooth mercury film is difficult. The supporting materials used for the mercury film show either high affinity with mercury which results in a fast Pt-mercury reaction or no affinity which results in the formation of mercury droplets loosely hanging from the surface of the supporting material. Platinum shows a certain affinity for mercury. The hanging mercury drop electrode supported by platinum has been shown to possess good stability with time. But the application of platinum as the supporting material for a mercury film electrode is handicapped by the difficulty involved in creating a thin smooth mercury film. As a consequence, the kinetic data for the Pt-Hg reaction is lacking from the literature partly due to the difficulty of achieving reproducible

results (29). This knowledge is important for the application of MFE in the electrochemical studies. The study of the effect of the surface state on the mercury deposit described in the previous chapters revealed that two types of mercury deposit exist on the platinum surface, namely mercury droplets and mercury patches. By lightly platinizing the platinum surface, the platinum surface can be coated with a smooth mercury film by an electroplating process. This finding is crucial for the study of the reaction rate of platinum and mercury because unless the mercury forms a smooth film on the platinum surface, the rate study can't be expected to generate reproducible data.

2. Relevant Results Obtained by Other Workers

a. Existence of the Pt-Hg Intermetallic Compound

The reaction of the platinum with the mercury coat leads to the formation of a Pt-Hg intermetallic compound. This compound has a definite composition. The structure has been determined as PtHg_4 (15, 33, 41). The intermetallic compound exhibits several electrochemical properties different from either the platinum electrode or the pure mercury electrode. The oxidation of the mercury in the

intermetallic compound occurs at a more anodic potential than that of metallic mercury. This property has been used in the scanning voltammetric(17) and the chronopotentiometric (29) studies of the Hg-Pt interaction. With a constant anodic current, the chronopotentiogram of the mercury stripping reaction using a mercury coated platinum electrode shows three potential plateaus. A typical plot is shown in Figure 5-1. The stripping is carried out in 0.1 M HClO_4 solution. The potentials of these plateaus are 0.54 V, 0.12 V and 1.7 V, corresponding to the ionization of the metallic mercury, the ionization of Hg in the Pt-Hg intermetallic compound and the oxidation of the supporting electrolyte respectively (29). Similar results were obtained with the scanning voltammetric method(17).

Since mercury has three oxidation states, 0, +1 and +2, the ionized product of the mercury oxidation has the possibility of taking either one of the two oxidized states. Theoretical calculations indicate that the oxidation state of the mercury ion generated by electrochemical oxidation depends on the applied potential. According to Hassen, Untereker and Bruckenstein (17), at $E < 0.85$ V, only Hg_2^{++} is produced; at $E > 1.10$ V, only Hg^{++} ion is produced; while at $1.10 \text{ V} > E > 0.85 \text{ V}$, a mixture of Hg_2^{++} and Hg^{++} is produced. Thus, in Fig. 5-1, the ionization product

HG STRIPPING

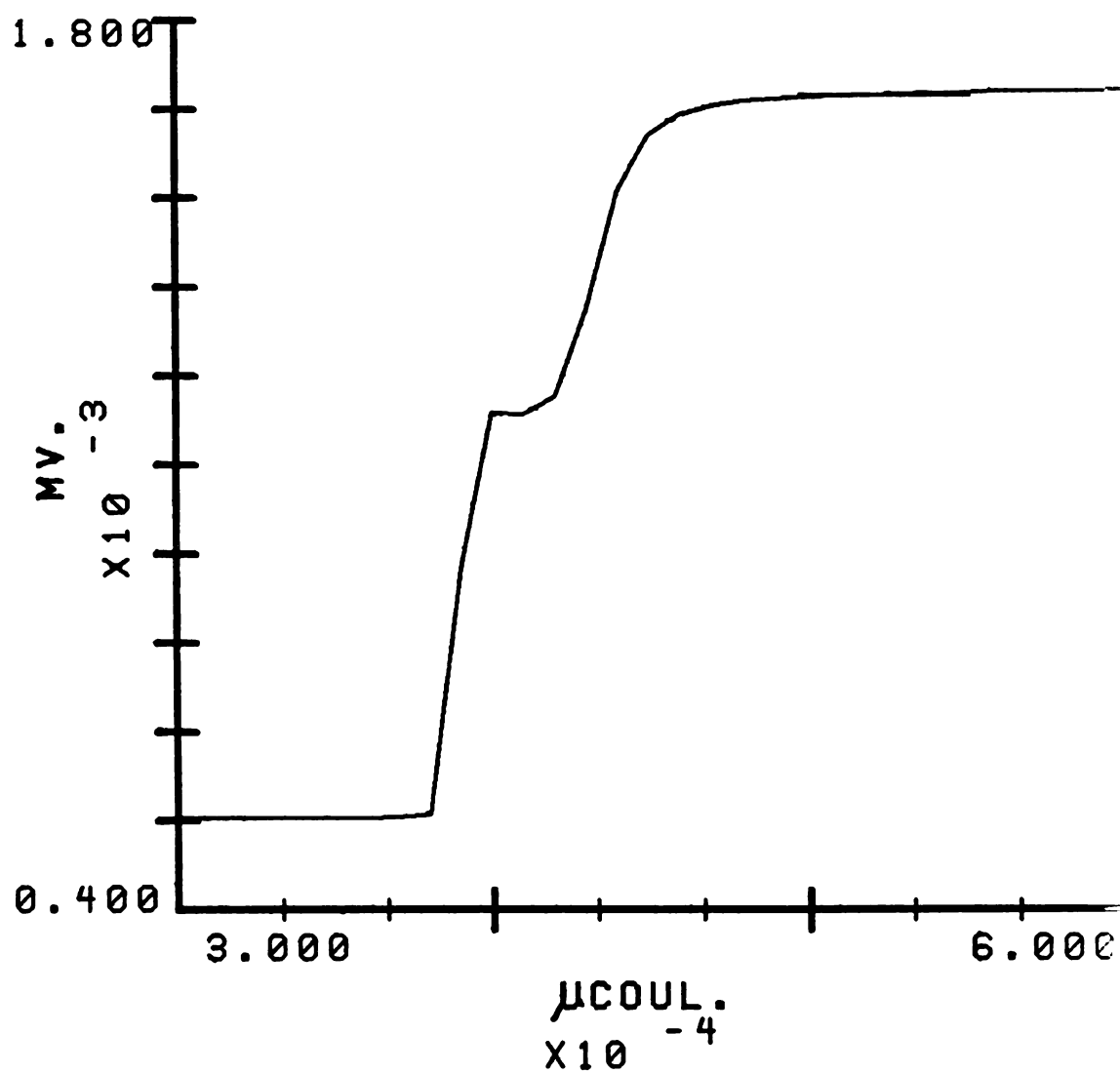


Figure 5-1. Potential-Charge Response of MFE under Anodic Current in 0.1 M HClO_4

during the second potential plateau is Hg^{++} ion while the ionization product during the first plateau is Hg_2^{++} . This was confirmed by UV spectrophotometric methods on the resulting solutions (29) and also by the electrochemical method (17).

b. Pt-Hg Reaction Rate Study

The rate of Pt-Hg reaction on the MFE is determined by measuring the quantity of the compound formed with time. Both a gravimetric method (33) and electrochemical methods have been used (29, 17). Barlow and Planting used a gravimetric method to determined the Pt-Hg reaction rate at elevated temperature. This technique is quite insensitive and is only applicable with a large quantity of Pt-Hg compound. The cyclic voltammetric technique was used by Hassen, Untereker and Bruckenstein (17) in their study of the Pt-Hg interaction involving a few atomic layers of Hg. Brubaker (29) used the chronopotentiometric method in his mercury-platinum system study. The second method enjoys the advantage of simple calculation for the number of coulombs involved in the process.

With the computer controlled coulostatic system, the Pt-Hg reaction can be studied within a much shorter period

of time than possible by other previous methods. Since a known amount of charge is delivered in each case, there is little difficulty in calculating the charge involved. In addition, the sequence of the polarization process is easily modified to meet the need of the study.

B. Experimental

1. Preparation of the Platinum Surface for the Rate Study

The reaction rate of Pt with Hg is apparently affected by the amount of Pt-Hg compound between the metallic mercury and the platinum. An analysis of the rate data has to include a consideration of the amount of the Pt-Hg compound already formed. For simplification of the mathematical treatment, the Pt-Hg compound covered Pt electrode is used. Such an electrode only has a layer of Pt-Hg compound on the surface, and is prepared by plating a certain amount of mercury and then stripping the metallic mercury off the surface after various periods of aging time allowed for the reaction to preceed.

The platinum electrodes in this study were lightly platinized using the procedure described previously. The RF of the lightly platinized electrodes ranged between 4.0 and 10.0.

2. Experimental Set-Up

The set-up is essentially identical to that used in the previous chapters. The Pt-Hg compound covered Pt electrode, PMCCPE, is obtained from the smooth MFE under the control of a program called STRIP. Under program control, the coulometric generator issues an anodic current to ionize the metallic mercury on the MFE. The potential during the stripping is measured every 30 microseconds. The stripping current is terminated when the metallic mercury on the surface is exhausted which is indicated by a sharp rise of potential. The potential value for the termination of current is 1.0 V vs. R.H.E.

C. Experimental Results

1. Methods Used for the Pt-Hg Reaction Rate Study

Two polarization techniques have been used for the Pt-Hg reaction rate study : the current reversal technique and the aging technique. In both cases two steps with mercury plating and stripping are included. The mercury to be plated is only a very small fraction compared to the amount of existing Pt-Hg compound on the electrode surface so that the amount of Pt-Hg compound can be treated as constant during study.

a. Current Reversal

In this technique, a short reduction current pulse is applied, immediately followed by an anodic current pulse. The current program is shown in Figure 5-2a. If the reducing current is made so that only reduction of mercurous ion is allowed, the charge consumed is equal to the amount of plated mercury. During the stripping step, part of the deposited mercury is oxidized and removed at a low potential value. The remaining plated mercury reacts with platinum and become indistinguishable from the existing compound. The mercury in the compound is oxidized at a higher potential. Analyzing the resulting potential-time curve during the stripping step gives the quantity of mercury which remained in metallic state. The difference in charge quantities used for plating of mercury and for removing metallic mercury gives the amount of mercury transformed into Pt-Hg compound.

b. Aging Method

In this technique, an additional period is incorporated in the polarization program. The scheme is shown in Figure 5-2b. The waiting period is included to vary the time available for the Pt-Hg reaction. The reaction rate can be determined in the same way as the previous technique.

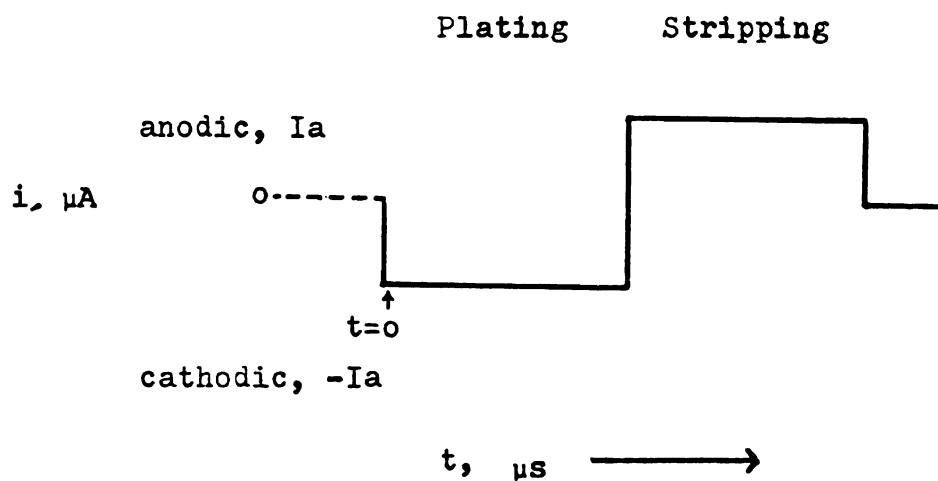


Figure 5-2 a . Current Program Used for Current Reversal Technique

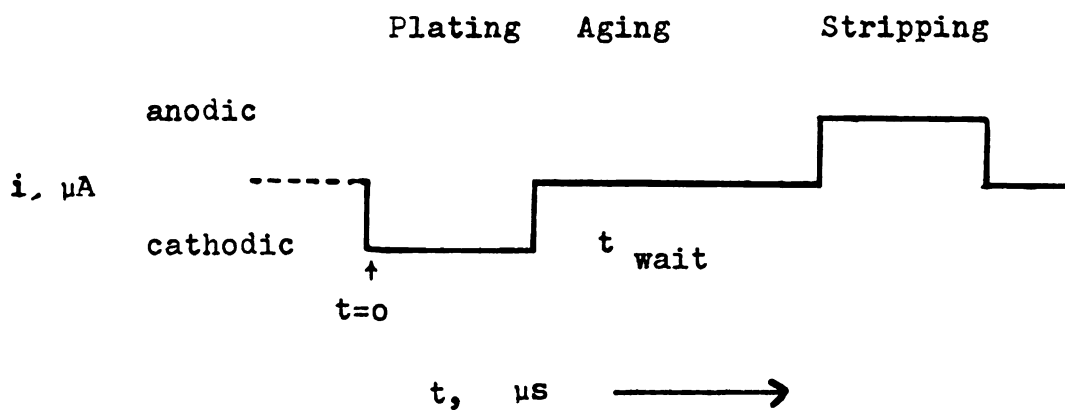


Figure 5-2 b . Current Program Used for Aging Technique

2. Anodic Stripping of MFE in Mercurous Solution

Since the transformation of the metallic mercury into Pt-Hg compound is known to be fast, particularly when the quantity of the Pt-Hg compound is small, it is impractical to change the supporting electrolytes during the deposition and the stripping of mercury. Thus the whole plating-stripping process has been performed in one supporting electrolyte, 0.1 M HgClO_4 in 0.1 M HClO_4 .

The potential response of the mercury stripping process from the MFE in 0.1 M HClO_4 solution containing 0.1 M HgClO_4 is similar to the response in the HClO_4 solution without HgClO_4 . But the corresponding numerical values of the potential plateaus are different in these two solutions.

Figure 5-3 shows a typical potential-charge variation during stripping in 0.1 M HClO_4 electrolyte solution containing 0.1 M HgClO_4 . This figure shows the stripping of the mercury on the MFE. The horizontal curve comes from the oxidation of the metallic mercury, a 11 mcouls of charge was consumed before the potential started to rise. The curve leveled off for the second time at 1.40 V. The potential hump at the transition appears only when the stripping is started with metallic mercury on the electrode surface.

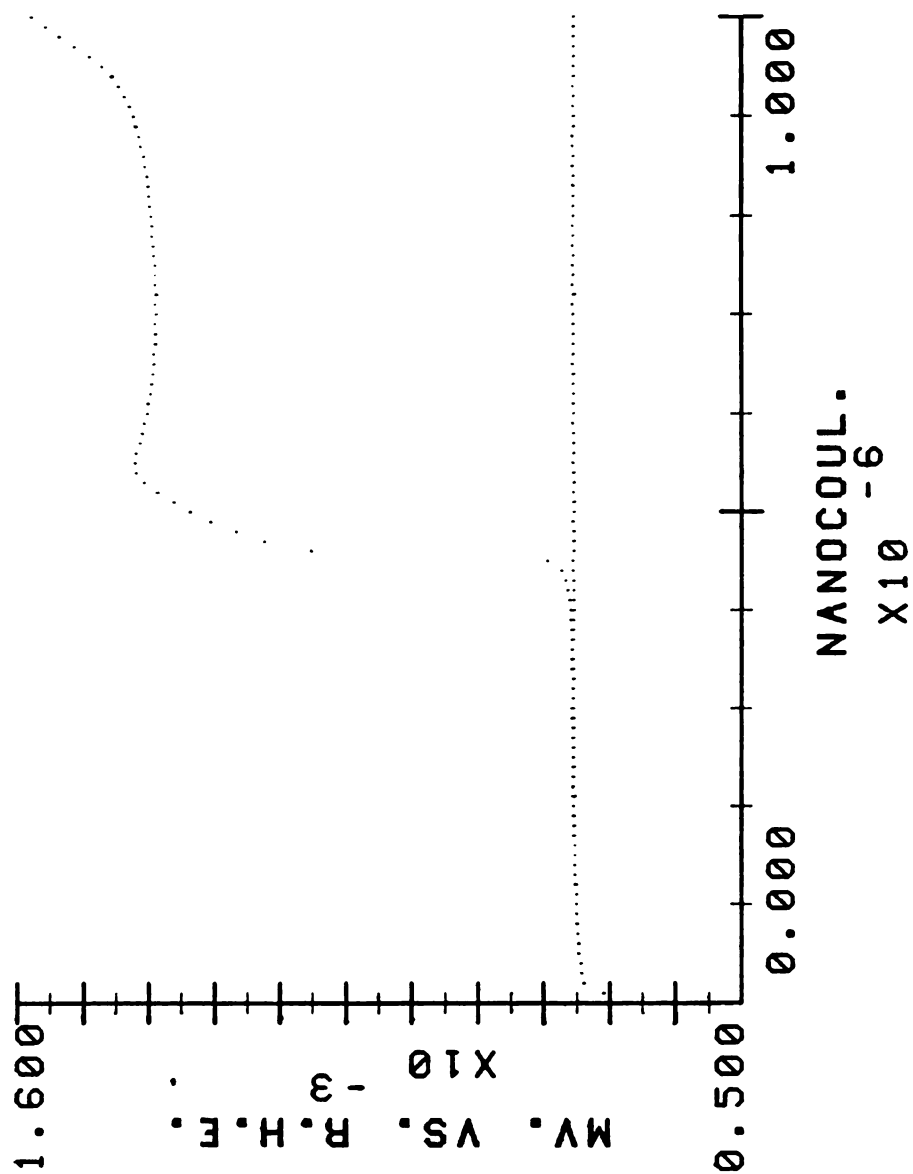


Figure 5-3. Anodic Potential-Charge Characteristic of the MFE
in 0.1 N Mercurous Solution

If the stripping process is halted during the potential rise such as at 1.0 V, and resumed after several minutes, a smooth transition is observed.

3. Disappearance of Metallic Mercury on the PMCCPE

a. Current Reversal Technique

A cathodic current is applied to the PMCCPE for 0.1 sec. and then the polarity of the current is made anodic with the same current amplitude. Figure 5-4 shows the potential-charge response using $\pm 150 \mu\text{A}$ current. The arrow indicates the switching point of current polarity. The potential during the mercury plating shows a slight variation. The duration of the potential plateau during the anodic step is always shorter than the cathodic step. This indicates that the metallic mercury recovered is less than that deposited. Table 5-1 shows the results of these experiments. The mercury in the compound was determined to be 3.0 mcoul.

Although these experiments were carried out within the same period of time, the deviation of deposited mercury increases with higher current amplitude. Assuming $160 \mu\text{coul}/\text{cm}^2$ of mercury atom is required to make a monolayer on platinum surface (17). A quantity of 0.4 $\mu\text{coul.}$ of

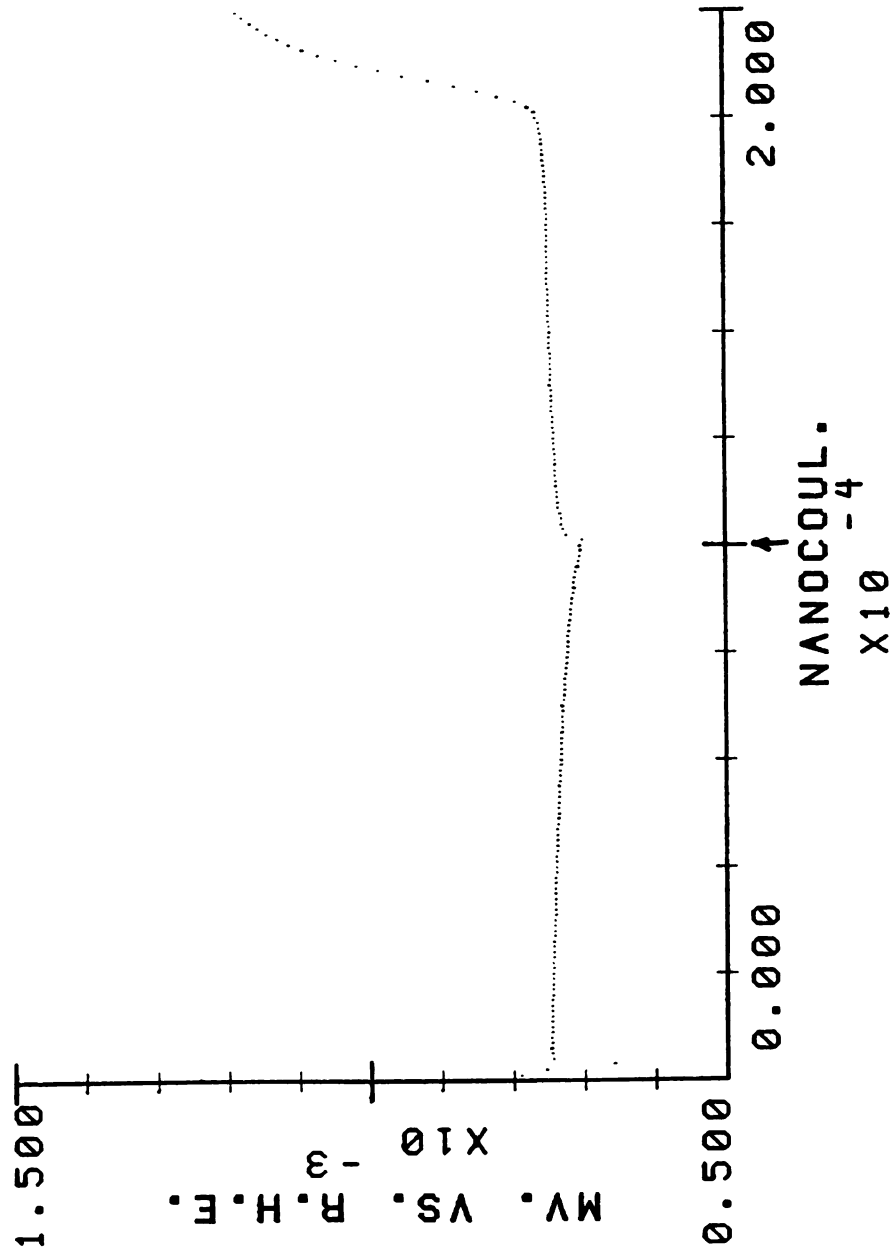


Figure 5-4. Current Reversal Experiment of Metallic Mercury
Stripped MFE in 0.1 M Mercurous Solution.
Current Amplitude = \pm 100 μ A, Overall Process = 0.20 sec.

Table 5-1. Disappearance of Metallic Mercury in
Current Reversal Experiment

Current Amplitude, μA	Q dep, $\mu coul$	Q strip, $\mu coul$	ΔQ , $\mu coul$
± 50.0	5.00	4.25	0.75
± 70.0	7.00	6.01	0.99
± 100.0	10.00	8.83	1.17

charge is required to plate one monolayer of mercury from mercurous ion. It takes a different period of time among the different current amplitudes used to supply this quantity of charge. Thus the actual contact time between the newly plated mercury and the Pt-Hg compound surface differs among these three cases. This should lead to a variation of the quantity of the mercury transformed into the compound.

b. Reduction of Mercurous Ion with High Amplitude Current

A reduction current of high amplitude, -2.400 mA, was chosen for the aging technique experiments. With this current amplitude, the mercurous ion at the electrode surface is depleted within a short time. Soon after the current is started, the charge supplied becomes predominantly used for the reduction of the supporting electrolyte. A potential-time curve is shown in Figure 5-5. At the beginning, the potential drops gradually which indicates that the concentration of the mercurous ion at the electrode surface is decreasing. Then, the potential plunges sharply

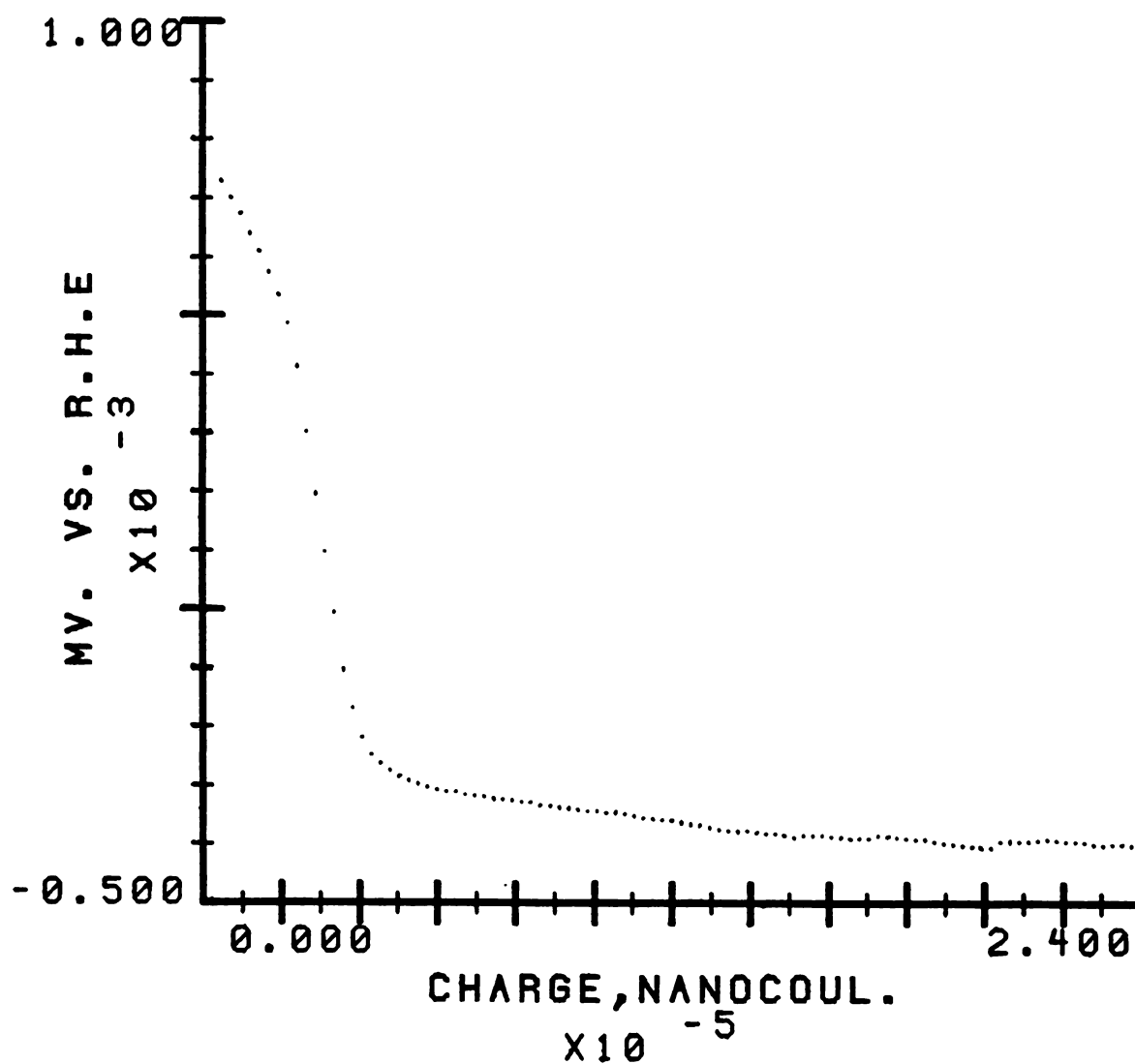


Figure 5.5. Potential-charge variation during reduction of mercurous ions from 0.1 M HgClO_4 using high reduction current

to a rather cathodic potential. After that, the potential varies only slowly with time. The reduction of hydrogen ion becomes predominant. To have a 100 % current efficiency for the reduction of mercurous ion, the current pulse should be restricted to within 20 $\mu\text{coul.}$ In the following experiments described, the current pulses used are 1 msec. long which contains 2.4 $\mu\text{coul.}$ of charge. According to calculation, this amount of charge is equivalent to 6 mercury monolayers on the electrode used. An aging period follows the mercury deposition, and then an anodic current pulse of 1.0 mA is issued. The potential-charge variation is recorded during this step at 40 μs intervals. This deposit-strip cycle is repeated with a longer aging period after several seconds with the same electrode. The whole process is repeated several times after the last cycle. Then, a longer anodic current is issued which ionizes the remaining mercury in the Pt-Hg compound. The quantity of mercury in the compound is determined from the resulting potential-charge curve. Figure 5-6 was obtained from one of the experiments. This electrode required 0.60 mcoul. charge to remove the mercury in compound. Table 5-2 lists the results obtained in this particular experiment. ΔQ is the averaged value from four repetitions of one single experiment.

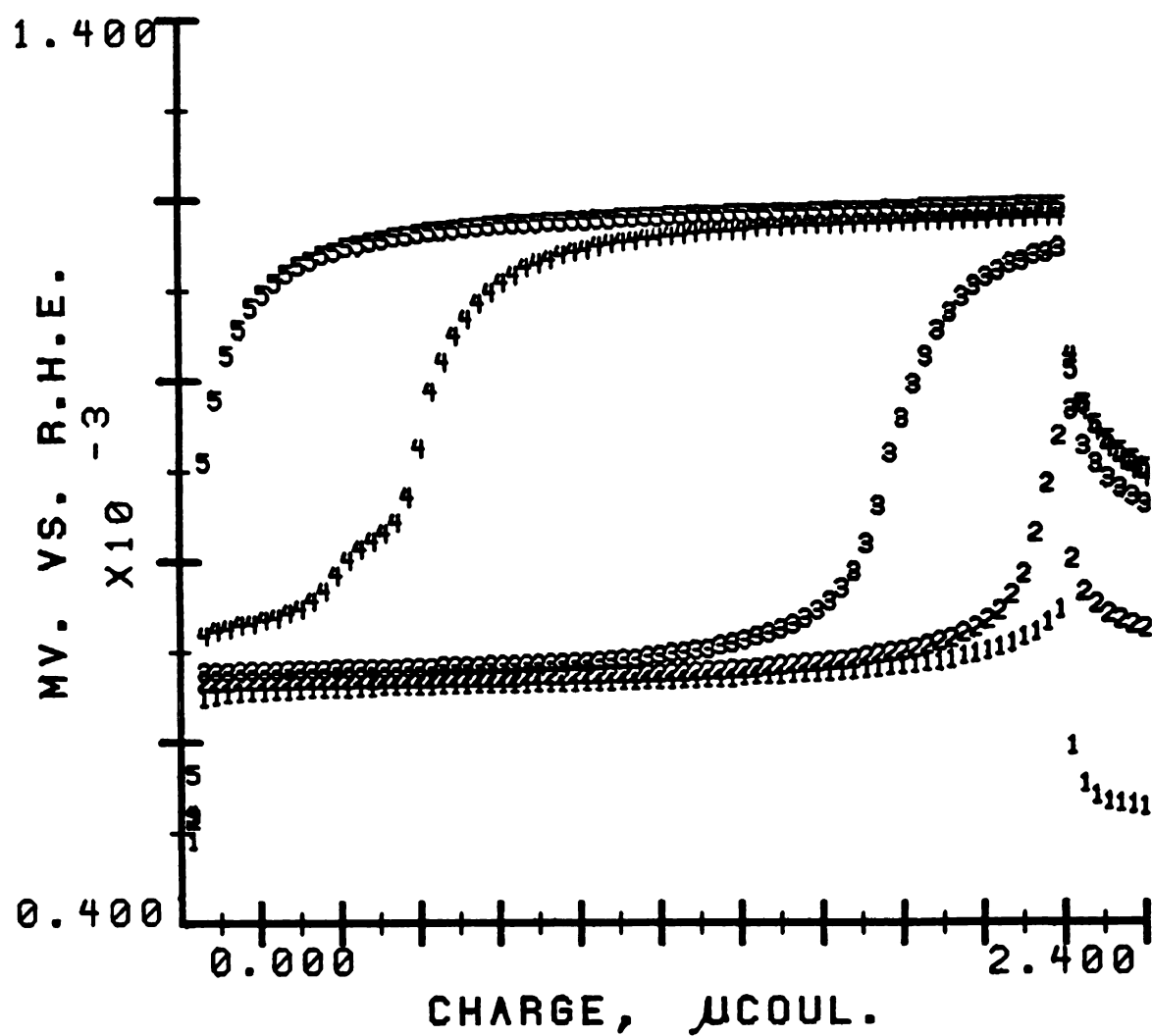


Figure 5-6. Potential-charge variations during repetitive deposition-stripping of mercury with varying aging intervals

Table 5-2. Disappearance of Metallic Mercury in the
Aging Experiment, $Q_{\text{Pt-Hg}} = 600 \text{ } \mu\text{coul.}$

T_{age} , sec.	ΔQ , $\mu\text{coul.}$
0.006	0.05 ± 0.01
0.024	0.15 ± 0.01
0.202	0.22 ± 0.01
0.600	0.49 ± 0.02
1.800	0.84 ± 0.02
5.400	1.60 ± 0.10

The aging period, T_{age} , is the sum of the time interval during the deposition of mercury, the waiting period, and the time required to strip all the metallic mercury remaining on the surface compound. ΔQ , the charge equivalent of mercury converted to the Pt-Hg compound increases with the aging period. A linear relationship is found when ΔQ is plotted vs. $(T_{\text{age}})^{1/2}$. Figure 5-7 shows the results from electrodes with varying amounts of Pt-Hg compound. Curves 1, 3 and 4 correspond to electrodes with 300 μcoul , 600 μcoul , and 750 μcoul equivalents of mercury in the compound respectively. Curve 5, the horizontal line, is obtained with 1.27 mcoul equivalents of mercury in the Pt-Hg compound. Curve 2 is obtained from a repetition of the experiment after the curve 1 data was obtained. Curve 2 shows a large curvature at the end. The metallic mercury has been reduced to less than one mercury monolayer during this time. After the deposit-strip cycle, not all the reduced mercurous ion is oxidized and removed from the electrode surface. However, since the quantity of mercury plated during these cycles is made very small compared to the amount of Pt-Hg compound already exists on the electrode surface, this accumulation of mercury is insignificant compared to the thickness of the compound. Results from consecutive runs show identical compound potential-time curves except for electrodes with very thin compounds such as in curve 1 and curve 2.

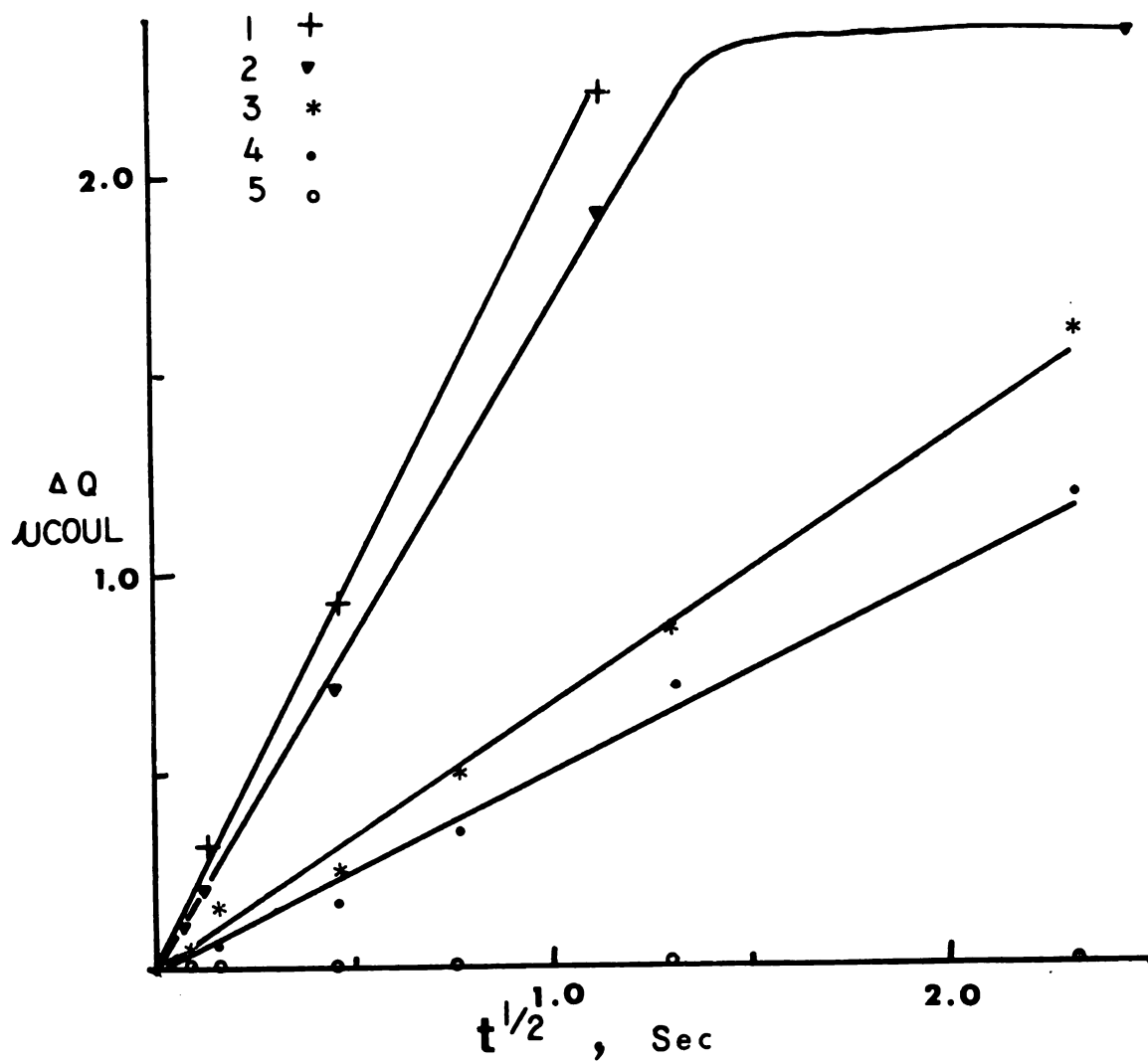


Figure 5-7. Disappearance of Metallic Mercury
with Aging Interval

The slopes of these potential-time curves are plotted in Figure 5-8. The influence of the quantity of the Pt-Hg compound on the rate of reaction is significant. As the compound thickness is increased, the slope of the curve decreases which indicates that the reaction rate is slowed down. When the mercury in the compound is as high as 1.27_{mcoul}, no detectable reaction occurred within the observation time span.

D. Discussion

1. Reaction of Platinum and Mercury on the PMCCPE

Both the current reversal experiments and the aging experiments indicate that the freshly plated mercury on the Pt-Hg compound covered platinum surface is gradually converted into Pt-Hg compound. The rate of this conversion is shown to be a function of the amount of compound already existing on the platinum surface. As the compound thickness increases, the reaction rate decreases which indicates that the Pt-Hg compound inhibits the reaction. This inhibition capability changes rapidly when the thickness of the compound is thin but becomes proportional to the compound thickness as soon as the mercury in the compound exceeds 600 _{ucoul}. The deviation of the reaction rate from the linearity together

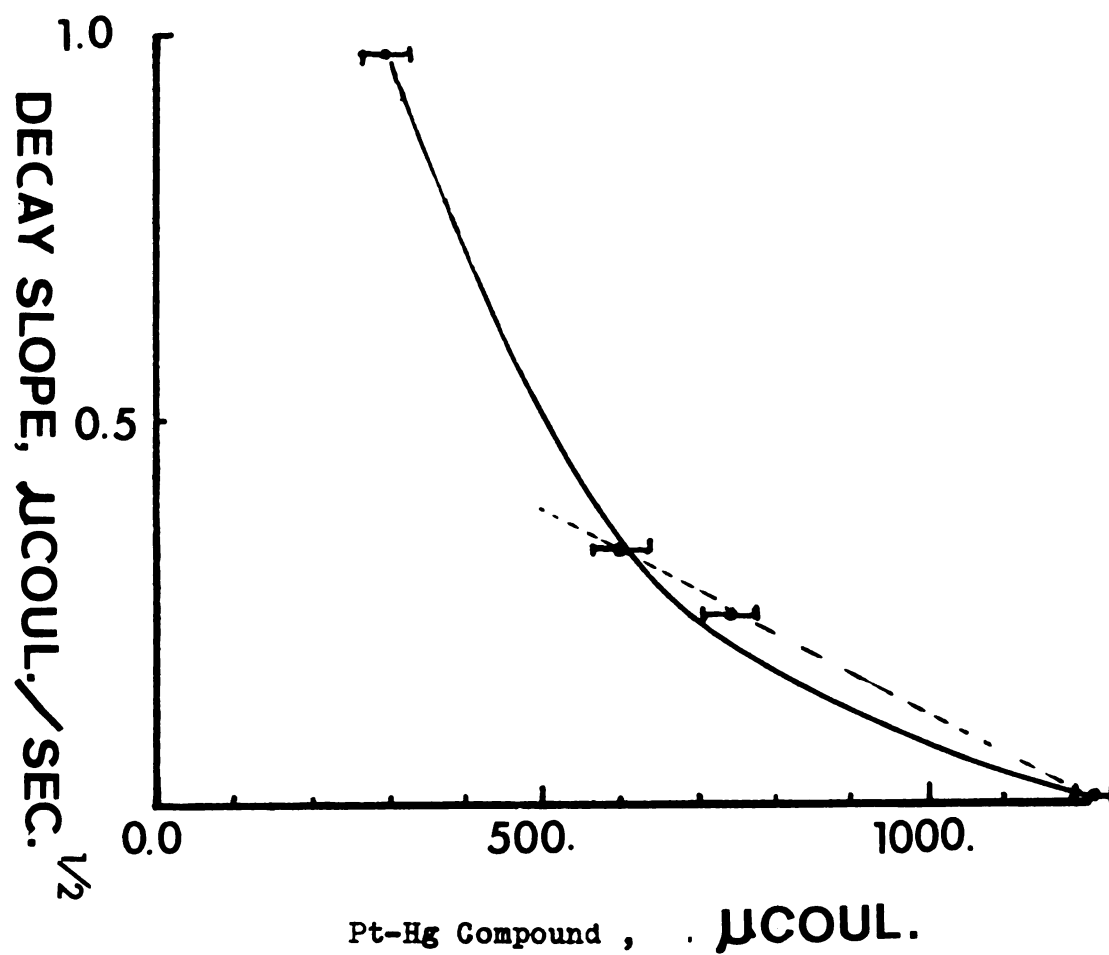


Figure 5-8. Effect of Pt-Hg Compound Thickness on the Reaction Rate of Pt and Hg

with the fact that the large variation of slopes between the repetition with the thin Pt-Hg compound seems to indicate that the Pt-Hg compound is undergoing a significant phase transition during the experiment. The results from the aging experiments indicate that for a given compound thickness, the amount of freshly plated mercury decreases in proportion to the square root of time.

2. Accounting for the Pt-Hg Reaction Rate

Once the mercury plating is initiated, the Pt-Hg reaction starts. Since 2.4 μcoul of charge is used during the mercurous ion reduction, several mercury atom layers are plated on the platinum-mercury compound surface. Therefore, the concentration of the mercury on the surface is equal to unity near the end of the reaction. The time segment of the concentration of the freshly plated mercury can be represented by Figure 5-9, where t_1 , t_2 and t_3 are the aging intervals.

The flux f of the metallic mercury at the interface between the metallic mercury and the Pt-Hg compound is given by :

$$f = \frac{dN}{dt}$$

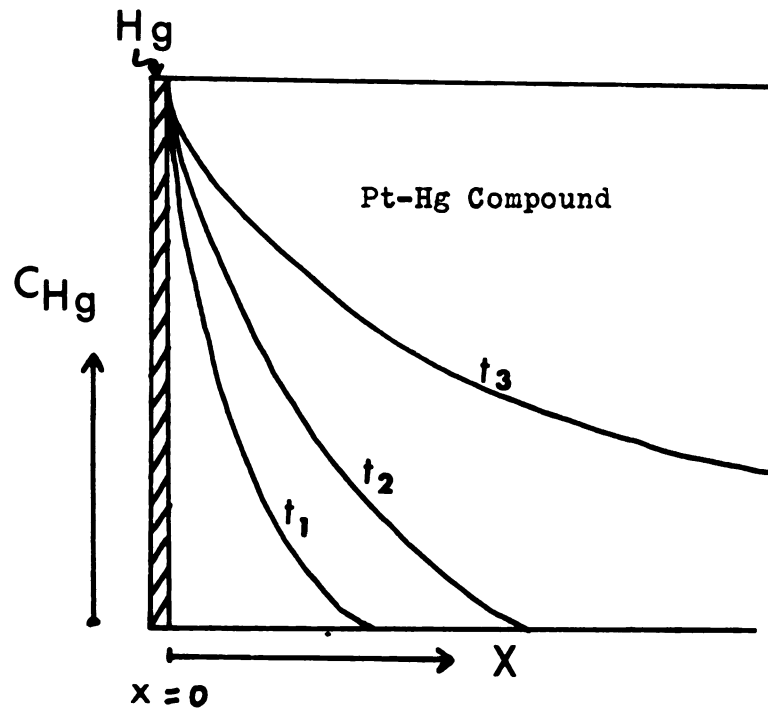


Figure 5-9. Concentration Profile of
Freshly Plated Mercury

where N is the amount of metallic mercury.

Application of Fick's First Law of Diffusion in this case gives

$$(1) \quad \frac{dN}{dt} = -D \frac{\partial C}{\partial x}$$

where C is the concentration of metallic mercury and D is the diffusion constant of the metallic mercury.

$$(2) \quad \frac{\partial C}{\partial t} = -D \frac{\partial^2 C}{\partial x^2}$$

To solve these differential equations, a Laplace transformation can be applied.

By taking the Laplace transform of equation (2) with respect to t ,

$$(3) \quad p C(x, p) - C(x, 0) = D \frac{d^2 C(x, p)}{dx^2}$$

Since at $t=0$ only Pt-Hg compound exists for all x ,

$$(4) \quad P C_{(x,p)} = D \frac{d^2 C_{(x,p)}}{d x^2}$$

Apply the Laplace transform to equation (4) with respect to x to obtain,

$$(5) \quad P C_{(q,p)} = D (q^2 C_{(q,p)} - q C_{(\emptyset,p)} - (\frac{\partial C_{(x,p)}}{\partial x})_{x=0})$$

Move $D q^2 C_{(q,p)}$ to the right side of equation and divide equation (5) by $(q^2 - \frac{P}{D})$ which gives

$$(6) \quad C_{(q,p)} = \frac{D}{q^2 - \frac{P}{D}} (q C_{(\emptyset,p)} + (\frac{\partial C_{(x,p)}}{\partial x})_{x=0})$$

By solving equation (6) for x using reverse Laplace transformation, we have

$$(7) \quad C_{(x,p)} = D C_{(\emptyset,p)} \cosh \left(\frac{P}{D} \right)^{\frac{1}{2}} x + \frac{D}{2P^{\frac{1}{2}}} \left(\frac{\partial C_{(x,p)}}{\partial x} \right)_{x=0} \sinh \left(\frac{P}{D} \right)^{\frac{1}{2}} x$$

By rearranging equation (7), we have

$$(8) \quad C_{(x,p)} = \left(\frac{C_{(\emptyset,p)}}{2} + \frac{D^{\frac{1}{2}}}{2P^{\frac{1}{2}}} \left(\frac{\partial C_{(x,p)}}{\partial X} \right)_{x=0} \right) e^{\left(\frac{P}{D}\right)^{\frac{1}{2}} x} \\ + \left(\frac{C_{(\emptyset,p)}}{2} - \frac{D^{\frac{1}{2}}}{2P^{\frac{1}{2}}} \left(\frac{\partial C_{(x,p)}}{\partial X} \right)_{x=0} \right) e^{-\left(\frac{P}{D}\right)^{\frac{1}{2}} x}$$

The first term on the right side of equation (8) is 0, because as $X \longrightarrow \infty$, $C_{(x,p)} = 0$. So that

$$(9) \quad C_{(\emptyset,p)} = - \frac{D^{\frac{1}{2}}}{2P^{\frac{1}{2}}} \left(\frac{\partial C_{(x,p)}}{\partial X} \right)_{x=0}$$

Since the concentration of the metallic mercury at $x=0$ is equal to 1,

$$C_{(\emptyset,t)} = 1,$$

$$C_{(\emptyset,p)} = L (C_{(\emptyset,p)}) = \frac{1}{P}$$

Thus,

$$(10) \quad C_{(\emptyset,p)} = - \frac{D^{\frac{1}{2}}}{P^{\frac{1}{2}}} \left(\frac{\partial C_{(x,p)}}{\partial X} \right)_{x=0}$$

or

$$(11) \quad \left(\frac{\partial c(x,p)}{\partial x} \right)_{x=0} = - \frac{1}{p^{\frac{1}{2}} D^{\frac{1}{2}}}$$

Reverse the transformation of equation (11) with respect to t which gives

$$\left(\frac{\partial c(x,t)}{\partial x} \right)_{x=0} = \frac{-1}{D^{\frac{1}{2}} t^{\frac{1}{2}} \pi^{\frac{1}{2}}}$$

$$(12) \quad \frac{dN}{dt} = \left(\frac{\partial c}{\partial x} \right)_{x=0} = - \frac{1}{D^{\frac{1}{2}} t^{\frac{1}{2}} \pi^{\frac{1}{2}}}$$

$$\text{or } dN = - \frac{2}{\pi^{\frac{1}{2}} D^{\frac{1}{2}}} dt^{\frac{1}{2}}$$

The decrease of metallic mercury dN is shown proportional to the square root of time.

A linear relationship between N, the amount of metallic mercury, and $t^{\frac{1}{2}}$ is expected from this derivation. For Pt-Hg reaction on the PMCCPE, this relationship is observed in the experiment as is shown in Figure 5-7.

In this derivation, Fick's Laws of Diffusion are used. The actual transportation mechanism of the metallic mercury through the reaction is not known. Since only one crystalline structure between mercury and platinum has been found on the mercury coated platinum electrode, the mercury atom transport in the Pt-Hg compound must be different from the diffusion phenomena occurring in the liquid state. Equation (2) shows that the decrease of metallic mercury is proportional to $t^{\frac{1}{2}}$ with the proportional constant $\frac{2}{\pi^{\frac{1}{2}} D^{\frac{1}{2}}}$. Unlike the diffusion process in liquid state, D, the diffusion constant, shows a large variation when the amount of compound is varied.

CHAPTER VI

FUTURE STUDY

A smooth mercury film electrode obtained by the chloride ion masking procedure has been applied in the anodic stripping analysis of cadmium ion. A preliminary study shows about a 10-fold increase in sensitivity, down to 10^{-7} M using the film electrode as compared to the hanging drop mercury electrode. Higher sensitivity is possible through the optimization of the procedures. This can be achieved through the usage of rotational MFE electrode, thinner mercury film, and the coulometric anodic stripping technique.

APPENDICES

APPENDIX 1:

Computer Interface

A special computer interfacing circuit called the 11-8 Emulator was designed by Dr. Enke's research group for the PDP 11/40 computer. This interface enables the PDP 11/40 to generate several control signals similiar to the PDP 8 computer.

The complete interface consists of a general device interface, the 11-8 Emulator and an interface buffer. The block diagram is shown in Figure A. 1.

The general device interface, DR11-C, provides the logic and buffer registers necessary for program - controlled parallel transfer of 16-bit data between a PDP 11 system and the external device. It has three registers : control and status, input buffer and output buffer. Each register has an address. Data is written into or read from the corresponding register when a particular register is addressed.

The 11-8 Emulator provides the logic necessary to generate control signal lines and data lines similiar to these of the PDP 8 system. These control lines are three IOP lines, six DS line and one $\overline{\text{SKP}}$ line.

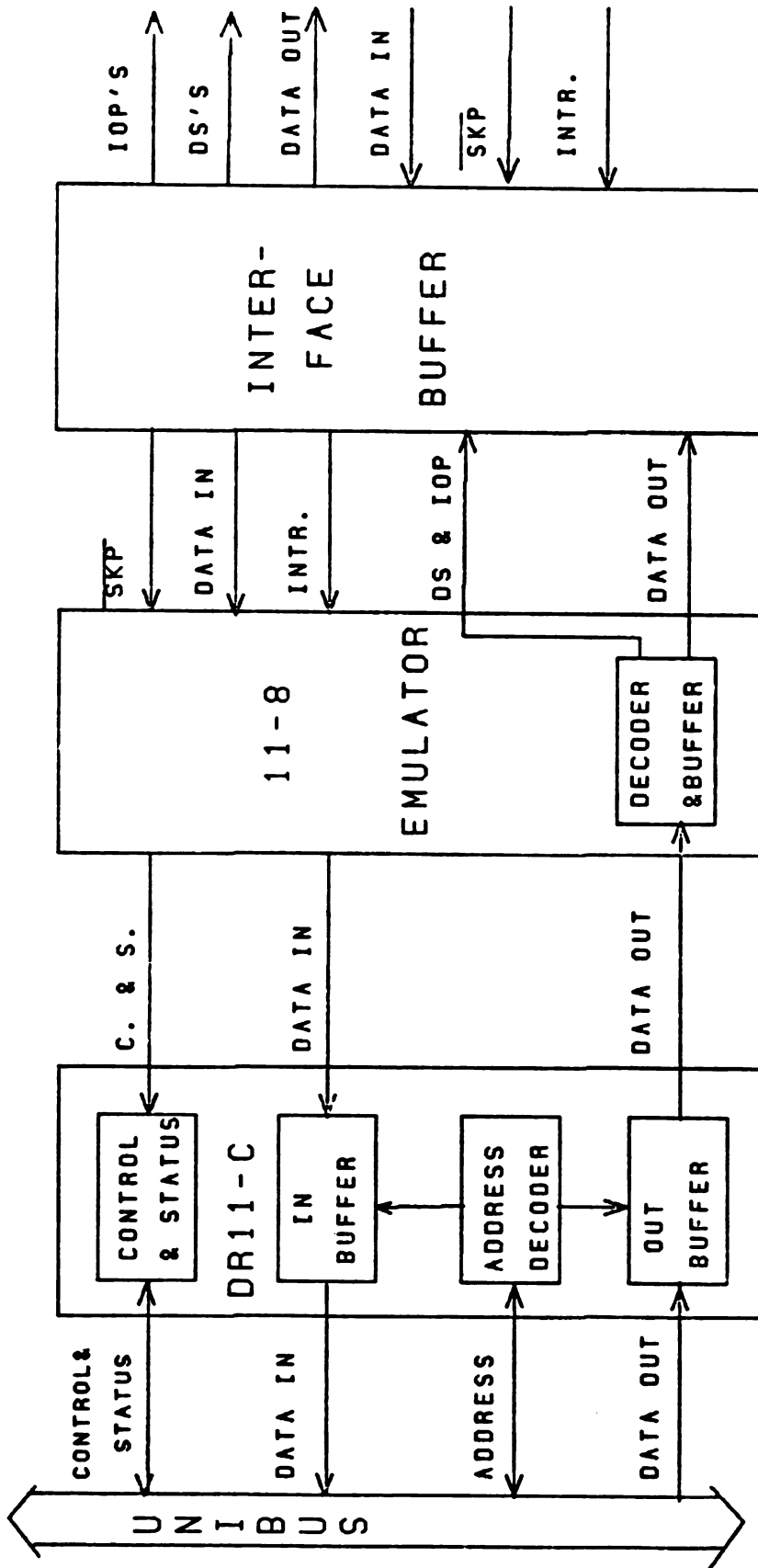


FIGURE A.1 COMPUTER INTERFACE

Each IOP line carries one IOP signal, namely IOP1, IOP2 or IOP4. When a particular IOP command is issued, a pulse of 0.2 μ sec is generated on the corresponding line. These pulses are used with the device select lines to accomplish all control functions.

The device - select (DS) lines are decoded into a two - digit octal number. Since each device is assigned with one particular number, it is chosen by selecting the proper number.

The $\overline{\text{SKP}}$ line is normally at a HI state. When the $\overline{\text{SKP}}$ line is grounded to a low state, the emulator pulls down bit zero of the status and control register of the DR11-C. It signals the CPU that certain condition of the external device has been reached and a decision could be made accordingly.

The interface buffer provides logic for buffering the input data, output data and all control signals.

Addresses of buffer registers in DR11-C

CSR = 167760

IN = 167764

OUT = 167762

APPENDIX 2

Program Listings

*****;

THESE ASSIGNMENTS ARE
COMMON TO ALL MACRO PROGRAMS

; REGISTERS

R0=%0
R1=%1
R2=%2
R3=%3
R4=%4
R5=%5
SP=%6
PC=%7
SR=177570

;

; 8/11 INTERFACE REGISTERS

;

CSR=167760
OUT=167762
IN=167764

;

; REAL TIME CLOCK REGISTERS

;

CKCSR=172540
PGCNTR=172542
CKINIT=172544
PGINEB=20000

; PGCNTR INTERRUPT ENABLE

;

; REGISTERS IN THE COULOSTATIC INSTRUMENT

;

ZERO=16011
PULSE=16157
HEIGHT=16142
LENGTH=16141
CONVRT=16561
DONE=16562
ADREAD=16564
TIMEBS=16121
CHANLD=16144

CONVENTIONS
MACROS

```
;
; THE FOLLOWING MACROS ARE DESIGNED TO FACILITATE THE
; PROGRAM DEVELOPMENT
;;
    .MACRO AXIS
        MOV #FTSTAK,R4
        MOV #0,(R4)
        JSR R5,T4010W
        MOV #FTSTAK,R4
        MOV #5,(R4)
        MOV #12,2(R4)
        MOV #7,4(R4)
        JSR R5,T4010W
    .ENDM
;;
    .MACRO PLOT
        MOV #FTSTAK,R4
        MOV #6,(R4)
        JSR R5,T4010W
    .ENDM
;;
    .MACRO WRITE MESSAGE
        MOV #MESSAGE,R1
        JSR R5,PUTR1
    .ENDM
;;
    .MACRO RSTCK AA
        BIS #4,CKINIT
CL'AA': BIT #40000,CKCSR
        BEQ CL'AA'
    .ENDM
;;
    .MACRO READ DATA
        MOV R4,-(SP)
        MOV #DATA,R4
        JSR R5,INPUT
    .ENDM
;;
    .MACRO FLAG IOPX,A
        NOP
'A'101: MOV #IOPX,OUT
        TSTB CSR
        BPL 'A'101
    .ENDM
;;
    .MACRO SETN DUM1,NUMB ;USE IOP DUM1 TO SET CONTROL
        MOV #NUMB,OUT ;WORD
        MOV #DUM1,OUT
    .ENDM
;;
    .MACRO READ DATA
        MOV R4,-(SP)
```

CONVENTIONS
MACROS

```
        MOV #DATA, R4
        JSR R5, INPUT
        . ENDM

;;

        . MACRO SETA DUM3, ADR1 ; DUM3 IS THE IOP
        MOV ADR1, OUT          ; TO SENT A DATA LOCATED
        NOP
        NOP
        MOV #DUM3, OUT         ; IN ADR1
        . ENDM

;;

;;

        . MACRO DATAAG DUM5, ADR2 ; DATA IS ACQUIRED WITH
        MOV #DUM5, OUT          ; IOP DUM5 AND PLACED IN ADR2
        NOP
        NOP
        NOP
        MOV IN, ADR2
        . ENDM

;;

        . MACRO SENT DUMMY
        MOV #DUMMY, OUT
        . ENDM
```

QUANTF

```
C
C
C      QUANTF. FTN
C
C      VERSION: A1
C
C      MINCHEN WANG
C
C      MARCH 24 77
C
C      PURPOSE: MEASURE PULSE CHARGE
C
C
C      A. CHANNEL 1,2,3,4
C
C      B VOLTAGE +-5,+-4,+-3,+-2,+-1,0 VOLT
C
C      C. PULSE WIDTH USEC. DEPENDS ON CHANNEL USED.
C
C
C      SUBROUTINE CALLED  QUANM. MAC
C      Q(IWIDTH)
C
C
C      DIMENSION IWIDTH(20),A(5),Q(10),AMP(50)
C      DOUBLE PRECISION VD
C      BYTE CNTR(4)
C      BYTE FNAME(40),TODAY(9)
C      EQUIVALENCE (FNAME(11),CNTR)
C      COMMON AMP
C      DATA IWIDTH/2,8,16,32,40,10,40,80,150,300,10,100,500,
C      11000,2000,50,100,500,1000,4000/
C      MM=0
C      II=0
C      WRITE(6,10)
C      READ(6,21)CAP
10  FORMAT('$CAPACITANCE OF CALIB. CAPACITOR ,MFD = ')
C      WRITE(6,49)
C      READ(6,51)ICH
C      WRITE(6,11)
11  FORMAT('$FILE NAME: ')
C      CALL AMPLI
C      READ(6,12)FNAME
12  FORMAT(40A1)
C
C      CHANNEL 1 TO 4
C
21  FORMAT(F10.5)
C      DO 60 JI=ICH,4
C      ICHAN=JI
```

QUANTF

```
C
C      PULSE HIGH
C
      DO 50 JK=1, 11
      JV=1000*(JK-1)-5000
C
C      5000 IS USED TO MAKE COMPLEMENT
C
C      2.441MV IS ONE BIT SIZE
C
C      COMPLEMENTARY VALUE IS LOADED
      VVO=FLOAT(JV)
      VO=FLOAT(JV)
      VO=-(VO-4998.78)/2.4414
      JV=IFIX(VO)
C      INCREMENT AMPLIFICATION INDEX
      MM=MM+1
      DO 40 K=1, 5
C
C      JJ POINTS TO THE PULSE WIDTH DATA
C
      JJ=(JI-1)*5+K
      JVOLT=IWIDTH(JJ)
      A(K)=FLOAT(IWIDTH(JJ))
      CALL QUANM(JVOLT, ICHAN, JV)
      Q(K)=FLOAT(JVOLT)*CAP
40    CONTINUE
      WRITE(6, 109)MM
109   FORMAT(I3)
      II=II+1
      ENCODE (4, 100, CNTR)II
100   FORMAT(I2)
      CALL ASSIGN(4, FNAME, 40, IERR)
      WRITE(4, 111)
111   FORMAT('; ')
      WRITE(4, 112) FNAME
112   FORMAT('; ', 40A1)
      WRITE(4, 113)
113   FORMAT('; ')
      CALL DATE(TODAY)
      WRITE(4, 104)TODAY
104   FORMAT('; '20A1)
      WRITE(4, 110)
110   FORMAT('; DATA FROM QUANF.FTN ')
      WRITE(4, 150)ICHAN
150   FORMAT('; CURRENT CHANNEL. ='I2)
      WRITE(4, 151)VVO
151   FORMAT('; VOLTAGE USED, MV, 'F15.0)
      WRITE(4, 105)
105   FORMAT('; THIS PROGRAM MEASURES PULSE CHARGE')
      WRITE(4, 108)
```


QUANTF

```
108  FORMAT(';  WIDTH MICROSEC.  CHARGE,  MICROCOUL.  ')  
      DO 2 I=1,5  
      A(I)=A(I)-0.44  
C  
C      PULSE WIDTH=IWIDTH-0.44  
C  
      Q(I)=Q(I)/(AMP(MM)*0.4096)  
2      WRITE(4,101)A(I),Q(I)  
101   FORMAT('RD',2F15.5)  
      N=I-1  
      WRITE(4,103) N  
103   FORMAT('ED END OF FILE. ',I5)  
      END FILE 4  
50    CONTINUE  
60    CONTINUE  
49    FORMAT('$START FROM CHANNEL  ')  
51    FORMAT(I1)  
      END
```

QUANM

```

        . TITLE PULSE CHARGE MEASUREMENT
        . IDENT /B2/
        . PSECT QUANT, RW, I, REL
        . NLIST TTM, BEX, MEB
;
;       MINCHEN
;       MARCH 24 77
;
        . GLOBL QUANM
        . MCALL . INIT, . WRITE, . WAIT, . EXIT, . READ, . RLSE
        . MCALL . BIN20, . F4DEF, . O2BIN
        . F4DEF 0
;
;
        . PSECT
QUANM:  MOV R5, RET
        MOV @2(R5), PL           ; PULSE LENGTH
        MOV @4(R5), ICHAN        ; CHANNEL #
        MOV @6(R5), PH           ; PULSE AMPLITUDE
        MOV #20, NPOINT          ; 16 POINTS AVERAGE
        BIC #170000, PH
        MOV #4000, CHANNO
        MOV #3, CKBASE           ; TIMEBASE OF THE DM CLOCK
                                   ; DEPENDS ON CHANNEL NO.

        SETA HEIGHT, PH
CNLSEL: DEC ICHAN
        BEQ CHAN
        MOV #4, CKBASE          ; WAIT 10 MS. BETWEEN DATA
                                   ; FOR CH. 2, 3 AND 4
        ROR CHANNO              ; NEXT CHANNEL
        BR CNLSEL
CHAN:   SETA CHANLD, CHANNO
        MOV CKBASE, CKCSR        ; SET TIME BASE FOR DM
        BIC #170000, PL
Q1:     SETA TIMEBS, TBASE        ; 1 USEC.
        SETA LENGTH, PL
;
;       CHECK STORAGE CAPACITOR
;
;       SET REAL TIME CLOCK
;
;       START DATA ACQUISITION
;
        RSTCK A2
DECHAR: BIS #200, CKINIT          ; CLEAR DM FLAG
        SENT CONVRT              ; CHECK POTENTIAL
        FLAG DONE, A3
        DATAQ ADREAD, PVOL      ; CAPACITOR DISCHARGE YET
        BIC #170000, PVOL        ; STRIP OFF THE FIRST 4 BITS
        CMP #7776, PVOL          ; .GE. 1 ?
        BMI CONT                 ; YES -> DECHARGE, OTHERWISE

```

QUANM

```

; CONTINUE
WRITE MS1
Q2:   MOV #16011,OUT      ; PUSH BUTTON IF READY HERE
      NOP
      TSTB CSR
      BPL Q2
CONT: RSTCK A1
      MOV #DATABF,R2
      BIS #200,CKINIT
      SENT PULSE
CKA4: BIT #100,CKCSR
      BEQ CKA4
      BIS #200,CKINIT
      SENT CONVRT
      FLAG DONE,B1
      DATAAQ ADREAD,(R2)
COMP: COM (R2)           ; THESE FOUR INSTRUCTIONS ARE
                        ; INSERTED HERE TO ALLOW 10 U.
                        ; SEC. BEFORE DATA CONVERSION

      BIC #170000,(R2)+
      DEC NPOINT
      BNE CKA4
      MOV #20,R4
      MOV #DATABF,R2      ; R2-> DATA BUFFER HEAD
SUM:  ADD (R2)+,R3
      SOB R4,SUM
      MOV #4,R4
DIV:  BIC #1,R3           ; CLEAR LEAST SIGNIFICANT BIT
      ROR R3
      SOB R4,DIV         ; DEVIDE BY 16
RETURN: MOV RET,R5
      MOV R3,@2(R5)
      RTS R5
FINISH: .EXIT
;
;
INPUT: MOV R0,-(SP)      ; SAVE R0
      MOV #BUFHD,R0      ; R0->BUFFERHEAD
      MOV R4,6(R0)       ; SET ADDRESS FOR LINE BUFFER
;
      MOV NUMW,(R0)      ; SET MAX WORD COUNT
READER: .INIT #LINBK
        .READ #LINBK, BUFHD
        .WAIT #LINBK
        .RLSE #LINBK
        MOV (SP)+,R0
        MOV (SP)+,R4
        RTS R5
PUTR1: MOV R5,-(SP)      ; SAVE R5
      MOV #BUFHD,R5      ; POINT TO BUFFER HEADER
      MOV R1,6(R5)       ; STORE THE CONTENT OF R1
      CLR R0             ; BYTE COUNT

```

QUANM

```

COUNT1: INC R0
          TSTB (R1)+          ; COUNTING THE NO. OF BYTE
          BNE COUNT1
          MOV R0, 4(R5)       ; STORE THE ACTUAL BYTE COUNT
          MOV #LINBK, R0      ; MOVE TO THE DEVICE HANDLER
          .INIT R0
          .WRITE R0, R5
          .WAIT R0
          .RLSE R0
          MOV (SP)+, R5
          RTS R5

;
          .EVEN
          .WORD FINISH
LINBK:    .WORD 0000
          .RAD50 /KB/
          .BYTE 1, 0
          .RAD50 /KB/

;
BUFHD:    .WORD 6
          .BYTE 6, 1
          .WORD 6
          .WORD 0
MS1:      .BYTE 15, 12
          .ASCIZ /SHORT CAP. /
          .EVEN
DATABF:   .BLKW 20
NPOINT:   .WORD 0
NPLSE:    .WORD 0
PVOL:     .WORD 0          ; PREPULSE POTENTIAL.
PH:        .WORD 0
COUNT:   .WORD 0
RET:       .WORD 0
DATAHD:   .WORD 0
TMP:       .WORD 0
N1:        .WORD 0
TBASE:    .WORD 0
CHANNO:   .WORD 0
PL:        .WORD 0
ICHAN:    .WORD 0
CKBASE:   .WORD 2
          .END QUANM

```

SLOPE

```
C
C
C      SLOPE. FTN
C
C      MINCHEN WANG
C
C      OCT. 29  1977
C
C
C      SUBROUTINE CALLED LINFIT(LINFIA. FTN)
C
C      PURPOSE: OPEN FILE SET AND CALCULATE THE SLOPES
C               OF EACH FILE, STORE THE RESULTS IN A NEW FILE.
C
C      USAGE: INPUT  NUMBER OF DATA FILES, FILE NAMES,
C               NO. OF DATA POINTS TO BE AVERAGED
C
C      DIMENSION Y(100), INTCPT(100), SLOPE(100), TIME(100)
C      DIMENSION SIGMAY(100)
C      BYTE FNAME(20), LINE(80), TODAY(10)
C      EQUIVALENCE (JFLAG, LINE(1))
C      WRITE(6, 101)
C      READ(6, 102) NFILE
C      WRITE(6, 103)
C      READ(6, 104) NPTS
C      DO 2 I=1, NFILE
C      WRITE(6, 105)
C      READ(6, 106) FNAME
C      CALL ASSIGN(4, FNAME, 20, IERR)
C      DO 1 J=1, NPTS
4      READ(4, 201) LINE
201  FORMAT(80A1)
      IF (JFLAG. EQ. 2HED) GO TO 1
      IF (JFLAG. EQ. 2HRD) GO TO 903
      GO TO 4
903  DECODE(32, 904, LINE) TIME(J), Y(J)
904  FORMAT(2X, 2E15. 7)
1    CONTINUE
      END FILE 4
C
C      CALL LEAST SQUARE FITTING ROUTINE
C
C      MODE=0
C      CALL LINFIT(TIME(1), Y(1), SIGMAY(1), NPTS, MODE, A, SIGMAA
1, B, SIGMAB, R)
C      INTCPT(I)=A
C      SLOPE(I)=B
2    CONTINUE
C
C      CREAT DATA FILE
C
```

SLOPE

```
        WRITE(6,125)
        READ(6,106)FNAME
        CALL ASSIGN(4,FNAME,20,IERR)
        WRITE(4,111)FNAME
111    FORMAT(';FNAME:'40A1)
        CALL DATE(TODAY)
        WRITE(4,113)TODAY
113    FORMAT('; ',20A1)
        WRITE(4,112)
112    FORMAT('; DATA NO.      SLOPE, MCOUL./SEC.      SIGMAY')
        DO 129 I=1,NFILE
            X=FLOAT(I)
            WRITE(4,129)X,SLOPE(I),SIGMAY(I)
129    FORMAT('RD',3F15.5)
        DO 140 I=1,NFILE
            WRITE(4,131)INTCPT(I)
131    FORMAT('YI',F15.5)
140    CONTINUE
        WRITE(4,132)SIGMAA,SIGMAB
132    FORMAT('; SIGMAA=',F15.5,' SIGMAB= 'F15.5)
        WRITE(4,134)R
134    FORMAT('; CORRELAION COEFFICIENT = ',F15.5)
        WRITE(4,133)
133    FORMAT('ED')
        END FILE 4
101    FORMAT('$NO. OF DATA FILES TO BE PROCESSED<*>  =')
102    FORMAT(I2)
103    FORMAT('$NO. OF DATA POINTS IN A FILE <***>=')
104    FORMAT(I3)
105    FORMAT('$ FILE NAME  ')
125    FORMAT('$NEW FILE NAME  ')
106    FORMAT(20A1)
        END
```

CAPF3

```
C
C
C      DIFFERENTIAL CAPACITANCE MEASUREMENT
C
C      CAPF3.FTN
C
C      MINCHEN WANG
C
C      SEP 5 77
C
C      SUBROUTINE CALLED: DCAP(CAPM3.MAC),LINFIT(LINFIB.FTN)
C
C      A MODIFICATION OF CAPF2.FTN TO ALLOW ENTERING OF
C      PULSE HIGH AND LENGTH
C
C      TWO DATA FILES ARE CREATED : ORIGINAL FILE AND FITTED
C      EXPOENTIAL DECAY DATA FILE .
C
C      CAP=Q/V
C      LOG V=LOG V(T=0)-[(NF/RT)*(I/CAP)*T]
C
C
C      DIMENSION IV(100),VI(100),IT(100),TIME(100)
C      DIMENSION VJ(100),SIGMAY(100)
C      BYTE FNAME(40),TODAY(9),AA(2)
C      EQUIVALENCE (IFLAG,AA(1))
C
C      MAXIMUN CURENT=2.5 M AMP
C      1 MAMP HAS A D/A SETTING OF 1600
C
C      1  WRITE(6,116)
C          READ(6,117)CURNT
C          VO=-(2.0*CURNT-5000.0)/2.4414
C          JPH=IFIX(VO)
C          WRITE(6,118)
C          READ(6,119)JPL
C          WRITE(6,11)
C          READ(6,12)AMP
C          WRITE(6,33)
C          READ(6,32)ICHAN
C          NPTS=100
C          IVEQ=ICHAN
C          CALL DCAP(IV(1),IVEQ,JPH,JPL)
C
C      IVEQ IS USED TO PASS CHANNEL NO.
C
C      DATA FITTING
C
C      VEG=FLOAT(IVEQ)/(AMP*.4096)
C      DO 10 I=1,NPTS
```

CAPF3

```

      VI(I)=FLOAT(IV(I))
10    VI(I)=ABS((VI(I)/(AMP*0.4096))-VEG)
      DO 20 I=1,NPTS
21    IF(VI(I).GT.0.0)GOTO 22
C
C    ASSIGN V(I) TO A NONZERO VALUE
C
      VI(I)=1.0
22    SIGMAY(I)=VI(I)
C
C    FOR THE LINEARIZED EXPOENTIAL EQ. FITTING,
C    SIGMAY IS EQUAL TO Y ITSELF
C
C    38.39 PER POINT, 10 USEC THE FIRST POINT
C
C    MODE =1, WEIGHT =1/SIGMAY(I)**2
C
C
      PERIOD=38.39
      TIME(I)=PERIOD*(I-1)+10.0
20    VJ(I)=ALOG(VI(I))
      MODE=1
      DO 15 I=1,NPTS
      WRITE(6,16) VI(I),VJ(I)
15    CONTINUE
11    FORMAT('$AMPLIFICATION FACTOR= ')
12    FORMAT(F10.5)
16    FORMAT(2F15.3)
      GO TO 44
31    WRITE(6,18)
      READ(6,19)NSTART,NSTOP
18    FORMAT('$ START AND STOP OF DATA FITTING **,*** ')
19    FORMAT(I2,I3)
      NTMP=NSTOP-NSTART+1
      DO 39 I=1,NTMP
      J=I+NSTART-1
      VJ(I)=VJ(J)
      TIME(I)=TIME(J)/1000.0
39    CONTINUE
      CALL LINFIT(TIME(1),VJ(1),SIGMAY(1),NTMP,MODE,A,
1SIGMAA,B,SIGMAB,R)
      VZERO=EXP(A)
C
C    SINCE CURRENT,CURNT HAS UNIT OF UAMP. UNIT CHANGE
C    IS REQUIRED TOGIVE UF FOR CAPACITANCE
C    VZERO: VOLTAGE CHANGED AT TIME 0, MVOLT.
C
C
C    PULSE LENGTH=JPL-0.53 *TIME UNIT( USEC. )
C

```


CAPF3

```

CAP=CURNT*((FLOAT(JPL)-0.53)/1000.0)/VZERO
RESIS=1.0/(CAP*B)
TMBASE=PERIOD/1000.0
DO 43 NN=1,NPTS
PERIOD=TMBASE*NN
43  VI(NN)=VZERO*EXP(B*PERIOD)
C
C
C  CREAT FILE
C
44  CONTINUE
WRITE(6,100)
100  FORMAT('$ FNAME: ')
READ(6,101)FNAME
101  FORMAT(40A1)
CALL ASSIGN(4,FNAME,40,IERR)
WRITE(4,102)FNAME
102  FORMAT('; FNAME: '40A1)
CALL DATE(TODAY)
WRITE(4,103)TODAY
103  FORMAT('; ',20A1)
WRITE(4,120)VEG
120  FORMAT('; EQUIL POTENTIAL ',F15.5,' MVOLT')
WRITE(4,122)VZERO
122  FORMAT('; POTENTIAL AT ZERO TIME ',F15.5,' MVOLT ')
DO 121 I=1,NPTS
TIME(I)=38.39*(I-1)+10.0
VOLT=VI(I)
TIME1=TIME(I)
WRITE(4,121)TIME1,VOLT
121  FORMAT('RD',2F15.5)
IF (CAP.EQ.0.0) GO TO 139
WRITE(4,130)CAP
WRITE(4,129)RESIS
129  FORMAT('; RESISTANCE= 'F15.5' KOHM ')
130  FORMAT('; DIFFERENTIAL CAP: 'F15.5,' UF')
WRITE(4,131)B
131  FORMAT('; SLOPE OF DECAY CURVE: ' F15.7' LOG(MVOLT)
1VERSUS MS. ')
WRITE(4,132)SIGMAA,SIGMAB
132  FORMAT('; SIGMAA= ,F15.5,' SIGMAB= 'F15.5)
WRITE(4,134)R
134  FORMAT('; CORRELAION COEFFICIENT = ',F15.5)
WRITE(4,133)
END FILE 4
C
C CAP=0.0 FOR THE DATA FILE
C
CAP=0.0
GOTO 1
139  WRITE(4,133)
```

CAPF3

```
133  FORMAT('ED')
      END FILE 4
      GO TO 31
116  FORMAT('$PULSE HIGH, MICROAMP= ')
117  FORMAT(F15.5)
118  FORMAT('$PULSE LENGTH, USEC  =  ****')
119  FORMAT(I4)
33   FORMAT('$CHANNEL NO.  ')
32   FORMAT(I1)
      END
```

CAPM3

```

        .TITLE CAPACITANCE
        .IDENT /3/
        .PSECT DCAP,RW,I,REL
        .NLIST TTM,BEX,MEB
; ;
;     MINCHEN
;     THIS IS A MODIFICACATION OF CAPME.MAC  ALLOWING
;     VARIATION OF PULSE SIZE.  USED WITH CAPF3.FTN
;
        .GLOBL DCAP
;
        .MCALL .INIT,.WRITE,.WAIT,.EXIT,.READ,.RLSE
        .MCALL .BIN20,.F4DEF,.O2BIN
        .F4DEF 0
DCAP:    MOV R5,RET
        MOV 2(R5),R3                ; STARTING ADDRESS OF DATA
        MOV @4(R5),ICHAN
        MOV @6(R5),PH                ; PULSE HIGHT
        MOV @10(R5),PL
        BIC #170000,PL
        BIC #170000,PH
        SETA HEIGHT,PH
        DEC ICHAN
        BNE CHAN2
CHAN1:   SETN CHANLD,4000
        BR TB
CHAN2:   DEC ICHAN
        BNE CHAN3
        SETN CHANLD,2000
        BR TB
CHAN3:   DEC ICHAN
        BNE CHAN4
        SETN CHANLD,1000
        BR TB
CHAN4:   SETN CHANLD,400
TB:      SETN TIMEBS,0                ; 1 USEC PULSE
        SETA LENGTH,PL
        MOV #4,TMP
        CLR VBSE
A1:      SENT CONVRT                ; CHECK POTENTIAL
        FLAG DONE,A1
        DATAAQ ADREAD,VBASE        ; CAPACITOR DISCHARGE YET
        COM VBASE
        BIC #170000,VBASE            ; STRIP OFF THE FIRST 4 BITS
        ADD VBASE,VBSE
        DEC TMP
        BNE A1
        CLR R0
        MOV VBSE,R1
        DIV #4,R0
        MOV R0,VBASE

```

CAPM3

```

      MOV #310, DATACT
PLSE:  SENT PULSE
      DIV #1, R1
      MUL #1, R1                ; 10 US AFTER PULSE
LOGGIN: SENT CONVRT
      MOV T1, T2                ; KILL SOME TIME
      NOP
      MOV T2, T1
      FLAG DONE, AB1
      DATAAG ADREAD, (R3)+
      DEC DATACT
      BNE LOGGIN
      MOV #310, DATACT
      MOV 2(R5), R3
MORE:  COM (R3)
      BIC #170000, (R3)+
      DEC DATACT
      BNE MORE
RETURN: MOV RET, R5
      MOV VBASE, @4(R5)
      RTS R5
FINISH: .EXIT
PL:     .WORD 0
PH:     .WORD 0
RET:    .WORD 0
TMP:    .WORD 0
VBSE:   .WORD 0
T1:     .WORD 0
T2:     .WORD 0
TBASE:  .WORD 0
ICHAN:  .WORD 0
DATACT: .WORD 0
VBASE:  .WORD 0
DATABF: .BLKW 400
        .END DCAP
```

LINFIA

```
C
C      SUBROUTINE LINFIT
C
C      MAKE A LEAST-SQUARES FIT OF DATA
C      Y= A + B*X
C
C      USAGE CALL:
C      LINFIT(X, Y, SIGMAY, NPTS, MODE, A, SIGMAA, B, SIGMAB, R)
C
C      SUBROUTINE LINFIT(X, Y, SIGMAY, NPTS, MODE, A, SIGMAA
1, B, SIGMAB, R)
      DOUBLE PRECISION SUM, SUMX, SUMY, SUMX2, SUMXY, SUMY2
      DOUBLE PRECISION XI, YI, WEIGHT, DELTA, VARNCE
      DIMENSION X(1), SIGMAY(1), Y(1)
11  SUM=0.
      SUMX=0.
      SUMY=0.
      SUMX2=0.
      SUMY2=0.
      SUMXY=0.
21  DO 50 I=1, NPTS
      XI=X(I)
      YI=Y(I)
      IF (MODE) 31, 36, 38
31  IF (YI) 34, 36, 32
32  WEIGHT=1. /YI
      GOTO 41
34  WEIGHT=1. /(-YI)
      GOTO 41
36  WEIGHT=1.
      GOTO 41
38  WEIGHT=1. /SIGMAY(I)**2
41  SUM=SUM+WEIGHT
      SUMX=SUMX+WEIGHT*XI
      SUMY=SUMY+WEIGHT*YI
      SUMX2=SUMX2+WEIGHT*XI*XI
      SUMXY=SUMXY+WEIGHT*XI*YI
      SUMY2=SUMY2+WEIGHT*YI*YI
50  CONTINUE
51  DELTA=SUM*SUMX2-SUMX*SUMX
      A=(SUMX2*SUMY-SUMX*SUMXY)/DELTA
53  B=(SUMXY*SUM-SUMX*SUMY)/DELTA
      IF (MODE) 62, 64, 62
62  VARNCE=1.
      GOTO 67
67  CONTINUE
64  CONTINUE
71  R=(SUM*SUMXY-SUMX*SUMY)/
      1 DSGRT(DELTA*(SUM*SUMY2-SUMY*SUMY))
      RETURN
      END
```

AMP FACTOR

```
C
C
C      AMP. FTN
C
C      DATA FOR AMPLIFICATION FACTOR
C
C      SUBROUTINE AMPLI
C      DIMENSION AMP(1)
C      COMMON AMP
C      DO 1 I=1,3
C      AMP(I)=0.792
1      CONTINUE
C      DO 2 I=1,5
C      J=I+3
C      AMP(J)=2.0
2      CONTINUE
C      DO 3 I=1,5
C      J=I+8
C      AMP(J)=0.792
3      CONTINUE
C      AMP(14)=0.792
C      AMP(15)=2.0
C      AMP(16)=4.0
C      AMP(17)=4.0
C      AMP(18)=4.0
C      AMP(19)=2.0
C      AMP(20)=0.792
C      DO 4 I=1,3
C      J=I+20
C      AMP(J)=0.792
4      CONTINUE
C      AMP(24)=2.0
C      AMP(25)=2.0
C      AMP(26)=4.0
C      AMP(27)=8.0
C      AMP(28)=8.0
C      AMP(29)=8.0
C      AMP(30)=4.0
C      AMP(31)=2.0
C      AMP(32)=2.0
C      AMP(33)=0.792
C      AMP(34)=4.0
C      AMP(35)=8.0
C      AMP(36)=8.0
C      AMP(37)=16.0
C      AMP(38)=16.0
C      AMP(39)=16.0
C      AMP(40)=16.0
C      AMP(41)=16.0
C      AMP(42)=8.0
```

AMP

AMP(43)=8.0
AMP(44)=4.0
END

VDEPOF

```
C      VDEPOF.FTN
C
C
C      WANG, MINCHEN
C
C      VERSION: A
C
C      AMP: AMPLIFICATION FACTOR , TO BE READ IN
C      CONTROLLED POTENTIAL ELECTROLYSIS OR DEPOSITION
C
C
C      DIMENSION JVOLT(500)
C      DOUBLE PRECISION VD
C      BYTE FNAME(40), TODAY(9)
C      WRITE(6,115)
C      READ(6,114)AMP
C      WRITE(6,207)
C      READ(6,208)REF
207  FORMAT('$POTENTIAL OF THE REF. ELECTRODE ')
208  FORMAT(F15.5)
C      ICHAN=2
C      1  WRITE(6,99)
99   FORMAT('$FILE NAME: ')
C      READ(6,100)FNAME
100  FORMAT(40A1)
201  FORMAT(I1)
C      WRITE(6,203)
C      READ(6,204)VMAINT
203  FORMAT('$VOLTAGE TO BE MAINTANED. = ')
204  FORMAT(F10.2)
C      VD=4000.0
C
C      2.441MV IS ONE BIT POTENTIAL
C
C      COMPLEMENTARY VALUE IS LOADED
C
C      IVD=VD
C      WRITE(6,205)
C      READ(6,206)VDROP
C      VDROP=VDROP*CURNT/100.0
205  FORMAT('$IR DROP PER 100UA. =')
206  FORMAT(F15.5)
C
C      JVOLT(1) IS THE FIRST HUMP POTENTIAL
C
C      JVOLT(1)=(VMAINT-REF+VDROP)*AMP/2.441+2048.0
C      CALL LINT(JVOLT(1), ICHAN, IVD)
C      CALL ASSIGN(4, FNAME, 40, IERR)
C      CALL DATE(TODAY)
C      WRITE(4,104)TODAY
```


VDEPOF

```
104  FORMAT('; '20A1)
      WRITE(4,110)
110  FORMAT('; DATA FROM VDEPO.LDA ')
      CURNT=-(FLOAT(ICHAN)*0.122)+250.0
C
C      CURNT=-(ICHAN*2.4414)/20.0+5000.0/20.0
C
      WRITE(4,151)CURNT
151  FORMAT('; CURRENT USED UA. , 'F15.0)
      JVDLT(1)=JVOLT(1)-2048
      JJ=JVOLT(1)/(AMP*0.4096)
      VOLT=FLOAT(JJ)-VDROP+REF
      WRITE(4,109)VOLT
109  FORMAT('; VOLTAGE MAINTAINED,MV = 'F15.2)
      WRITE(4,103)
103  FORMAT('ED END OF FILE. ')
114  FORMAT(F10.5)
115  FORMAT('$AMPLIFICATION FACTOR  = ')
      END FILE 4
      GOTO 1
      END
```

VDEPOM

```

. TITLE CONTROLLED POTENTIAL DEPOSITION
. IDENT /A/
. PSECT VDEPO, RW, I, REL
. NLIST TTM, BEX, MEB
;
; MINCHEN
;
; VDEPOM. MAC
;
; 1000 S. POTENTIAL MAINTAINENCE
;
. GLOBL LINT
. MCALL . INIT, . WRITE, . WAIT, . EXIT, . READ, . RLSE
. MCALL . BIN20, . F4DEF, . Q2BIN
. F4DEF 0
;
LINT:  MOV R5, RET
      MOV 2(R5), R2          ; STARTING ADDRESS OF DATA
      MOV @2(R5), VFIRST    ; POTENTIAL OF THE FIRST HUMP
      MOV @4(R5), ICHAN     ; CHANNEL NO.
      MOV @6(R5), IVO       ; PULSE HIGHT
      MOV #16011, OUT       ; ZERO BUFFER OA
      MOV #6, TBASE        ; MAKE LONG PULSE
      SETA TIMEBS, TBASE    ; PULSE TIME BASE, 1 M SEC
      DEC ICHAN             ; CHANNEL ONE ?
      BNE CHANB
CHAN1: SETN CHANLD, 4000     ; CHANNEL ONE
      JMP START
CHANB: DEC ICHAN
      BNE CHANC
CHAN2: SETN CHANLD, 2000    ; 2 CHANNEL
      JMP START
CHANC: DEC ICHAN
      BNE CHAND
CHAN3: SETN CHANLD, 1000    ; CHANNEL 3
      JMP START
CHAND: SETN CHANLD, 400     ; CHANNEL 4
START: SETA HEIGHT, IVO
      SETA LENGTH, PL
      MOV #11, CKCSR        ; MS. AS TIME BASE FOR DM
      MOV #1, CKINIT
      SENT PULSE
A1:   BIT #100, CKCSR
      BEQ A1
      BIS #200, CKINIT      ; CLEAR DM FLAG
PLS:  SETA HEIGHT, IVO
      NOP
      NOP
      SENT CONVRT
      FLAG DONE, AB
      DATAQ ADREAD, (R2)

```

VDEPOM

```

        COM (R2)
        BIC #170000, (R2)
        BIT #40000, CKCSR      ; FLAG UP ?
        BIT #100, CKCSR
AG2:     CMP (R2), VFIRST
        BMI PLS1
        BPL PLS2
        JMP PLS
A3:      SETN TIMEBS, 0
        SETN CHANLD, 0
        MOV #007, 177566
RETURN:  MOV RET, R5
        MOV (R2), @2(R5)
        MOV IVO, @4(R5)
        RTS R5
PLS1:    DEC IVO
        JMP PLS
PLS2:    INC IVO
        CMP IVO, #7777
        BPL OVER
A6:      NOP
        JMP PLS
OVER:    MOV #7777, IVO
        BR A6
FINISH:  .EXIT
INCNT:   INC COUNT
        BIS #100, CKINIT      ; CLEAR PG FLAG
        BR AG2
;
        .PSECT FLTSTK, OVR
FTSTAK:  .BLKW 10
;
RET:     .WORD 0
N1:      .WORD 0
TBASE:   .WORD 0
PL:      .WORD 7000
IVO:     .WORD 0
ICHAN:   .WORD 0
VFIRST:  .WORD 0
        .END LINT
```

CHRONF

```
C
C      CHRONF.FTN
C
C      MAY 5 78
C      WANG
C      VERSION: C
C
C      USAGE: APPLY A CONSTANT CURRENT AND MONITOR THE
C      RESULTING VOLTAGE
C
C      AMPLIFICATION FACTOR IS TO BE READ IN
C
C      FOUR CURRENT CHANNELS ARE TESTED
C      SUBROUTINE CALLED CHRONM.MAC
C
C      DIMENSION JVOLT(500)
C      DOUBLE PRECISION VD
C      BYTE FNAME(40), TODAY(9)
C      BYTE CNTR(4)
C      EQUIVALENCE (FNAME(11), CNTR)
C      WRITE(6, 115)
C      READ(6, 114) AMP
C      WRITE(6, 207)
C      READ(6, 208) REF
207  FORMAT('$POTENTIAL OF THE REF. ELECTRODE ')
208  FORMAT(F15.5)
C      WRITE(6, 200)
C      READ(6, 201) ICHAN
200  FORMAT('$CHANNEL NO. = ')
C      WRITE(6, 11)
11   FORMAT('$TIME INTERVAL PER DATA 10**AAAAA MS. ')
C      READ(6, 12) INTER
12   FORMAT(I5)
C      WRITE(6, 99)
99   FORMAT('$FILE NAME: ')
C      READ(6, 100) FNAME
100  FORMAT(40A1)
201  FORMAT(I1)
C      WRITE(6, 203)
C      READ(6, 204) CURNT
203  FORMAT('$CURRENT, UA. = ')
204  FORMAT(F10.2)
C      VD=CURNT*2.*10** (ICHAN-1)
C      VD=- (VD-5000.0)/2.4414
C
C
C      2.441MV IS ONE BIT SIZE
C
C      COMPLEMENTARY VALUE IS LOADED
C
```

CHRONF

```
      IVD=VD
      WRITE(6,205)
      READ(6,206)VDROP
205  FORMAT('$IR DROP PER 100UA.=')
      VDROP=VDROP*CURNT/100.0
      WRITE(6,76)
76   FORMAT('$NO. OF FILES ')
      READ(6,77)NFILE
77   FORMAT(I2)
206  FORMAT(F15.5)
      DO 1 II=1,NFILE
      JVOLT(1)=INTER
      CALL LINT(JVOLT(1),ICHAN,IVD)
      ENCODE(4,107,CNTR)II
107  FORMAT(I2)
      CALL ASSIGN(4,FNAME,40,IERR)
      CALL DATE(TODAY)
      WRITE(4,104)TODAY
104  FORMAT('; '20A1)
      WRITE(4,110)
110  FORMAT('; DATA FROM CHRON.LDA ')
      WRITE(4,151)CURNT
151  FORMAT('; CURRENT USED UA., 'F15.0)
      JVOLT(1)=JVOLT(1)-2048
      JJ=JVOLT(1)/(AMP*0.4096)
      VOLT=FLOAT(JJ)+REF
      WRITE(4,109)VOLT
109  FORMAT('; INITIAL POTENTIAL,MV ='F15.2)
      WRITE(4,108)
108  FORMAT('; CHARGE, MUCOUL. VOLTAGE,MV')
      DO 2 I=3,101
      J=I-1
      JVOLT(I)=JVOLT(I)-2048
      JVD=JVOLT(I)/(AMP*0.4096)
      VOLT=FLOAT(JVD)-VDROP+REF
      A=FLOAT(J)*(10**INTER)*ABS(CURNT)
2    WRITE(4,101)A,VOLT
101  FORMAT('RD',2F15.0)
      N=I-2
      WRITE(4,103) N
103  FORMAT('ED END OF FILE. ',I5)
114  FORMAT(F10.5)
115  FORMAT('$AMPLIFICATION FACTOR   = ')
      END FILE 4
1    CONTINUE
      END
```

CHRONO

```

. TITLE CHRONNOPOTENTIOMETRY
. IDENT /B1/
. PSECT LINNEA, RW, I, REL
. NLIST TTM, BEX, MEB
;
;   MINCHEN
;   MARCH 9 77
;
;   A MODIFICATION OF LINTF.MAC(LINEAR TEST)
;
;   CHRONM. MAC
. GLOBL LINT
;

. MCALL . INIT, . WRITE, . WAIT, . EXIT, . READ, . RLSE
. MCALL . BIN2D, . F4DEF, . O2BIN
. F4DEF 0
. PSECT

;
LINT:  MOV R5, RET
      MOV 2(R5), R2           ; STARTING ADDRESS OF DATA
      MOV @2(R5), TBASE      ; TIME BASE
      MOV @4(R5), ICHAN      ; CHANNEL NO.
      MOV @6(R5), IVD        ; PULSE HIGHT
      MOV #16011, OUT        ; ZERO BUFFER OA
      . BIN2D #TMP, IVD
      WRITE MS1
      BIC #170000, IVD
      . BIN2D #TMP1, IVD
      WRITE MS2
      MOV IVD, OUT
      ADD #3, TBASE          ; MSEC AND UP
      SETA TIMEBS, TBASE     ; PULSE TIME BASE, 1 M SEC
      DEC ICHAN              ; CHANNEL ONE ?
      BNE CHANB
CHAN1: SETN CHANLD, 4000      ; CHANNEL ONE
      JMP START
CHANB: DEC ICHAN
      BNE CHANC
CHAN2: SETN CHANLD, 2000     ; 2 CHANNEL
      JMP START
CHANC: DEC ICHAN
      BNE CHAND
CHAN3: SETN CHANLD, 1000     ; CHANNEL 3
      JMP START
CHAND: SETN CHANLD, 400      ; CHANNEL 4
START: MOV NDATA, COUNT
      MOV TBASE, CKCSR
      SETA LENGTH, PL
      SETA HEIGHT, IVD
      RSTCK A1

```

CHRONO

```

        BIS #200,CKINIT           ; CLEAR DM FLAG
        SENT CONVRT
        FLAG DONE,AA
        SENT PULSE
        DATAAQ ADREAD,(R2)+
AGAIN:   NOP
CKA2:    BIT #100,CKCSR           ; TIME YET?
        BEQ CKA2
        SENT CONVRT
        FLAG DONE,AB
        DATAAQ ADREAD,(R2)+
        BIS #200,CKINIT
        DEC COUNT
        BNE AGAIN
        SETN CHANLD,0
RETURN:  MOV RET,R5
        MOV 2(R5),R2
        MOV NDATA,COUNT
COMP:    COM (R2)
        BIC #170000,(R2)+       ; AUTO INCREMENT TO NEXT DATA
        DEC COUNT               ; COMPLEMENTARY DATA
        BNE COMP
        RTS R5
FINISH:  .EXIT
;
        .PSECT FLTSTK,DVR
FTSTAK:  .BLKW 10
;
INPUT:   MOV R0,-(SP)            ; SAVE R0
        MOV #BUFHD,R0           ; R0->BUFFERHEAD
        MOV R4,6(R0)            ; SET ADDRESS FOR LINE BUFFER
READER:  .INIT #LINBK
        .READ #LINBK, BUFHD
        .WAIT #LINBK
        .RLSE #LINBK
        MOV (SP)+,R0
        MOV (SP)+,R4
        RTS R5
PUTR1:   MOV R5,-(SP)            ; SAVE R5
        MOV #BUFHD,R5           ; POINT TO BUFFER HEADER
        MOV R1,6(R5)            ; STORE ADDRESS OF LINE HEAD
        CLR R0                  ; DATA COUNT
COUNT1: INC R0
        TSTB (R1)+              ; COUNTING THE NO. OF DATA
        BNE COUNT1
        MOV R0,4(R5)            ; STORE THE ACTUAL COUNT
        MOV #LINBK,R0           ; MOVE TO THE DEVICE HANDLER
        .INIT R0
        .WRITE R0,R5
        .WAIT R0
        .RLSE R0
```

CHRONO

```
        MOV (SP)+, R5
        RTS R5
;
        . EVEN
        . WORD FINISH
LINBK:   . WORD 0000
        . RAD50 /KB/
        . BYTE 1, 0
        . RAD50 /KB/
;
BUFHD:   . WORD 6
        . BYTE 6, 1
        . WORD 6
        . WORD 0
MS1:     . BYTE 15, 12
        . ASCII /DAC OUT = /
TMP:     . BLKB 6
        . WORD 0
MS2:     . BYTE 15, 12
        . ASCII /DAC OUT = /
TMP1:    . BLKB 6
        . WORD 0
COUNT:  . WORD 0
RET:     . WORD 0
DATAHD:  . WORD 0
N1:      . WORD 0
TBASE:   . WORD 0
PL:      . WORD 200
IVO:     . WORD 0
ICHAN:   . WORD 0
NDATA:   . WORD 145
        . END LINT
```


DEPOSF

```

C
C
C      DEPOSF.FTN
C
C
C      MINCHEN WANG
C      APRIL 20 1978
C
C      A MODIFICATION VERSION OF THE CURRENT REVERSAL EXP.
C
C      SUBROUTINE CALLED DEPOSM.MAC
C
C      Q, DEP=2.4 MA*1000  USEC.
C      ENTER FILE NAME AS FL: DEPOSA.01
C
C      2.4 UCUL NEGATIVE CHARGE IS DUMPED ON
C      THE WORKING ELECTRODE. STRIPPING IS STARTED
C      AFTER A PRESELECTED WAITTING PERIOD.
C
C
C
C      DIMENSION A(260), TIME(260), IV(260)
C      BYTE FNAME(20), LINE(80), TODAY(10), CNTR(2)
C      EQUIVALENCE (JFLAG, LINE(1)), (FNAME(11), CNTR)
C      FIVE DATA FILES ARE CREATED
C
C      WRITE(6, 11)
C      READ(6, 12) AMP
11      FORMAT(' $AMPLIFICATION FACTOR ')
12      FORMAT(F10.5)
C      WRITE(6, 13)
13      FORMAT(' $ REF. ELECTRODE POTENTIAL VS. R.H.E ')
C      READ(6, 12) REF
C      WRITE(6, 20)
20      FORMAT(' $IR DROP, MV. PER 100 UA CURRENT ')
C      READ(6, 21) BSE
21      FORMAT(F15.6)
C      CATHO=-2400.0
C      FCTR=2.4
C      WRITE(6, 125)
C      READ(6, 106) FNAME
C      WRITE(6, 106) FNAME
C      NPTS=100
C
C      WAIT FOR 10**ITWAIT USEC. -1000USEC.
C
C      ANODI=-CATHO/FCTR
C      BSE=-BSE*ANODI/100.0
C      VCATHO=-(CATHO*2.0-5000.0)/2.4414
C      VANODI=-(ANODI*2.0-5000.0)/2.4414
C      IANODI=IFIX(VANODI)

```

DEPOSF

```
      ICATHO=IFIX(VCATHO)
      IFCTR=IFIX(FCTR)
      ITWAIT=3
      II=1
99    CONTINUE
      CALL DEPOS(IV(1), ICATHO, IANODI, ITWAIT)
      DO 1 I=1, NPTS
      IV(I)=IV(I)-2048
      A(I)=FLOAT(IV(I))/(AMP*0.4096)
1     CONTINUE
      ENCODE(4, 109, CNTR) II
      CALL ASSIGN(4, FNAME, 20, IERR)
      WRITE(4, 111) FNAME
111   FORMAT( ', FNAME: '40A1)
      CALL DATE(TODAY)
      WRITE(4, 113) TODAY
113   FORMAT( ', ', 20A1)
      WRITE(4, 110) CATHO, ANODI
110   FORMAT( ', CATHODIC CURRENT='F15.6,
1      ' ANODIC CURRENT='F15.6)
      WRITE(4, 112) BSE
      WRITE(4, 115) ITWAIT
115   FORMAT( ', WAITING FOR 10**'I2'   USEC. - 1 MSEC. ')
112   FORMAT( ', IR DROP IS ', F15.5, 'MV. PER 100 UA')
      WRITE(4, 114)
114   FORMAT( ', MUCOUL.   MV. VS. R.H.E. ')
      DO 126 I=1, 100
      VOLT=A(I)+BSE+REF
      CHARGE=FLOAT(I)*ANODI*0.04
      WRITE(4, 129) CHARGE, VOLT
126   CONTINUE
129   FORMAT( 'RD', 2F15.5)
      WRITE(4, 133)
133   FORMAT( 'ED')
      END FILE 4
102   FORMAT(I2)
104   FORMAT(I3)
105   FORMAT( '$ FILE NAME ')
125   FORMAT( '$NEW FILE NAME ')
106   FORMAT(20A1)
107   FORMAT( ' NEXT FILE '20A1)
108   FORMAT( '$NEW CHAR. ')
      ITWAIT=ITWAIT+1
      II=II+1
109   FORMAT(I2)
      IF (ITWAIT.LT.8) GOTO 99
      END
```

DEPOSM

```

        . TITLE DEPOSITION
        . IDENT /A/
        . PSECT PARAME,RW,I,REL
        . NLIST TTM,BEX,MEB
        . GLOBL DEPOS
;
; APPLY A SHORT CURRENT PULSE FOLLOWED BY A WAITING PERIOD
; THEN, A STRIPPING PULSE IS ISSUED
;
        . MCALL . INIT,. WRITE,. WAIT,. EXIT,. READ,. RLSE
        . MCALL . BIN20,. F4DEF,. D2BIN
        . F4DEF 0
;
        . PSECT
DEPOS:  MOV 2(R5),BFADDR
        MOV BFADDR,R2
        MOV R5,RET
        MOV @4(R5),PH1
        MOV @6(R5),PH2           ; CATHODIC CURRENT
        MOV @10(R5),WAIT         ; WAITING PERIOD
        MOV #47,PGCNTR           ; 40 U SEC.
        MOV #2,TMP               ; 2 * TWAIT
        MOV #144,NDATA           ; 100 POINTS
        CMP WAIT,#6
        BMI CONT
        BNE T7
        MOV #6,TMP
        BR CONT1
T7:     CMP WAIT,#7
        BNE T8
        MOV #22,TMP              ; 1.8 S
        BR CONT1
T8:     MOV #100,TMP              ; 6.4 S.
        BR CONT1
CONT:   MOV WAIT,TWAIT
CONT1:  MOV TWAIT,CKCSR
;
; PL=1000 US, PL2= 3200 US.
;
        MOV #1750,PL1
        MOV #6200,PL2
        BIS #14000,CKCSR         ; DOWN, PRESET , 1 MSE. TB
        SETA HEIGHT,PH1
        SETA LENGTH,PL1
        SETN TIMEBS,0
CHAN1:  SETN CHANLD,4000
        SENT PULSE
        MOV #1,CKINIT           ; CLEAR DM DIVIDER
A1:     BIT #100,CKCSR
        BEQ A1
        BIS #200,CKINIT
A2:     BIT #100,CKCSR

```

DEPOSM

```
BEG A2
BIS #200,CKINIT
DEC TMP
BNE A2
SETA HEIGHT,PH2
SETA LENGTH,PL2
MOV #0,CKCSR
MOV #14000,CKCSR
RSTCK A3
SENT PULSE
BIS #100,CKINIT
A3: SENT CONVRT
A4: BIT #40000,CKCSR
BEG A4
DATAAG ADREAD,(R2)+
DEC NDATA
BEG TRANS
BIS #100,CKINIT
BR A3
TRANS: MOV #7,177566
MOV BFADDR,R2
BIS #1,CKINIT
A6: COM (R2)
BIC #170000,(R2)+
INC NDATA
CMP #144,NDATA
BPL A6
BIS #200,CKINIT
MORE: BIT #100,CKCSR
BNE MORE
RTS R5
FINISH: .EXIT
WAIT: .WORD 0
PH1: .WORD 0
PL1: .WORD 0
PL2: .WORD 0
PH2: .WORD 0
RET: .WORD 0
TMP: .WORD 0
N1: .WORD 0
TWAIT: .WORD 0
ICHAN: .WORD 0
NDATA: .WORD 4
BFADDR: .WORD 0
.END DEPOS
```

ETREAF

```
C
C
C      ETREAF.FTN
C
C
C      MINCHEN WANG
C
C      FEB 14 1978
C
C      THIS PROGRAM  CALCULATE THE CELL IR FROM THE
C      EXTRAPOLATED POTENTIAL VALUE , DOSE IR CORRECTION
C
C      DIMENSION A(210),TIME(210),IV(210)
C      BYTE FNAME(20),LINE(80),TODAY(10),CNTR(1)
C      EQUIVALENCE (JFLAG,LINE(1)),(FNAME(9),CNTR)
C      DATA FILE CREATED
C
99      WRITE(6,125)
        READ(6,106)FNAME
        WRITE(6,106)FNAME
        NPTS=200
        CALL ETREAT(IV(1))
        WRITE(6,11)
        READ(6,12)AMP
11      FORMAT('$AMPLIFICATION FACTOR ')
12      FORMAT(F10.5)
        WRITE(6,13)
13      FORMAT('$ REF. ELECTRODE POTENTIAL VS. R.H.E ')
        READ(6,12)REF
        DO 1 I=1,NPTS
          IV(I)=IV(I)-2048
          A(I)=FLOAT(IV(I))/(AMP*0.4096)
1      CONTINUE
C
C
C
C
        BSE=(A(100)-A(101))/2.0
        CALL ASSIGN(4,FNAME,20,IERR)
C
        WRITE(4,111)FNAME
111      FORMAT(';FNAME: '40A1)
        CALL DATE(TODAY)
        WRITE(4,113)TODAY
113      FORMAT('; ',20A1)
        WRITE(4,112)BSE
112      FORMAT('; IR DROP IS ',F15.5,'MV. ')
        WRITE(4,114)
114      FORMAT('; MUCDUL.  MV. ')
        DO 126 I=1,100
```

ETREAF

```
VOLT=A(I)-BSE+REF
CHARGE=FLOAT(I)*50.0
WRITE(4,129)CHARGE,VOLT
126 CONTINUE
DO 127 I=101,NPTS
VOLT=A(I)+BSE+REF
CHARGE=FLOAT(I)*50.0
WRITE(4,129)CHARGE,VOLT
127 CONTINUE
129 FORMAT('RD',2F15.5)
WRITE(4,133)
133 FORMAT('ED')
END FILE 4
102 FORMAT(I2)
104 FORMAT(I3)
105 FORMAT('$ FILE NAME ')
125 FORMAT('$NEW FILE NAME ')
106 FORMAT(20A1)
107 FORMAT(' NEXT FILE '20A1)
108 FORMAT('$NEW CHAR. ')
109 FORMAT(1A1)
GO TO 99
END
```

ETREMA

```
. TITLE ELECTROCHEMICAL TREATMENT
. IDENT /A1/
. PSECT ETREAT, RW, I, REL
. NLIST TTM, BEX, MEB
. GLOBL ETREAT
;
;   USAGE: THIS SUBROUTINE IS CALLED BY ETREAT.FTN
;
;   PURPOSE: DELIVER 250. UAMP ALTERNATING CURRENT
;   STEPS FOR 51 CYCLES. PERIOD IS 0.2 S.
;
;   FEB 16 78
;   .MCALL .INIT, .WRITE, .WAIT, .EXIT, .READ, .RLSE
;   .MCALL .BIN20, .F4DEF, .O2BIN
;   .F4DEF 0
;   .PSECT
;
;   . =. +100
ETREAT: MOV 2(R5), R2
        MOV R2, DATAK
        MOV R5, RET
        MOV #144, CYCLE
        MOV #5, TBASE           ; 100 MS TIME BASE
        MOV #16011, OUT         ; ZERO BUFFER OA
        SETA TIMEBS, TBASE      ; PULSE TIME BASE, 10 M SEC
CHAN2:  SETN CHANLD, 2000       ; 2 CHANNEL
        SETA LENGTH, PL
        MOV #3, CKCSR           ; MS. FOR TIME BASE
        RSTCK A1
        BIS #200, CKINIT       ; CLEAR DM FLAG
        SENT PULSE
POINV:  NOP
        SETA HEIGHT, IVO
        MOV #144, COUNT
CKA1:   BIT #100, CKCSR         ; TIME YET?
        BEQ CKA1
        BIS #200, CKINIT
        DEC COUNT
        BNE CKA1
        COM IVO
        BIC #170000, IVO
        DEC CYCLE
        BEQ START
        JMP POINV
START:  MOV DATAK, R2
        MOV #2, INDEX
POLINV: SETA HEIGHT, IVO
        MOV #144, COUNT
AGAIN:  MOV #4, NDATA
CONV:   SENT CONVRT
        FLAG DONE, AA
```

ETREMA

```
DATAAG ADREAD, -(SP)
ADD (SP)+, (R2)
DEC NDATA
BNE CONV
CKA2: BIT #100, CKCSR           ; TIME YET?
      BEQ CKA2
      ASR (R2)+
      BIS #200, CKINIT
      DEC COUNT
      BNE AGAIN
      DEC INDEX
      BEQ LAST
      COM IVD                 ; INVERT VOLTAGE
      BIC #170000, IVD
      MOV #144, COUNT
      JMP POLINV
LAST:  SETN TIMEBS, 0
      MOV RET, R5
      MOV #310, COUNT
      MOV DATALK, R2
MORE:  ASR (R2)
      COM (R2)
      BIC #170000, (R2)+
      DEC COUNT
      BNE MORE
      RTS R5
FINISH: .EXIT
INPUT:  MOV R0, -(SP)         ; SAVE R0
      MOV #BUFHD, R0         ; R0->BUFFERHEAD
      MOV R4, 6(R0)          ; SET ADDRESS FOR LINE BUFFER
      MOV NUMW, (R0)         ; SET MAX WORD COUNT
READER: .INIT #LINBK
      .READ #LINBK, #BUFHD
      .WAIT #LINBK
      .RLSE #LINBK
      MOV (SP)+, R0
      MOV (SP)+, R4
      RTS R5
PTR1:  MOV R5, -(SP)         ; SAVE R5
      MOV #BUFHD, R5         ; POINT TO BUFFER HEADER
      MOV R1, 6(R5)          ; STORE ADDRESS OF LINE
                                   ; HEADER
                                   ; DATA COUNT
COUNT1: CLR R0
      INC R0
      TSTB (R1)+             ; COUNTING THE NO. OF DATA
      BNE COUNT1
      MOV R0, 4(R5)          ; STORE THE ACTUAL COUNT
      MOV #LINBK, R0         ; MOVE TO THE DEVICE HANDLER
      .INIT R0
      .WRITE R0, R5
      .WAIT R0
```


ETREMA

```
        .RLSE R0
        MOV (SP)+,R5
        RTS R5
;
        .EVEN
        .WORD FINISH
LINBK:   .WORD 0000
        .RAD50 /KB/
        .BYTE 1,0
        .RAD50 /KB/
;
BUFHD:   .WORD 6
        .BYTE 6,1
        .WORD 6
        .WORD 0
MS1:     .BYTE 15,12
        .ASCII /DAC OUT = /
TMP:     .BLKB 6
        .WORD 0
MS2:     .BYTE 15,12
        .ASCII /DAC OUT = /
TMP1:    .BLKB 6
        .WORD 0
COUNT:  .WORD 0
RET:     .WORD 0
DATAHD:  .WORD 0
CYCLE:   .WORD 0
INDEX:   .WORD 0
N1:      .WORD 0
TBASE:   .WORD 0
PL:      .WORD 310
IVD:     .WORD 0
ICHAN:   .WORD 0
DATALK:  .WORD 0
NDATA:   .WORD 4
        .END ETREAT
```

PLATINIZE

```
. TITLE PLATINIZATION
. IDENT /B1/
. PSECT PLATINZ, RW, I, REL
. NLIST TTM, BEX, MEB
. GLOBL ETREAT
;
; EACH RUN CONSISTS OF 20480 CYCLE, 30 MS.
; CURRNET STEPS
;
; MAY 78
;
. MCALL . INIT, . WRITE, . GAIT, . EXIT, . READ, . RLSE
. MCALL . BIN20, . F4DEF, . D2BIN
. F4DEF 0
. PSECT
;
ETREAT: WRITE MS1
        READ NDCYC
        . D2BIN #NDCYC
        MOV (SP)+, CYCCNT
        MOV (SP)+, JUNK          ; CLEAR STAKE
E1:     MOV #50000, CYCLE        ; 20480 CYCLES
        MOV #5, TBASE           ; 100 MS TIME BASE
        MOV #16011, OUT         ; ZERO BUFFER DA
        SETA TIMEBS, TBASE      ; PULSE TIME BASE, 10 M SEC
        MOV #2314, IVD          ; 1000 UAMP ON CHANNEL 1
CHAN1:  SETN CHANLD, 4000        ; CHANNEL 1
        SETA LENGTH, PL
        MOV #3, CKCSR           ; MS. FOR TIME BASE
        RSTCK A1
        BIS #200, CKINIT        ; CLEAR DM FLAG
        SENT PULSE
POINV:  NOP
        SETA HEIGHT, IVD
        MOV #17, COUNT
CKA1:   BIT #100, CKCSR          ; TIME YET?
        BEQ CKA1
        BIS #200, CKINIT
        DEC COUNT
        BNE CKA1
        COM IVD
        BIC #170000, IVD
        DEC CYCLE
        BEQ START
        JMP POINV
START:  MOV #2, INDEX
POLINV: SETA HEIGHT, IVD
        MOV #17, COUNT
AGAIN:  NOP
CKA2:   BIT #100, CKCSR          ; TIME YET?
        BEQ CKA2
```

PLATINIZE

```

        BIS #200,CKINIT
        DEC COUNT
        BNE AGAIN
        DEC INDEX
        BEQ LAST
        COM IVD ; INVERT VOLTAGE
        BIC #170000,IVD
        MOV #144,COUNT
        JMP POLINV
LAST:    SETN TIMEBS,0
        DEC CYCNT
        BEQ FINISH
        JMP E1
FINISH:  .EXIT
INPUT:   MOV RO,-(SP)           ; SAVE RO
        MOV #BUFHD,RO          ; RO->BUFFERHEAD
        MOV R4,6(RO)           ; SET ADDRESS FOR LINE BUFFER
;
;   MOV NUMW,(RO)              ; SET MAX WORD COUNT
READER:  .INIT #LINBK
        .READ #LINBK, BUFHD
        .WAIT #LINBK
        .RLSE #LINBK
        MOV (SP)+,RO
        MOV (SP)+,R4
        RTS R5
PUTR1:   MOV R5,-(SP)           ; SAVE R5
        MOV #BUFHD,R5          ; POINT TO BUFFER HEADER
        MOV R1,6(R5)           ; STORE CONTENT OF R1
        CLR RO                  ; BYTE COUNT
COUNT1: INC RO
        TSTB (R1)+              ; COUNTING THE NO. OF BYTES
        BNE COUNT1
        MOV RO,4(R5)            ; STORE THE ACTUAL COUNT
        MOV #LINBK,RO          ; MOVE TO THE DEVICE HANDLER
        .INIT RO
        .WRITE RO,R5
        .WAIT RO
        .RLSE RO
        MOV (SP)+,R5
        RTS R5
;
        .EVEN
        .WORD FINISH
LINBK:   .WORD 0000
        .RAD50 /KB/
        .BYTE 1,0
        .RAD50 /KB/
;
BUFHD:   .WORD 6
        .BYTE 6,1
        .WORD 6
```

PLATINIZE

```
      . WORD 0
MS1:  . BYTE 15, 12
      . ASCII /NO. OF REPEAT, (DECIMAL)/
      . EVEN
      . WORD 0
COUNT: . WORD 0
RET:    . WORD 0
DATAHD: . WORD 0
CYCLE:  . WORD 0
INDEX:  . WORD 0
N1:     . WORD 0
TBASE:  . WORD 0
PL:     . WORD 7640
IVO:    . WORD 0
ICHAN:  . WORD 0
DATAHK: . WORD 0
NDATA:  . WORD 4
NOCYC:  . BLKB 6
JUNK:   . WORD 0
CYCCNT: . WORD 0
      . END ETREAT
```

STRIPF

```
C
C      STRIPF.FTN
C
C      FEB. 13 78
C
C      WANG
C      VERSION: A
C
C
C      AMP AMPLIFICATION FACTOR IS TO BE READ IN
C      SUBROUTINE CALLED: LINT(FROM STRIPM.MAC)
C
C
C      DIMENSION JVOLT(500)
C      DOUBLE PRECISION VD
C      BYTE FNAME(40), TODAY(9)
C      WRITE(6, 115)
C      READ(6, 114) AMP
C      WRITE(6, 207)
C      READ(6, 208) REF
207  FORMAT('$POTENTIAL OF THE REF. ELECTRODE ')
208  FORMAT(F15.5)
C      WRITE(6, 200)
C      READ(6, 201) ICHAN
200  FORMAT('$CHANNEL NO. = ')
1    WRITE(6, 99)
99   FORMAT('$FILE NAME: ')
C      READ(6, 100) FNAME
100  FORMAT(40A1)
201  FORMAT(I1)
C      WRITE(6, 203)
C      READ(6, 204) CURNT
203  FORMAT('$CURRENT, UA. = ')
204  FORMAT(F10.2)
C      VD=CURNT*2.*10**(ICHAN-1)
C      VD=-(VD-5000.0)/2.4414
C
C      2.441MV IS ONE BIT SIZE
C
C      COMPLEMENTARY VALUES OF VOLTAGE SETTING ARE LOADED
C
C      IVD=VD
C      WRITE(6, 205)
C      READ(6, 206) VDROP
C      VDROP=VDROP*CURNT/100.0
205  FORMAT('$IR DROP PER 100UA. =')
206  FORMAT(F15.5)
```

STRIPF

```
C      JVOLT(1) IS THE FIRST HUMP POTENTIAL
C      850.0MV IS ASSUMED
      JVOLT(1)=(850.0-REF+VDROP)*AMP/2.441+2048.0
      CALL LINT(JVOLT(1), ICHAN, IVO)
      CALL ASSIGN(4, FNAME, 40, IERR)
      CALL DATE(TODAY)
      WRITE(4, 104) TODAY
104    FORMAT(';', '20A1')
      WRITE(4, 110)
110    FORMAT(';', DATA FROM STRIP.LDA  ')
      TIME=FLOAT(ICHAN)*65.536+FLOAT(IVO)/1000.0
      CHARGE=CURNT*TIME
      WRITE(4, 151) CURNT
151    FORMAT(';', CURRENT USED UA., 'F15.0')
      WRITE(4, 108) CHARGE
108    FORMAT('CHARGE, UCOUL. 'F15.5)
      JVOLT(1)=JVOLT(1)-2048
      JJ=JVOLT(1)/(AMP*0.4096)
      VOLT=FLOAT(JJ)-VDROP+REF
      WRITE(4, 109) VOLT
109    FORMAT(';', POTENTIAL PRIOR TO V RISING, MV = 'F15.2)
      WRITE(4, 103)
103    FORMAT('ED END OF FILE.  ')
114    FORMAT(F10.5)
115    FORMAT('$AMPLIFICATION FACTOR    =  ')
      END FILE 4
      GOTO 1
      END
```

STRIPM

```

. TITLE STRIP
. IDENT /A/
. PSECT LINNEA, RW, I, REL
. NLIST TTM, BEX, MEB
;
; MINCHEN
; MARCH 9 77
;
; PURPOSE: STRIP HG TO THE FIRST POTENTIAL HUMP
;
;
. GLOBL LINT
. MCALL . INIT, . WRITE, . WAIT, . EXIT, . READ, . RLSE
. MCALL . BIN20, . F4DEF, . O2BIN
. F4DEF 0
. PSECT
;
LINT:  MOV R5, RET
      MOV 2(R5), R2          ; STARTING ADDRESS OF DATA
      MOV @2(R5), VFIRST    ; POTENTIAL OF THE FIRST HUMP
      MOV @4(R5), ICHAN     ; CHANNEL NO.
      MOV @6(R5), IVO       ; PULSE HIGHT
      MOV #16011, OUT       ; ZERO BUFFER DA
      MOV #0, TBASE        ; MAKE LONG PULSE
      SETA TIMEBS, TBASE    ; PULSE TIME BASE, 1 M SEC
      DEC ICHAN             ; CHANNEL ONE ?
      BNE CHANB
CHAN1: SETN CHANLD, 4000     ; CHANNEL ONE
      JMP START
CHANB: DEC ICHAN
      BNE CHANC
CHAN2: SETN CHANLD, 2000    ; 2 CHANNEL
      JMP START
CHANC: DEC ICHAN
      BNE CHAND
CHAN3: SETN CHANLD, 1000    ; CHANNEL 3
      JMP START
CHAND: SETN CHANLD, 400     ; CHANNEL 4
START: SETA HEIGHT, IVO
      SETA LENGTH, PL
      MOV #1400, CKCSR      ; PG: UP, MS. CLEAR MODE
      RSTCK A1
      BIS #100, CKINIT     ; CLEAR PG FLAG
      CLR COUNT
      MOV #30, CKINIT      ; CLEAR PGCNTR
PLS:  SENT PULSE
      NOP
      NOP
      SENT CONVRT
      FLAG DONE, AB
      DATAAG ADREAD, (R2)

```

STRIPM

```

                                COM (R2)
                                BIC #170000, (R2)
                                BIT #40000, CKCSR           ; FLAG UP ?
                                BNE INCNT
AG2: SETA LENGTH, PL
      CMP (R2), VFIRST
      BMI PLS
      MOV #40, CKINIT           ; LATCH PGCNTR
      SETN TIMEBS, 0
      SETN CHANLD, 0
      MOV #007, 177566
RETURN: MOV RET, R5
        MOV (R2), @2(R5)
        MOV PGCNTR, @6(R5)
        MOV COUNT, @4(R5)
        RTS R5
FINISH: .EXIT
INCNT:  INC COUNT
        BIS #100, CKINIT       ; CLEAR PG FLAG
        BR AG2
;
        .PSECT FLTSTK, OVR
FTSTAK: .BLKW 10
;
COUNT: .WORD 0
RET:     .WORD 0
DATAHD:  .WORD 0
N1:      .WORD 0
TBASE:   .WORD 0
PL:      .WORD 200
IVO:     .WORD 0
ICHAN:   .WORD 0
VFIRST:  .WORD 0
NDATA:   .WORD 145
        .END LINT
```


REFERENCES

1. Adams, R., "Electrochemistry at Solid Electrodes", Marcel Dekker, Inc., New York, 1969.
2. Anson, F. C. and King, D. M., Anal. Chem., 34 (1962) 362.
3. Hammett, L. P., J. Amer. Chem. Soc., 46 (1924) 7.
4. Feltham, A. M. and Spiro, M., Chemical Review 71 (1971) 177.
5. Anson, F. C., Anal. Chem., 33 (1961) 934.
6. Gardiner, K. W. and Rogers, L. B., Anal. Chem., 25 (1953) 393.
7. Marple, T. L. and Rogers, L. B., Anal. Chem., 25 (1953) 1351.
8. Woods, R., "Electroanalytical Chemistry", Ed. A. J. Bard, Vol. 9, P. 1, Marcel Dekker, Inc., New York, 1976.
9. Kemula, W., Kublic, Z. and Galus, Z., Nature, 184 (1959) 1795.
10. Neeb, R., Z. Anal. Chem., 180 (1961) 161.
11. Bruckenstein, S., and Nagai, T., Anal. Chem., 33 (1961) 1201.
12. Moros, S. A., Anal. Chem., 34 (1962) 1584.
13. Ramaley, L., Brubaker, R. L. and Enke, C. G., Anal. Chem., 33 (1961) 1201.
14. Hartley, A. M., Hiebert, A. G. and Cox, J. A., Electroanal. Chem., 17 (1968) 81.
15. Robins, G. D. and Enke, C. G., J. Electroanal. Chem., 23 (1969) 343.
16. Bruckenstein, S. and Hassen, M. Z., Anal. Chem., 43 (1971) 928.
17. Hassen, M. Z., Untereker, D. F. and Bruckenstein, S., J. Electroanal. Chem., 42 (1973) 161.

18. Schuldiner, S., Rosen, M. and Flinn, D. R.,
Electrochim. Acta, 18 (1973) 19.
19. Plaksin, I. M. and Survorovskaya, N. A., Acta Physiochim.,
URSS, 13 (1940) 83.
20. Elliott, P., "Constitution of Binary Alloys", 1st Supplement
p. 535, Mc Graw Hill, New York, 1965.
21. Biegler, T., Rand, D. A. J. and Wood, R., J. Electroanal.
Chem., 29 (1971) 269.
22. Pugh, W., J. Chem. Soc. (London), (1937) 1824.
23. Biegler, T., J. Electrochem. Soc., 116 (1969) 1131.
24. Woods, R., Electrochim. Acta, 13 (1968) 1967.
25. Bittles, J. A. and Littaner, E. L., Corros. Sci., 10 (1970)
29.
26. Gorbinova, K. M. and Polukorov, Yu. M., "Advances in
Electrochemistry and Electrochemical Engineering", Vol. 5,
ed. Tobias, C. W., Wiley, 1967.
27. Untereker, D. F. and Bruckenstein, S., J. Electrochem.
Soc., 121 (1974) 360.
28. Delahay, P., J. Phy. Chem., 66 (1963) 2204.
29. Brubaker, R. L., Thesis, Princeton Univ. 1966.
30. Hahn, B., Thesis, M.S.U. 1975.
31. Hansen, M., "Constitution of Binary Alloys", p. 832,
McGraw Hill, 2nd Edition, New York, 1958.
32. Malmstadt, H. V., Enke, C. G. and Crouch, S. R.,
"Digital and Analog Conversion" (Benjamin, 1973).
33. Barlow, M. and Planting, P. J., Z. Metallkde. Bd.
60 (1968) 292.
34. Daum, P., Thesis, M.S.U. 1969.
35. Nicholson, M. M., Anal. Chem., 29 (1957) 7.

36. Will, F. C., J. Electrochem. Soc., 112 (1965) 451.
37. Kolthoff, I. M. and Miller, C. S., J. Am. Chem. Soc., 63 (1941) 451.
38. Davis, D., "Electroanalytical Chemistry", Ed. A. Bard, p. 157, Vol. 1, Marcel Dekker, Inc., 1966.
39. Underkofler, W. L. and Shain, I., Anal. Chem., 33 (1961) 1966.
40. Vander Leest, R., Analchem. Acta, 52 (1970) 151.
41. Sutyyagina, A. A., Fadeeva, V. I., Golyanitskaya, I. N., Vovohenko, G. D., Russian J. of Phy. Chem., 45 (1971) 7.
42. Reinmuth, R. H., Anal. Chem., 34 (1962) 1272.
43. Kudirka, J. M., Daum, P. H. and Enke, C. G., Anal. Chem., 44 (1972) 309.
44. Gileadi, E., Kirowa-Eisner, E. and Penciner, J., "Interfacial Electrochemistry" Addition-Wesley Pub. Co., Massachusetts, 1975.
45. Wier, W. D. and Enke, C. G., J. Physical Chem. 71 (1967) 280.
46. Gerischer, H., Anal. Chem., 31 (1959) 33.
47. Kolthoff, I. M. and Miller, C. S., J. Amer. Chem. Soc., 63 (1941) 2732.
48. Caphill, F. P. J. and Vanloon, G. W., Amer. Lab., Aug. (1976) 11.
49. Frantisek Vydra, Karel Stulik and Eva Julakova, "Electrochemical Stripping Analysis", John Wiley and Sons Inc., New York, 1976.
50. Shain, I. and Lewinson, J., Anal. Chem., 33 (1961) 187.
51. Gerischer, H., Z. Physik. Chem., 202 (1953) 302.
52. Barendrecht, E., Nature, 181 (1958) 764.
53. Zakharov, M. S. and Thrushina, L. F., Zh. Anal. Khim., 22 (1967) 1219.

54. Igolinski, V. A. and Stromber, A. G., Zavodok. Lab., 30 (1964) 659.
55. Anderson, J. E. and Tallman, D. E., Anal. Chem., 48 (1976) 209.
56. Watson, W. R., Roe, D. K. and Carritt, D. E., Anal. Chem., 37 (1965) 1594.
57. Clem, R. G., Litton, G. and Ornelas, L. D., Anal. Chem., 45 (1973) 1306.
58. Stulikova, M., J. Electroanal. Chem., 48 (1973) 33.
59. McLaren, K. G. and Batley, G. E., J. Electroanal. Chem., 79 (1977) 169.
60. Clem, R. G., Anal. Chem., 47 (1975) 1778.
61. Batley, G. E. and Florence, T. M., J. Electroanal. Chem., 55 (1974) 23.
62. Stojek, Z. and Kublik, Z., J. Electroanal. Chem., 60 (1975) 349.
63. Stojek, Z. and Kublik, Z., J. Electroanal. Chem., 77 (1977) 205.
64. Stojek, Z., Osterpczuk, P. and Kublik, Z., J. Electroanal. Chem., 67 (1976) 301.
65. D.J.G. Ives and G.J. Janz, " Reference Electrodes", Academic Press, New York 1961